UTILISING HAEM ENZYMES IN CATALYTIC

OXIDATION CHEMISTRY

A thesis submitted for the

Degree of Doctor of Philosophy

by

AYHAN ÇELIK B.Sc. (Hons), M.Sc.

Department of Chemistry

Faculty of Science

University of Leicester

January 2001

UMI Number: U149125

UMI

Dissertation Publishing

ProQuest

STATEMENT

The accompanying thesis submitted for the degree of Doctor of Philosophy entitled "Utilising Haem Enzymes in Catalytic Oxidation Chemistry" is based on work conducted by the author in the Department of Chemistry of the University of Leicester during the period between January 1997 and January 2001.

All the work recorded in this thesis is original unless otherwise acknowledged in the text or by references. None of the work has been submitted for another degree in this or any other University.

© Ayhan Celik

Signed:............................ Date:....................

ACKNOWLEDGEMENTS

Utilising Haem Enzymes in Catalytic Oxidation Chemistry

Ayhan Çelik

Abstract

The catalytic oxidation of a range of substrates by recombinant pea cytosolic ascorbate peroxidase (rAPX), cytochrome P450 BM3 (P450 BM3) and poly-L-leucine has been examined and, for rAPX and P450 BM3, the results rationalised using computer-based molecular modelling.

Transient and steady state kinetics, together with a range of chromatographic and spectroscopic techniques, have been used to establish the mechanism and the products of the H_2O_2-dependent oxidation of p-cresol by rAPX. The results are discussed in the more general context of APX-catalysed aromatic oxidations.

The oxidation of a number of thioethers by rAPX and a site-directed variant of rAPX (W41A) has been examined. Steady state oxidation of the majority of sulphides studied, gave values for k_{cat} that are approximately 10-fold to 100-fold higher for W41A than for rAPX. For rAPX, essentially racemic mixtures of R- and S-sulphoxides were obtained for all sulphides. The W41A variant shows substantial enhancements in enantioselectivity Structure-based modelling techniques have provided a fully quantitative rationalisation of all the experimentally determined enantioselectivity and have indicated a role for Arg38 in the control of stereoselectivity.

Cytochrome P450 BM3 is shown to be a versatile catalyst for the oxidation of a wide range of organic molecules. In this study we have shown that the enzyme is able to catalyse the regio- and stereo-selective oxidation of alkyl aryl sulphides to corresponding sulphoxides with varying degrees of enantioselectivity. The effects of both the nature of the alkyl group and the electronic properties of the aryl group on both rate and the stereoselectivity of the biotransformation have been explored. The results from this study have been compared to the theoretical prediction for the asymmetric induction expected for cytochrome P450 BM3 catalysed reactions.

Poly-L-leucine proved to be a satisfactory catalyst for the oxidation of alkyl aryl sulphides, although this has been shown to occur with no significant asymmetric induction.

Contents

CHAPTER 2

SPECTROSCOPIC AND KINETIC STUDIES ON THE

CATALYTIC OXIDATION of *p*-CRESOL BY APX

CHAPTER 3

ALKYL ARYL SULPHIDE OXIDATION CATALYSED BY APX AND THE W41A VARIANT

CHAPTER 4

SULPHIDE OXIDATION CATALYSED BY

CYTOCHROME P450 BM3

CHAPTER 5

STUDIES ON THE ARTIFICAL ENZYME: POLY-L-LEUCINE-CATALYSED SULPHIDE OXIDATION

CHAPTER 6

EXPERIMENTAL

ABBREVIATIONS AND UNITS

Enzymes and Chemicals

APX   -ascorbate peroxidase

rAPX   -recombinant pea ascorbate peroxidase

W41A   -wariant of rAPX (Trp 41 is replaced with an Ala.)

MBP   -maltose binding protein

P450 BM3   -cytochrome P450 BM3

PLL   -poly-L-leucine

DNase   -deoxyribonuclease

ABTS   -2,2'-Azino, di-(3-Ethyl-Benzothiazoline-6-Sulphonic Acid)

DBU   -1,8-diazobicyclo [5.4.0]undec-7-ene

DTT   -dithiothreitol

EDTA   -ethylenediaminetetraacetic acid

FAD   -flavin adenine dinucleotide

FMN   -flavin mononucleotide

IPTG   -isopropyl-β-D-thiogalactoside

NADH   -nicotinamide adenine dinucleotide

NADPH   -nicotinamide adenine dinucleotide phosphate

PMSF   -phenylmethylsulphonyl fluoride

SDS   -sodiumdodecylsulphate

Units/Symbols

δ -chemical shift

A   -absorbance

ε -absorption coefficient

μ -ionic strength

kDa   -kilo Daltons

k_{cat} -catalytic constant

K_m -equilibrium constant

v -initial rate of catalysis

V_{max} -maximum rate of catalysis

J -coupling constant

ppm   -parts per million

Experimental

EI	-electron ionisation
FAB	-fast atom bombardment
GC	-gas chromatography
HQ-dH$_2$O	-high quality deionised water
HPLC	-high performance liquid chromatography
IR	-infra-red
M.pt.	-melting point
MS	-mass spectrometry
GC-MS	-gas chromatography-mass spectrometry
NMR	-nuclear magnetic resonance spectrometry
PAGE	-polyacrylamide gel electrophoresis
Rz	-reinheitzahl
Uv-vis	-ultra-violet and visible
PCR	-polymerase chain reaction

Amino acids are abbreviated according to the three-letter codes recommended by the I.U.P.A.C. Joint commission on Biochemical Nomenclature (1985).

CHAPTER ONE

General Introduction

1.1 INTRODUCTION

There are two important issues in the catalysis of chemical reactions that need to be addressed. The first is the development of environmentally friendly processes, for example by replacement of heavy metal salts as oxidants by hydrogen peroxide or oxygen, which is a cleaner alternative. The second is the need for catalytic reactions of high chemo-, regio- or stereoselectivity as there is an ever-increasing demand for more selective and clean oxidation catalysts, especially in the production of enantiomerically pure compounds.

Enzymes are commonly used in reactions requiring a high enantioselectivity. So far, mostly hydrolytic enzymes have been used on an industrial scale.[1,2] However, it is becoming increasingly clear that haem proteins can be used to carry out oxidation reactions which are difficult or impossible to carry out using classical synthetic chemistry methods. For example, cytochrome P450s, which are responsible for monooxygenation reactions in biological systems, can be utilised for the hydroxylation and epoxidation of fatty acids (or related compounds) and alkenes in synthetic chemistry.[3] Similarly, it was recently shown that haem peroxidases could, in principal, provide an alternative to hydrolytic enzymes since they are 'universal redox enzymes' and found abundantly in nature.[4,5] Theoretical and applied research in the field of peroxidase structure and mechanism is connected with the prospect of using peroxidase enzymes in an industrial or biotechnological context, for example in biochemical and immunochemical assays, biosensors, transformation of drugs, production of chemicals, degradation of aromatic compounds and environmental control.[2]

1.2 HAEM PROTEINS

Haem proteins are widespread in all groups of living organism and have an extraordinary number of different biological functions, including oxygen and electron transport, charge separation in photosynthesis and catalysis in the synthesis and breakdown of chemicals in the cell. The area has been reviewed fairly extensively.[4,6-14]

The common structural feature of all haem proteins is the prosthetic group. A large number of haem proteins contain *ferriprotoporphrin IX* as a prosthetic group (Figure 1.1).[15] As such, the different functions that arise within the haem proteins must derive from differences in the manner in which the haem interacts with amino acids residues and small molecules (*e.g.* substrate) in the active site. Further modifications to function can be imposed on the molecule by modification of the haem prosthetic group itself, for example by modification of the substitutents on the haem or by introduction of covalent links between the haem and the protein (*e.g.* in cytochrome *c*). These modifications have been discussed in the literature.[16] The diversity in the structure of various haems is beyond the scope of this thesis and will not be discussed in detail here.

In *ferriprotoporphyrin IX*, the coordination number of iron (III) is usually five or six, with the sixth ligand being provided by either a protein amino acid ligand or any exogenous ligand (such as water, cyanide, CO or azide). Different ligands impose different spin state requirements on the metal itself: strong field ligands lead to a low-spin haem whereas weak field ligands lead to high-spin haem. By variation of the spin-state and coordination number of the haem structure, the function and behaviour of various haem proteins may vary drastically, providing a convenient means for utilisation of the same prosthetic group in a number of biological contexts. In peroxidases, for example, the haem, which is generally high-spin, is attached to the apoprotein by a dative bond between a proximal histidine amino acid and the metal site. The resting state of cytochrome P450 also contains iron (III) protoporphrin IX, but the ligand on the proximal side is a thiolate (provided by a cysteine residue).

1.2.1 Haem Peroxidases

Peroxidases are haem-containing enzymes that are remarkable in their ability to catalyse a very wide range of oxidations of organic and inorganic substrates using hydrogen peroxide or hydroperoxides,[4,7,17,18] equation [1.1].

$$2RH + H_2O_2 \rightarrow 2R^{\cdot} + 2H_2O \qquad \qquad ...[1.1]$$

(A)

VI   *Distal site*

Fe^{III}

Proximal site
V

(B)
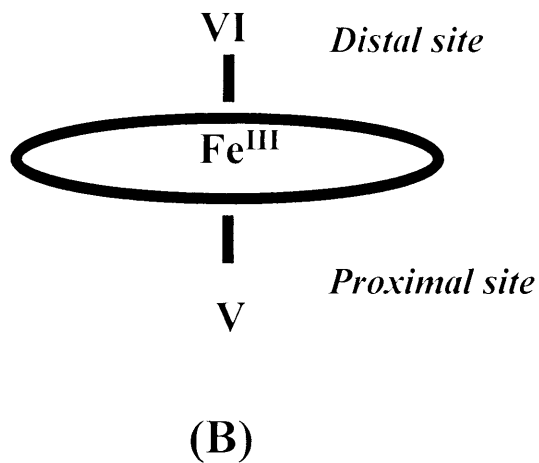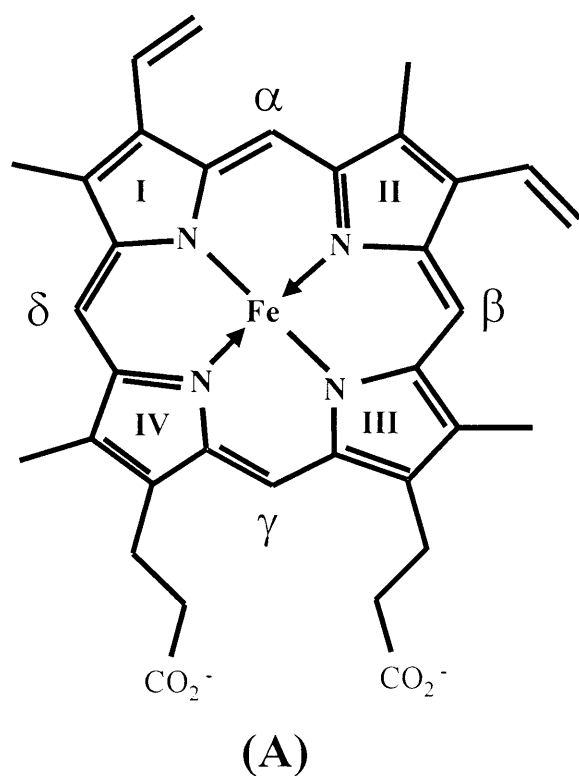
FIGURE 1.1

Ferriprotoporphyrin IX, the co-ordination positions of the iron are numbered: (**A**)

positions I-IV are occupied by the four pyrrole nitrogen atoms, (**B**) position V is

located on the *proximal side* of the haem and, position VI is located on the *distal side*

of the haem and is vacant in the native enzyme.

4

The peroxidase literature can be traced back to the early 1920s and studies on peroxidases by Willstätter and Sumner (reviewed by Dunford[4]) played an important part in the development of modern theories of biological oxidation. The biological function of haem peroxidases appears to be prevention of peroxide build-up. Indeed, the emergence of the theory of toxicity of oxygen free radicals in the late 1960s has led to an increased appreciation that one of the main functions of peroxidases is to provide a vital defence against activated oxygen species that are released in normal metabolic processes. The production of toxic superoxide free radicals appears to be universal problem in aerobic cells. The elimination of superoxide by superoxide dismutase (SOD) produces another toxic substance, hydrogen peroxide that is subsequently removed by various peroxidases or catalases. In addition to their role in detoxification, peroxidases also have a variety of other roles, such as biosynthesis and the oxidation of small aromatic molecules in the plant and fungal enzymes.[19]

1.2.1.1 Classification of Plant and Bacterial Haem Peroxidases

The fungal, plant and bacterial haem peroxidases have been classified as members of the plant peroxidase superfamily, in which there are different classes.[20]

Class I, *the intracellular peroxidases*, includes: yeast cytochrome c peroxidase (CcP), a soluble protein found in the mitochondrial electron transport chain, where it probably protects against toxic peroxides; ascorbate peroxidase (APX), the main enzyme responsible for hydrogen peroxide removal in chloroplasts and cytosol of higher plants; and bacterial peroxidases, exhibiting both peroxidase and catalase activities. It is thought that catalase-peroxidase provides protection to cells under oxidative stress.

Class II *consists of secretory fungal peroxidases* and includes ligninases, or lignin peroxidases (LiPs), and manganese dependent peroxidases (MnPs). These are monomeric glycoproteins involved in the degradation of lignin. In MnP, Mn^{2+} serves as the reducing substrate. Class II proteins contain four conserved disulphide bridges and two conserved calcium-binding sites.[4]

Class III *consists of the secretory plant peroxidases*, which have multiple tissue-specific functions: e.g., removal of hydrogen peroxide from chloroplasts and cytosol; oxidation of

toxic compound, biosynthesis of the cell wall, defence responses towards wounding, indole-3-acetic acid catabolism and ethylene biosynthesis.[19] The most intensively studied example is horseradish peroxidase isoenzyme C. Class III peroxidases are also monomeric glycoproteins, containing four conserved disulphide bridges and two calcium ions, although the placement of the disulphides differs from class II enzymes.

1.2.1.2 Catalytic Cycle of Peroxidases

The overall catalytic cycle, which is common to all haem peroxidases examined so far, is depicted in Figure 1.2. This reaction transfers the two oxidising equivalents of hydrogen peroxide or hydroperoxide to the enzyme, producing a metal-oxo derivative of the enzyme, called Compound I,[21] in which one of the oxidising equivalents resides in the iron, oxidized from the ferric to the ferryl state,[22] and the other oxidising equivalent on either the porphyrin ring (as a cation radical) or an amino acid residue (as a protein radical).[23,24] The formation of a protein radical on hydrogen peroxide or alkyl hydroperoxide reduction requires the presence of an easily oxidizable residue in close proximity to the haem, the most famous example of which is seen in cytochrome *c* peroxidase.[25-27]

The second step of the peroxidase reaction is regeneration of the resting enzyme by reduction of the oxidised Compound I intermediate. This requires the input of two electrons from a reducing-substrate, and is complicated by the wide range of possibilities including phenols, amines, heterocyclic compounds, organic acids, thiols and some inorganic ions. Reduction usually occurs in two, one–electron transfers, but in some cases, two-electron transfer has been reported.[28] One-electron reduction of Compound I produces Compound II, which contains a ferryl-oxo complex. Reduction of compound II by a single electron regenerates the resting enzyme. This step is about one to two orders of magnitude slower than reduction of Compound I and usually represents the rate-limiting step in the overall peroxidase catalytic cycle. This reduction of Compound I is normally associated with transfer of the oxo ligand from the peroxidase higher oxidation state to the substrate in monoxygenase enzymes.
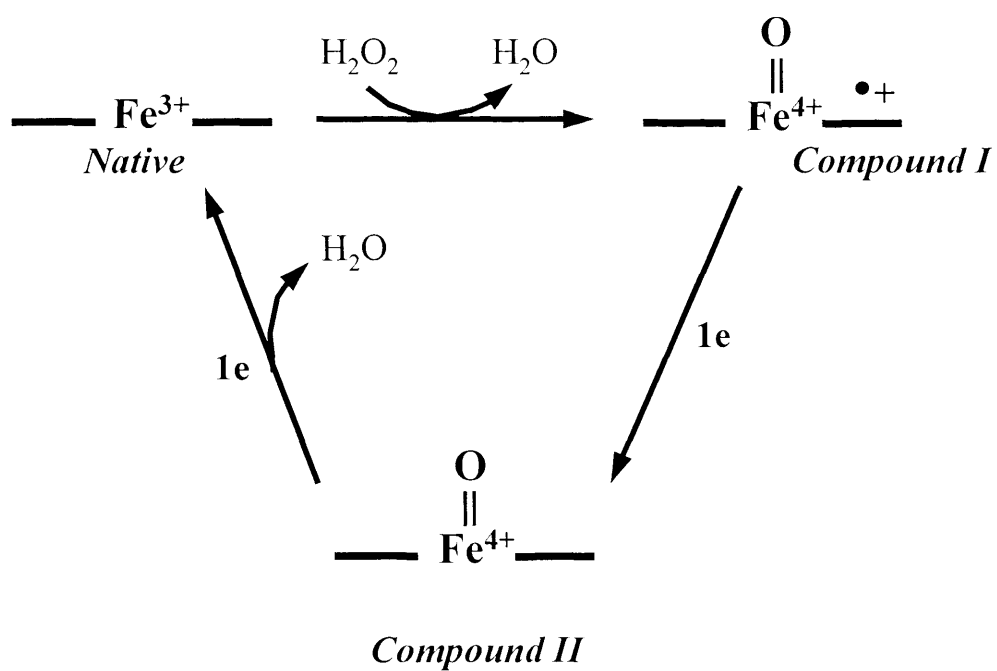
FIGURE 1.2

The general haem peroxidases catalytic cycle.

1.2.1.3 Types of Reactions Catalysed by Peroxidases

Hydrogen peroxide or hydroperoxide-dependent oxidations by peroxidases have been investigated for a long time and have provided a wealth of spectroscopic, mechanistic and structural information. In fact, the ability of the protein to react with hydrogen peroxide to generate a strong oxidant is one of the oldest known catalytic activities. Planche, who reported formation of a blue pigment in an alcoholic tincture of guaiac resin, first described this kind of activity in 1810 using various plant materials including an extract of horseradish root.[29] The use of peroxidases in various oxidation reactions has since been extended, some of which are summarised in Table 1.1.

1.2.1.4 Ascorbate Peroxidase

The discovery of ascorbate peroxidase was first reported in 1979.[30,31] Ascorbate peroxidase therefore is a relatively new member of the peroxidase family in comparison with other peroxidases, such as horseradish peroxidase (first identified in 1903[32]) and cytochrome *c* peroxidase (first identified in 1940[33]). Since the initial reports, studies on APX have expanded, most notably to include isolation and characterization from various sources,[34,35] the development of an expression system[36] and the publication of a crystal structure for the recombinant pea cytosolic enzyme.[37] The APX area has been reviewed by Dalton in 1991,[38] by Dunford in 1999[4] and, most recently, by Raven in 2000.[39]
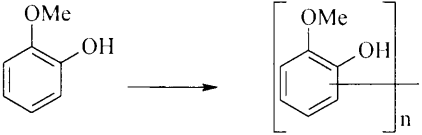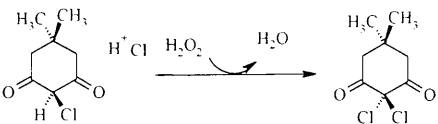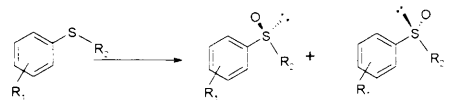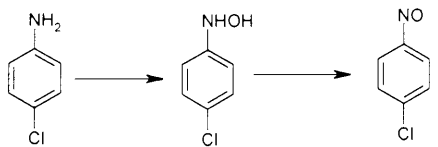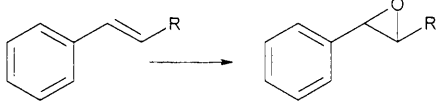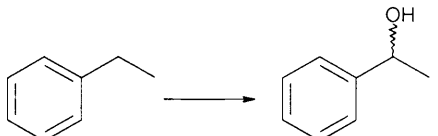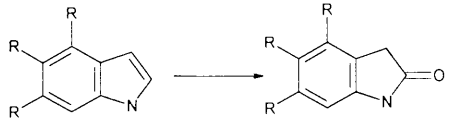
Scavenging of H_2O_2 in plants is usually accomplished by ascorbate peroxidase (APX, ascorbate; hydrogen peroxide oxidoreductase, EC 1.11.1.11). The enzyme catalyzes a reaction in which ascorbate acts as an electron donor and H_2O_2 is reduced to water, equation [1.2].

$$2 \text{ Ascorbate} + H_2O_2 \rightarrow 2 \text{ Monodehydroascorbate} + 2 H_2O \quad \text{...[1.2]}$$
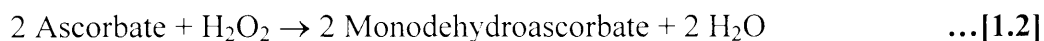
The immediate product of this reaction is the monodehydroascorbate radical, which may spontaneously disproportionate to ascorbate and dehydroascorbate (Scheme 1.1). Alternatively, monodehydroascorbate may be reduced back to ascorbate in a NAD(P)H dependent reaction catalysed by monodehydroascorbate reductase (NADH; monodehydroascorbate oxidoreductase, EC.1.6.5.4).

TABLE 1.1

Oxidation of various organic substrates catalysed by peroxidases.

Reaction type	Example	References
Oxidative dehydrogenation		40
Oxidative halogenation		Reviewed in [2]
Hydrogen peroxide disproportionation	$2H_2O_2 \rightarrow 2H_2O + O_2$	Reviewed in [2]
Oxygen-transfer reaction (*S*-oxidation)		14,41-48
Oxygen-transfer reaction (*N*-oxidation)		49
Oxygen-transfer reaction (Epoxidation)		2,50-56
CH bond oxidation (Benzylic/allylic oxidation)		57
CH bond oxidation (Alcohol oxidation)		58,59
CH bond oxidation (Indole oxidation)		2,60

9
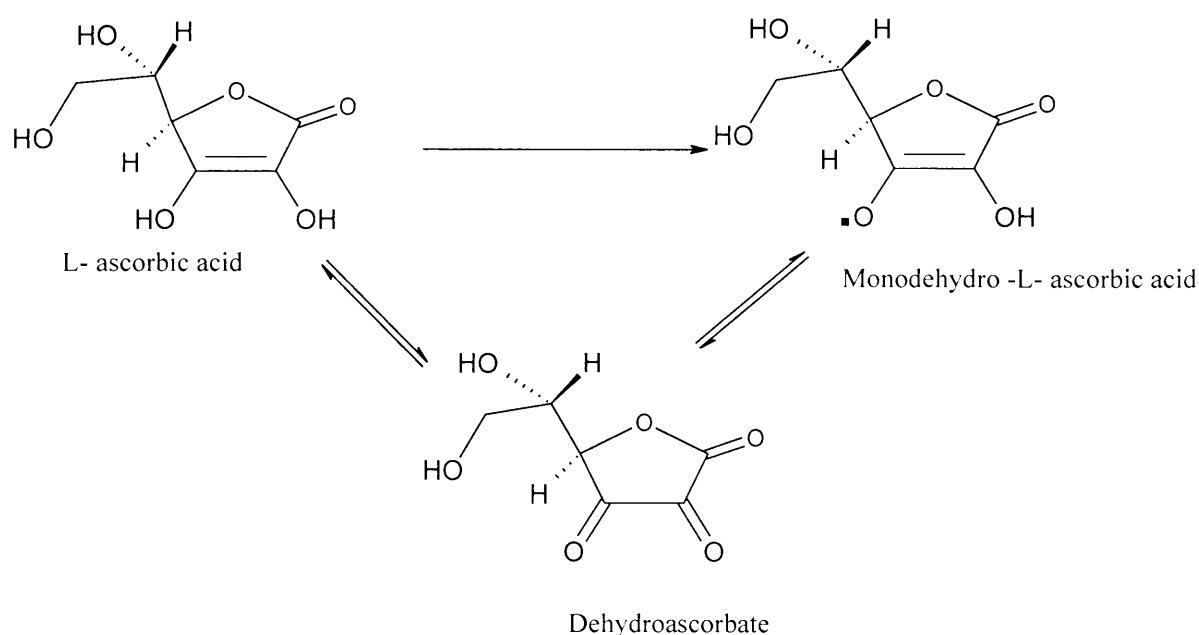
SCHEME 1.1

Conversion of ascorbate into monodehydroascorbate and dehydroascorbate[61]

Thus, APX is a key enzyme in plant defences against activated forms of oxygen. Since the identification of the physiological role of this enzyme, it has become evident that oxygen toxicity and H_2O_2 scavenging are particularly critical in two plant systems, chloroplasts and nitrogen-fixing root nodules.[61]

Ascorbate peroxidases were originally believed to exist in two different forms, one in chloroplasts, and the other in the cytosol. Four different types of ascorbate peroxidase, rather than two, have now been identified. These are: cytosolic ascorbate peroxidases,[35,62-71] chloroplastic, stromal ascorbate peroxidases,[62,72-74] chloroplastic, thylakoid-bound ascorbate peroxidases[62,72-75] and glyoxysomal ascorbate peroxidases.[62,72,76,77]

1.2.1.5 Structure of Ascorbate Peroxidase

The 3-dimentional structures of several peroxidases have been determined, including yeast cytochrome *c* peroxidase (CcP),[78] lignin peroxidase (LiP),[79-81] manganese peroxidase (MnP),[82] chloroperoxidase (ClP),[83] *Arthromyces ramosus* peroxidase (ARP),[84] peanut

10

peroxidase (PNP)[85] and horseradish peroxidases (HRP).[86] One of the milestones of the APX area was the determination of the crystal structure for the recombinant pea cytosolic enzyme (pAPX).[37] The ascorbate peroxidase structure confirmed that the pea cytosolic enzyme is a noncovalent homodimer held together by a series of ionic interactions arranged around the 2-fold noncrystallographic dimer axis. Ascorbate peroxidase shares the same architecture as other peroxidases, consisting of two antiparallel helices which form a crevice in which the haem group is inserted[37] (Figure 1.3 and 1.4). One helix, contributed by the C-terminal domain, contains the fifth (proximal) haem iron ligand (His-163 in APX). The imidazole ring of the proximal histidine lies approximately perpendicular to the porphyrin plane with N2 bonded to haem iron and N1 hydrogen bonded to the buried carboxylate group of an Asp residue (Asp-208). Many peroxidases (C*c*P, ARP, LiP, MnP) also contain an aromatic residue (Trp or Phe) parallel to and in Van der Waals contact with the imidazole ring of the proximal histidine. The other helix, on the distal side of the haem, contributes three conserved residues (Arg-38, Trp-41, and His-42) that form a ligand pocket for H_2O_2. Table 1.2 lists the haem active site residues identified in various known peroxidase structures.

11
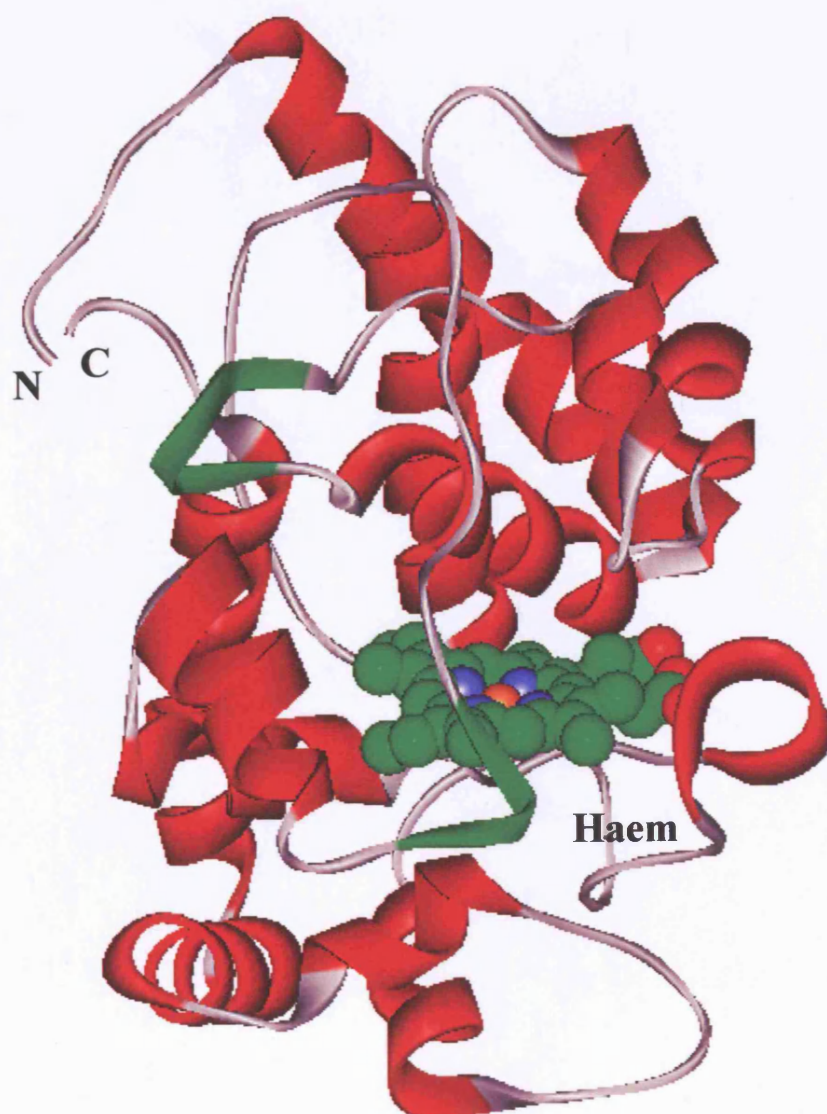
FIGURE 1.3

Ribbon drawing of ascorbate peroxidase. The crystal structure data[37] is taken from Protein Data Bank (PDB), entry 1APX and the picture is produced using WL ViewerPro. v.3.5. software.
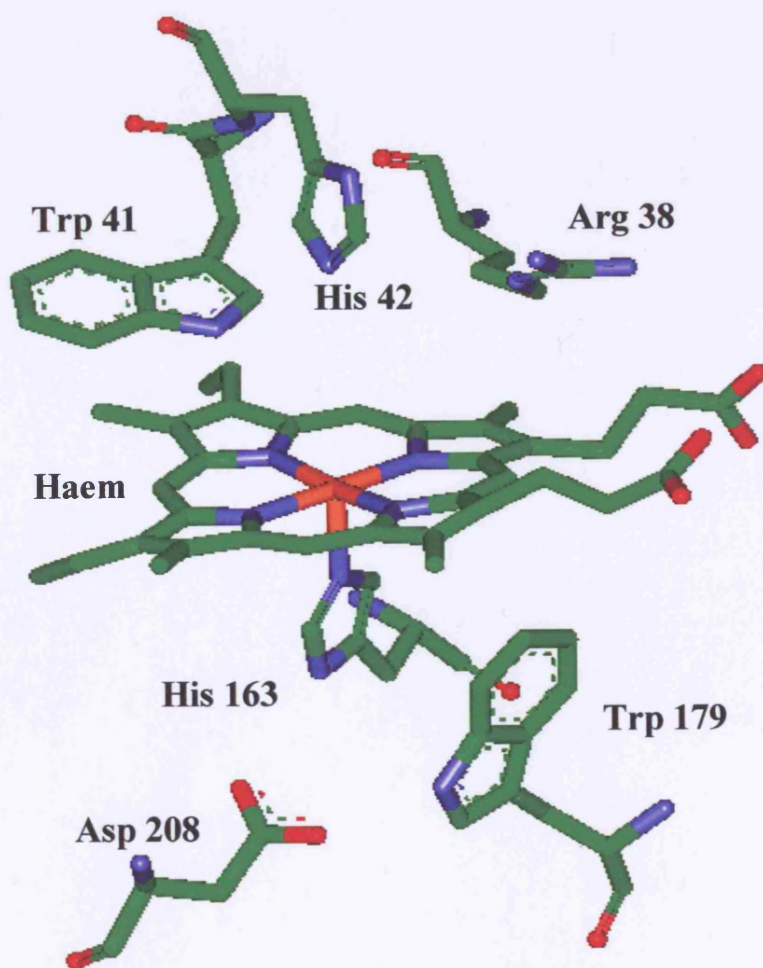
FIGURE 1.4

Active site structure of ascorbate peroxidase[37] showing key residues. The crystal structure data is taken from Protein Data Bank (PDB), entry 1APX and the picture is produced using WLViewerPro. v.3.5. software.

TABLE 1.2

Haem active site residues identified in various in known peroxidase structures.

Enzyme	Distal pocket	Proximal pocket
CcP[78]	Arg 48, Trp 51, His 52	His 175, Trp 191, Asp 235
HRP[86]	Arg 38, Phe 41, His 42	His 170, Phe 221, Asp 247
LiP[80,81]	Arg 43, Phe 46, His-47	His 176, Phe 193, Asp 238
MnP[82]	Arg 42, Phe 45, His 46	His 173, Phe 190, Asp 242
ARP[84]	Arg 52, Phe 55, His 56	His 184, Leu 201, Asp 246
APX[37]	Arg 38, Trp 41, His 42	His 163, Trp 179, Asp 208
PNP[85]	Arg 38, Phe 41, His 42	His 169, Phe 213, Asp 239

1.2.1.6 Role of Active Site Residues

It was recognised early on that the amino acid residues in and around the active site in haem peroxidases are likely to have a substantial influence on the reactivity towards hydrogen peroxide. The role of various residues in the peroxidase catalytic cycle was first proposed by Poulos and Kraut.[87] With the advent of site-directed mutagenesis techniques, the roles of individual residues in peroxidase catalysis and function has since been the subject of intense study for both CcP and HRP.[6-8,88-90] The distal histidine and arginine residues have, perhaps, been the most extensively studied: the distal histidine is believed to play several roles: the most is that it acts as a general base that aids deprotonation of the substrate peroxide and protonation of the product water after heterolytic cleavage of the hydroperoxide (Scheme 1.2). To maintain the resting state general base character of the distal histidine, a strong hydrogen bond is conserved with a distal asparagine which maintains the N^ε of the distal histidine in a deprotonated form.[37,82,85] For example, the hydrogen bond network comprises His 42, Asn 70 and Glu 64 in HRP. Mutation of Asn induces reorientation of the distal histidine, loss of the His42-Asn70 hydrogen bond, and decreases the rate of compound I formation.[145]
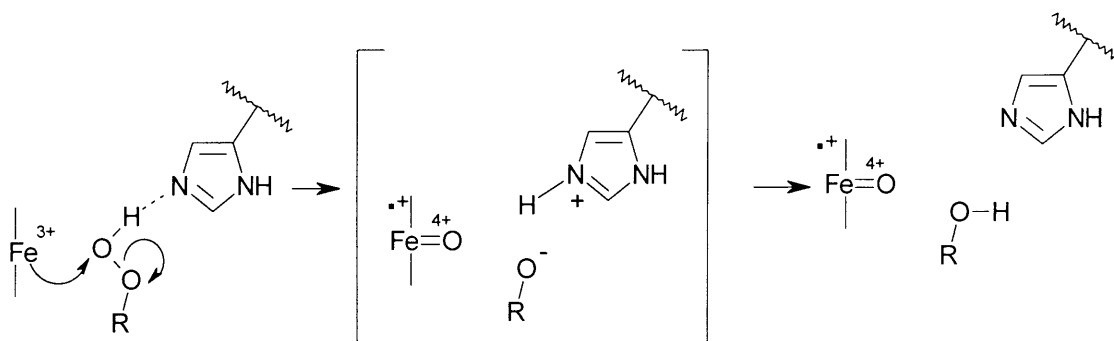
SCHEME 1.2

Proposed role of distal residues of peroxidases in facilitating heterolysis of O-O bond.

(Modified from[87])

The distal arginine group has been hypothesized to help Compound I formation by stabilizing the developing negative charge on the leaving group oxygen during heterolytic cleavage.[87] Other residues close to the haem (*e.g.* Trp-191 in CcP, and the proximal histidine and aspartic acid residues) have also been targeted and their effects on the

spectroscopic, function and mechanistic properties examined in detail. Discussion of the range of mutations examined is well beyond the scope of this review, and the reader is referred to a number of key review articles.[4,6,7,13,18,91-92]

1.2.2 Cytochrome P450 Enzymes

Cytochrome P450 enzymes (P450s) are a class of haem-containing monooxygenases so-called as a result of their absorbance band at 450 nm in the carbon monoxide (CO) form. These enzymes are present in mammals, plants, yeast, insects and bacteria. In all of these different organisms, the strong oxidising properties of the cytochrome P450 have been exploited for many purposes: P450s are involved in a number of vital processes including drug metabolism, biosynthesis of steroids or lipids, and degradation of *xenobiotics*.[3] The diversity of P450-catalysed reactions *in vivo*, as well as *in vitro*, has been expanding into the fields of biochemistry, pharmacology, toxicology and nutrition, amongst others.

There are two main categories of P450s: those involved in steroid biosynthesis and those involved in *xenobiotics* metabolism, namely "Phase I" and "Phase II" metabolism. In "Phase I" metabolism, various isoforms of P450s are able to catalyse the functionalisation of steroids, fatty acids, prostaglandins, leucotrienes, biogenic amines and pheromones.[93] Here, a functional group, *e.g.* –OH, is introduced into a substrate, ready for the next step of metabolism, "Phase II", which involves the addition of chemical compounds or groups (e.g. glucuronic acid, sulphate, glucose), and which usually makes the compounds less toxic to body tissues and easy to excrete.

The specificity of cytochrome P450 enzymes changes dramatically from one member of the family to another. Hence, microsomal P450 enzymes show broad overlapping substrate specificity, whilst mitochondrial and bacterial P450 enzymes are more specific for the reaction they catalyse in terms of substrate and stereochemistry of the reaction.

Members of the P450 enzymes are able to catalyse more than twenty different reactions: examples include dehydrogenation, hydroxylation, epoxidation and many more.[94] These reactions are discussed in more detail in Chapter 4.

1.2.2.1 Historical Background of Cytochrome P450 Enzymes

In 1958, Garfinkel[95] and Klingenberg[96] independently described the presence of a CO-binding pigment in liver microsomes of pigs and rats. This pigment, reducible by either NADPH or dithionite, exhibited an unusual absorption band maximum of the reduced CO-bound complex at 450 nm. However, the haemoprotein nature of the CO-binding pigment was not established until 1964, by Omura and Sato[97] The identification of this pigment as one of the cytochrome types (containing protohaem IX, Figure 1.1) with unusual absorption maximum at 450 nm led the authors to name it as cytochrome P450, despite the absence of any knowledge about its function. The ability of reduced P450 to induce absorption at 450 nm upon CO binding is still used for estimating the P450 content.

In 1963-1965, Estabrook and co-workers[98] and Cooper and co-workers[99] demonstrated that P450 is the key enzyme responsible for the biotransformation of many drugs and steroids; a particularly important discovery was to show a catalytic role for the pigment in the C-21 hydroxylation of 17-hydroxyprogesterone by adrenal cortex microsomes.

In 1968, a major breakthrough was achieved by Katagiri[100] and Coon,[101] showing that these monooxygenase systems are composed of different proteins. This discovery started a series of studies leading to the purification and characterisation of the components of the cytochrome P450 system and to their reconstitution in an *in vitro* system.

In 1982, the primary sequences of two isoforms were solved.[102,103] However, it was not until 1985 that the first three-dimensional structure, of the soluble, bacterial camphor-hydroxylating P450$_{cam}$, was reported by Poulos and co-workers.[104] During the 1980s, heterologous expression of cytochrome P450 in *Escherichia coli*, yeast, and cell cultures became available, including a major advance in studies on the mechanism of P450 action and the regulation of the gene expression of this enzymes. Furthermore, over 450 different P450 enzymes are now known to exist. They have been found in virtually every mammalian tissue and organ as well as plants and insects. A system of nomenclature has been developed to relate each P450 sequence based on their structural homology.[105]

1.2.2.2 Cytochrome P450 Electron Transport Systems

The activation of molecular oxygen by cytochrome P450 enzymes occurs by the insertion of one atom of oxygen into a substrate with the concomitant reduction of the second oxygen atom to water. As such, these enzymes are termed haem monooxygenases. In catalysing the monooxygenation reaction, P450 is able to utilise either NADH or NADPH as the electron donor, equation [1.3], Where, RH represents a substrate and ROH represents the corresponding product

$$RH + O_2 + NAD(P)H + H^+ \rightarrow ROH + H_2O + NAD(P)^+ \qquad ...[1.3]$$
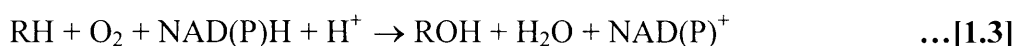
Since the haem moiety of the P450 domain cannot be directly reduced by NADPH, the two electrons derived from NAD(P)H for oxygen activation must be transferred to the haem via an electron transport protein(s). There are two types of auxiliary protein systems, termed Class I and Class II. The Class I system is employed in the mitochondrial and most bacterial P450 systems. In this system, which consists of a flavin adenine dinucleotide (FAD)-containing reductase and a small iron-sulphur protein (ferredoxin), electrons flow from NADPH to a FAD-containing protein to an iron-sulphur protein and finally to P450, where oxygen activation occurs by converting the substrate (S) to product (SO), Figure 1.5 (A).

In bacterial P450s, all components are soluble, whereas in the mitochondrial systems the electron transfer proteins are soluble in the matrix while the P450 domain is membrane bound. The Class II system is present in the endoplasmic reticulum of eukaryotic organisms and is the largest of the two classes. In contrast to Class I, this system utilizes a single flavoprotein, NADPH-cytochrome P450 reductase (containing both flavin adenine dinucleotide, and flavin mononucleotide (FMN), to transport electrons from NADPH to P450, where oxygen activation occurs (Figure 1.5 (B)).

Finally, a very unusual bacterial P450 from *Bacillus megaterium*, P450 BM3 has been studied that utilises the microsomal type electron transport system (Figure 1.5 (C)). P450 BM3 is "self-sufficient" (requires no auxiliary proteins for electron transfer) in that it has both the electron carrier component and the monooxygenase haem moiety present in one large single subunit protein. P450 BM3 enzyme is discussed in detail in the latter section of this chapter.

NAD(P)H

Substrate (S)

Ferrodoxin Reductase Fe-S P450

O_2

H_2O

NAD(P)$^+$

Product(s) (SO)

(A)

NADPH

Substrate (S)

NADPH Reductase P450

O_2

H_2O

NADP$^+$

Product(s) (SO)

(B)

NADPH

Substrate (S)

Reductase P450

O_2

H_2O

NADP$^+$

Product(s) (SO)

(C)

FIGURE 1.5

Cytochrome P450s **(A)** Class I, **(B)** Class II and **(C)** P450 BM3 electron transfer protein system
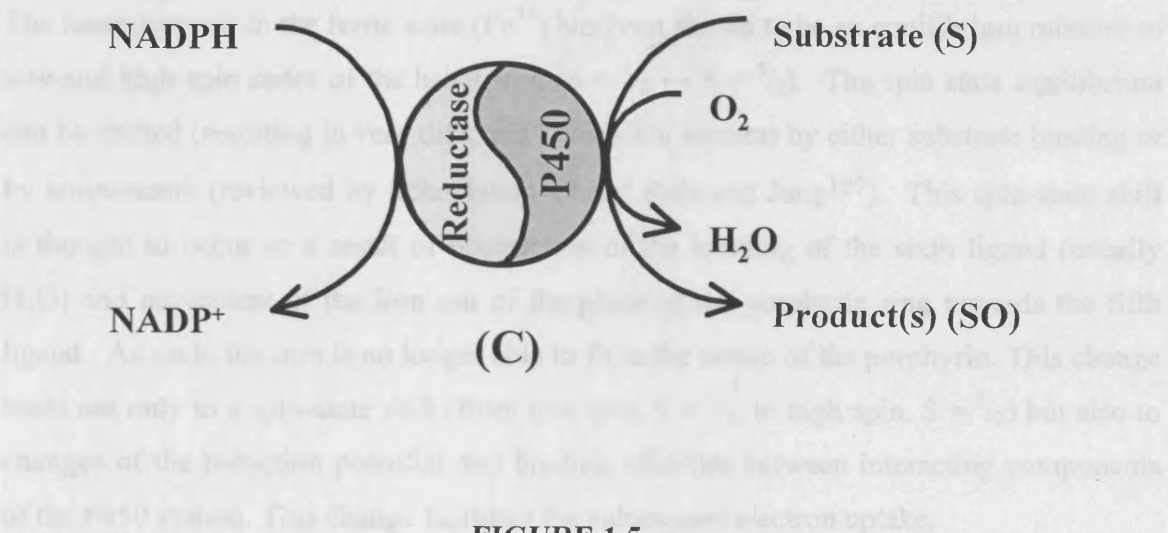
1.2.2.3 The Catalytic Pathway of Cytochrome P450 Enzymes

The principal catalytic cycle of cytochrome P450 has been much discussed and often reviewed,[3,94] but essential features have been agreed upon now for some time. The essential steps involve (Figure 1.6): **(1)** binding of the substrate, **(2)** reduction of ferric, resting cytochrome P450 to the ferrous state, **(3)** binding of molecular oxygen to give a ferrous cytochrome P450-dioxygen complex, **(4)** transfer of the second electron to this complex to give a peroxyiron (III) complex, **(5)** protonation and cleavage of the O-O bond with concurrent incorporation of the distal oxygen atom into a molecule of water and **(6)**, the formation of a reactive iron-oxo species, **(7)** oxygen atom transfer from this iron-oxo complex to the bound substrate and **(8)**, the dissociation of the product. The individual steps of the catalytic cycle are discussed in detail in the following sections.

(1) Substrate binding

The first step of in the reaction cycle is the formation of the enzyme substrate complex.

$$Fe^{3+} + Substrate\ (RH) \longrightarrow Fe^{3+}\ (RH)$$
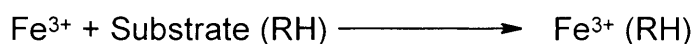
The haemoprotein in the ferric state (Fe^{3+}) has been shown to be an equilibrium mixture of low-and high-spin states of the haem iron ($S = {}^1/_2 \leftrightarrow S = {}^5/_2$). The spin state equilibrium can be shifted (resulting in very different Uv-visible spectra) by either substrate binding or by temperature (reviewed by Schenkman[106] and Rein and Jung[107]). This spin-state shift is thought to occur as a result of obstruction of the bonding of the sixth ligand (usually H_2O) and movement of the iron out of the plane of the porphyrin ring towards the fifth ligand. As such, the iron is no longer able to fit in the centre of the porphyrin. This change leads not only to a spin-state shift (from low spin, $S = {}^1/_2$, to high spin, $S = {}^5/_2$) but also to changes of the reduction potential and binding affinities between interacting components of the P450 system. This change facilities the subsequent electron uptake.

(2) First electron transfer to the enzyme –substrate complex

The second step of the reaction cycle is the introduction of the first electron.

$$Fe^{3+} (RH) \xrightarrow{\quad + e \quad} Fe^{2+} (RH)$$

P450 enzymes accept an electron from NAD(P)H via an electron carrier protein route. The rate of electron transfer is generally regulated by the intermolecular transfer steps within the ... structures of the protein...

(3) Oxygen binding to the enzyme-substrate ...

In the third step of the reaction cycle the one-electron reduced...

ROH Fe^{3+} **RH**   •NADPH-reductase •[2Fe-2S]-protein

(ROH) Fe^{3+} **Shunt**   (RH) Fe^{3+} e

(R.) $(Fe\text{-}OH)^{3+}$ XOH   XOOH   (RH) Fe^{2+} O_2

$2e, 2H^+$ (RH) $(Fe\text{-}O)^{3+}$ (RH) $Fe^{2+}(O_2)$

(peroxy complex)   (oxy complex)   (RH) $Fe^{3+}(O_2 \cdot ^-)$

H_2O H_2O (RH) $Fe^{3+}(O_2^{2-})$ e

$2H^+$ $2H^+$

H_2O_2 •NADPH-reductase •[2Fe-2S]-protein •Cytochrome b$_5$

FIGURE 1.6

The catalytic cycle of a cytochrome P450 enzyme

Molecular oxygen binds with the reduced ... and iron atom ... of the cysteine residue, to form a ternary ... enzyme complex, ... distinct and characterised by clearly identifiable transitions in the UV-visible region. From this complex, a superoxide anion radical can be released, depending on the efficiency of electron transfer in the next step. The negatively charged dioxygen ligand favours binding of a proton[11] or at least hydrogen bonding.

(4) Introduction of the second electron

The acceptance of a second electron is usually via the reductase protein - in some cases the second electron is provided by another microsomal heme protein - cytochrome b$_5$.[12] This yields a ferric peroxide adduct, which can be protonated to give a hydroperoxide complex (not shown in the P450 cycle, Figure 1.6).

(2) First electron transfer to the enzyme –substrate complex

The second step of the reaction cycle is the introduction of the first electron.

$$Fe^{3+} (RH) \xrightarrow{\quad + \ e^- \quad} Fe^{2+} (RH)$$
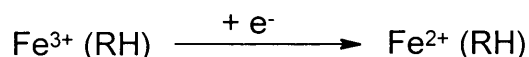
P450 enzymes accept an electron from NAD(P)H via an electron carrier protein route. The rate of electron transfer is generally regulated by the intermolecular transfer steps within the amino acid structures of the protein.

(3) Oxygen binding to the enzyme –substrate complex

In the third step of the reaction cycle the one-electron reduced haem binds oxygen.

$$Fe^{2+} (RH) \ + \ O_2 \longrightarrow \ \overset{O-O\bullet}{\underset{Fe^{3+} (RH)}{|}}$$
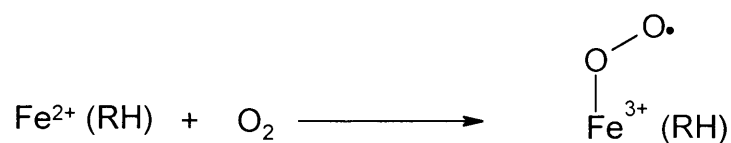
Molecular oxygen binds with co-ordination to the iron atom *trans* to the sulphur atom of the cysteine residue, to form a ternary ferrous-oxy complex, which is spectroscopically distinct and characterised by clearly identifiable transitions in the UV-visible region.[108-110] From this complex, a superoxide anion radical can be released, depending on the efficiency of electron transfer in the next step. The negatively charged dioxygen ligand favours binding of a proton[111] or at least hydrogen bonding.

(4) Introduction of the second electron

The acceptance of a second electron is usually via the reductase protein - in some cases the second electron is provided by another microsomal haem protein - cytochrome b_5.[112] This yields a ferric peroxide adduct, which can be protonated to give a hydroperoxide complex (not shown in the P450 cycle, Figure 1.6).

$$\underset{\underset{\displaystyle \text{Fe}^{3+}\ \text{(RH)}}{|}}{\text{O}}\diagup{}^{\displaystyle \text{O}\bullet} \quad \xrightarrow{+\ e} \quad \underset{\underset{\displaystyle \text{Fe}^{3+}\ \text{(RH)}}{|}}{\text{O}}\diagup{}^{\displaystyle \text{O}^{-}} \quad \xrightarrow{+\ H^{+}} \quad \underset{\underset{\displaystyle \text{Fe}^{3+}\ \text{(RH)}}{|}}{\text{O}}\diagup{}^{\displaystyle \text{OH}}$$
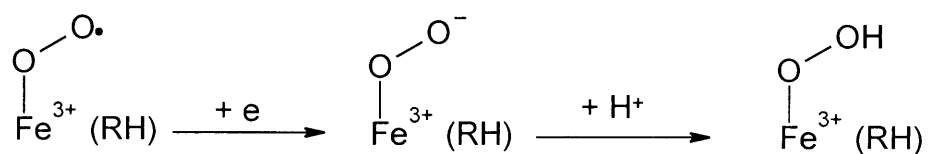
This step has been found to be the rate-limiting step for the overall reaction in P450 enzymes.[113] It is thought that if the second electron is not delivered efficiently, the oxygen complex can dissociate to give ferric P450 and a superoxide radical.[114]

(5) Cleavage of the dioxygen bond

A second protonation leads to heterolytic O-O bond cleavage (since the insertion of the second electron into the dioxygen complex in step 4 induces destabilisation of the dioxygen π-bond[111]) releasing water and generating the proposed oxo-ferryl intermediate ((RH) (Fe-O)$^{3+}$), which is equivalent to the high-valent iron oxo intermediate of the peroxidase enzymes, called compound I, as previously discussed in section 1.2.3. This intermediate has only very recently been detected.[115,116]

$$\underset{\underset{\displaystyle \text{Fe}^{3+}\ \text{(RH)}}{|}}{\text{O}}\diagup{}^{\displaystyle \text{OH}} \quad \xrightarrow{+\ H^{+}} \quad \underset{\underset{\displaystyle \text{Fe}^{5+}\ \text{(RH)}}{||}}{\text{O}} \quad +\quad H_2O$$
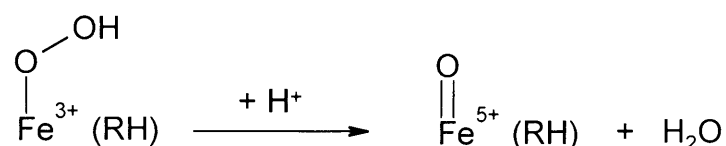
(6 & 7) Substrate radical formation and oxygen insertion

In these steps, hydrogen atom abstraction (step 6) is probably followed immediately by the recombination of two radicals to produce stable products (step 7). Although the actual process of oxygen insertion mechanism remains elusive, an "oxygen rebound" mechanism has been used to explain this step (Scheme 1.3).

$$R\text{—}\overset{\frown}{C}\text{—H} \quad \longrightarrow \quad R\bullet$$

$$\overset{\frown}{C}\text{—O} \quad \longrightarrow \quad \overset{\frown}{C}\text{—OH} \quad \longrightarrow \quad Fe^{3+} + ROH$$

$$Fe^{5+} \qquad Fe^{4+}$$
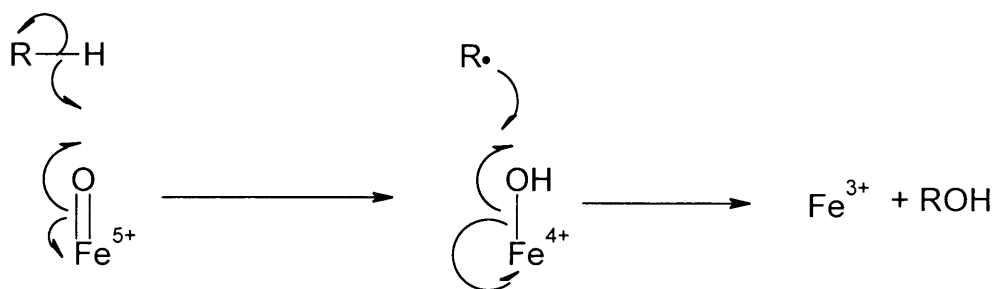
SCHEME 1.3

Oxygen rebound mechanism

(8) Dissociation of the product

$$(ROH)\ Fe^{3+} \quad \longrightarrow \quad Fe^{3+} + ROH$$
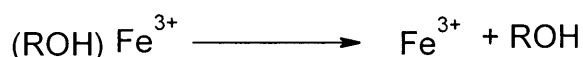
Finally, product dissociation completes the cycle. On release of the product, the P450 enzyme resumes its ferric, low spin hexa-coordinate state, to start the catalytic cycle again.

(9) Short circuit or peroxide shunt

In the so called "short circuit" or "peroxide shunt", the substrate can be hydroxylated immediately by peroxides such as hydrogen peroxide, cumene hydroperoxide, and *tert*-butyl hydroperoxide without the need for interaction with the electron donating system by virtue of formation of the 'Compound I' intermediate directly from ferric haem and peroxide. Some P450 enzymes are able to turn over using H_2O_2 as the source of oxygen atom,[3] presumably via the short circuit route. In this sense, the peroxide shunt mechanism closely resembles that known to be utilised by haem peroxidase enzymes (section 1.2.3).

1.2.2.4 Cytochrome P450 from Bacillus megaterium (P450 BM3)

Due to the difficulties associated with the isolation of class II P450 enzymes, which are largely membrane-bound, early research concentrated on soluble P450 enzymes from

bacterial sources. In particular, a P450 from *Pseudomonas putida* (P450$_{cam}$) is well characterised both structurally (the crystal structure of P450$_{cam}$ was solved by Poulos' group in 1985 at 1.6 Å resolution[104]) and mechanistically.[117] P450$_{cam}$ is a member of the Class I type system and catalyses the regio- and stereospecific hydroxylation of camphor at the 5-exo position (Scheme 1.4).
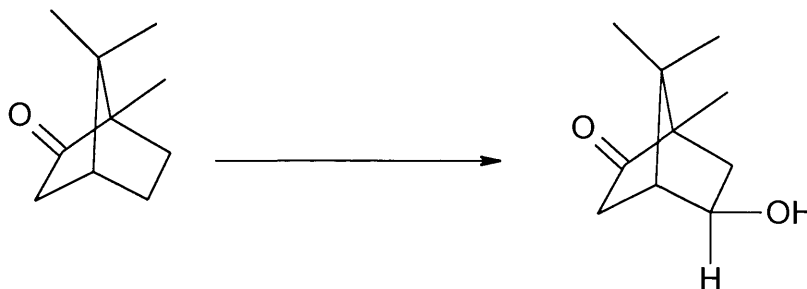
SCHEME 1.4

Although a significant volume of information has been gathered from studies on P450$_{cam}$, the limited sequence homology and the difference in electron transfer pathways between P450$_{cam}$ and majority of P450 enzymes has raised questions concerning the validity of any generalisations concerning mammalian P450 enzymes made on the basis of P450$_{cam}$ studies. As a result, efforts have concentrated on the identification of a P450 enzyme which is soluble and more closely related to Class II P450 enzymes. P450 BM3 from *Bacillus megaterium* is an attractive candidate as it is a unique P450 regarded as being in a class of its own. P450 BM3 is similar to Class II P450 enzymes, as it contains a FAD/FMN reductase domain, but is unusual in the sense that the two domains are linked by a small amino acid chain. The anchoring of the two domains seems to be analogous to the restriction imposed by the membrane binding domains of the mammalian P450 enzymes. In addition, P450 BM3 has high sequence homology with mammalian P450 enzymes. For these reasons, P450 BM3 is a better model than P450$_{cam}$ for P450s generally and the mammalian systems in particular.

During the mid 1970's, Fulco and co-workers discovered a fatty acid hydroxylase in a soluble enzyme preparation from *Bacillus megaterium* ATCC 14581.[118] The enzyme was later identified as a cytochrome P450 enzyme, and named as P450 BM3. In the presence of oxygen and NADPH the enzyme catalyses the hydroxylation of fatty acids (and will also catalyse the hydroxylation of fatty alcohols and fatty amides) at the positions of ω-1,

ω-2 and ω-3 on long chain fatty acids(Scheme 1.5).[118,119] The terminal methyl group in the substrate has never been observed to be hydroxylated during this reaction.
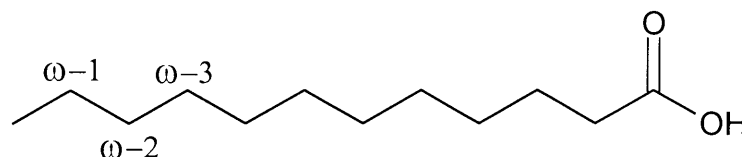
SCHEME 1.5

The isolation purification and subsequent characterisation of P450 BM3 was initially hampered by its low concentration in the cell and by virtue of it not being inducible by its own substrate. Addition of phenobarbital (Scheme 1.6) to the growth media, however, induced formation of P450 BM3 several-fold.[120] Although phenobarbitol itself is not a substrate in the P450 BM3 system, it is a well-recognised specific P450 inducer in the liver of higher animals and bacterial monooxygenases.[121]
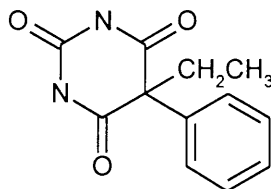
SCHEME 1.6

The discovery of P450 BM3, discussed earlier, uncovered a range of substrates for this P450 system that were not previously appreciated. Fatty acids, fatty amides and fatty alcohols are all hydroxylated by P450 BM3 at the corresponding ω-1, ω-2 and ω-3 monohydroxy metabolites. Other saturated derivatives, fatty acid methyl esters and long chain hydrocarbons, are not substrates for P450 BM3.

1.2.2.5 The Domain Architecture of Cytochrome P450 BM3

Cytochromes P450 utilize redox partners to deliver electrons from NADPH/NADH to the P450 haem center. Microsomal P450s utilize an FAD/FMN reductase. The bacterial fatty acid hydroxylase, P450 BM3, is similar except that the P450 haem and FAD/FMN

proteins are linked together in a single polypeptide chain arranged as haem-FMN-FAD as discussed in Section 1.2.2.2. Therefore the domain architecture of cytochrome P450 BM3 can be divided into three groups, namely the reductase domain structure, the linker region structure and the haem domain structure.

First, in 1987, Narhi and Fulco[122] utilized limited trypsin proteolysis in the presence of substrate to cleave P450 BM3 into two polypeptides (domains) of about 66,000 and 55,000 daltons. The 66-kDa domain contains both FAD and flavin mononucleotide FMN, but no haem, reduces cytochrome c in the presence of NADPH, and is derived from the C-terminal portion of P450 BM3. This flavoprotein domain of P450 BM3 (BMR) is soluble and contains an equimolar ratio of FAD and FMN and is functionally analogous to microsomal nicotinamide adenine dinucleotide phosphate (NADPH)-P450 reductases.

Limited trypsinolysis of BMR removed the NH_2-terminal with 122 residues. This region has been postulated to contain amino acids residues that are important for FMN binding.[123]

The domain (BMR) was sub-cloned and expressed in *E. coli* by Oster and co-workers[124] to investigate the properties further. Several studies on the domain properties and functions have also been published.[125-128]

The linker region connecting the C-terminal end of the haem domain and the N-terminal end of the reductase domain of P450 BM3 (BMR) was investigated by Munro and co-workers.[129] The amino acid sequence of the linker region is rich in charged residues, including lysine, arginine and glutamic acid. The amino acid sequence as a whole does not resemble any other well-characterized linker region, but it does contain a number of amino acids considered favourable as constituents of inter-domain linkers. Spectroscopic studies have indicated that the linkage of the domains in intact P450 BM-3 alters the haem and aromatic amino acid environments which presumably provides the correct structural arrangement for efficient electron transfer between the redox centres. Deleting three or six residues or changing an Arg-Lys-Lys stretch in the middle of the linker to Ala-Ala-Ala does not alter the functional properties of the individual domains of P450 BM3. However, the six amino acid deletion variant exhibits nearly undetectable levels of fatty acid hydroxylase activity, the three amino acid deletion mutant about 10% activity, and the three alanine substitution mutant about 50% activity, indicating that the linker region has a

very important role in the activity of the intact enzyme. The variants also have slower electron transfer rates, which correlate to the lower monooxygenase activity. It seems that the length of the linker and, to a lesser extent, the sequence, are important for the correct orientation of the two domains to achieve efficient reductase-to-haem electron transfer.[130] The extension of the linker region with the insertion of three alanines has only a small effect on the enzyme activity, indicating that the longer linker extends into the solution and that the deletion of amino acids tightens the connection between domains and forces reorientation.[131]

Finally, comprehensive work from Ravichandran and co-workers[132] used data from the crystallisation and x-ray diffraction analysis to determine the crystal structure of the haem domain of P450 BM3 (Figure 1.7).

The active site is accessible through a long channel, 8 to 10 Å in diameter and about 20 Å in length, and is lined with mostly non-aromatic hydrophobic residues (Figure 1.8). The crystal structure has allowed the identification of a number of active site residues likely to interact with the substrate and/or involved in the catalytic process. These include Arg47, Tyr51, Phe87 and Phe42. The charged Arg47 residue (located at the open end of the binding pocket close to the molecular surface) is proposed to anchor the carboxylate ion of fatty acid substrates together with Tyr51. The phenylalanine residue (Phe87) forms close van der Waals interactions with the haem. The phenyl ring of this residue is located almost perpendicular to the porphyrin plane. It was proposed[133,134] that Phe87 may be important in the sequestering the terminal methyl group of fatty acid substrates, shielding the position from hydroxylation (it is known is that Phe87 undergoes dramatic movement on substrate binding and is vital in the control of the regiospecificity of substrate oxidation). Phe42, which is located at the mouth of the long hydrophobic fatty acid binding pocket of the P450, places a phenyl 'cap' over the mouth of the active site.

The structure of the haem domain of P450 BM3 provided a long-awaited atomic model for the class II P450 enzymes. The substrate-bound X-ray crystal structure (2.7 Å) of P450 BM3 haem domain was solved by Li and Poulos,[135] in the presence of a fatty acid substrate, palmitoleic acid (Figure 1.9). A comparison of the substrate-bound and substrate-free forms reveals major conformational differences and provides detailed picture of substrate-induced conformational changes in a P450.
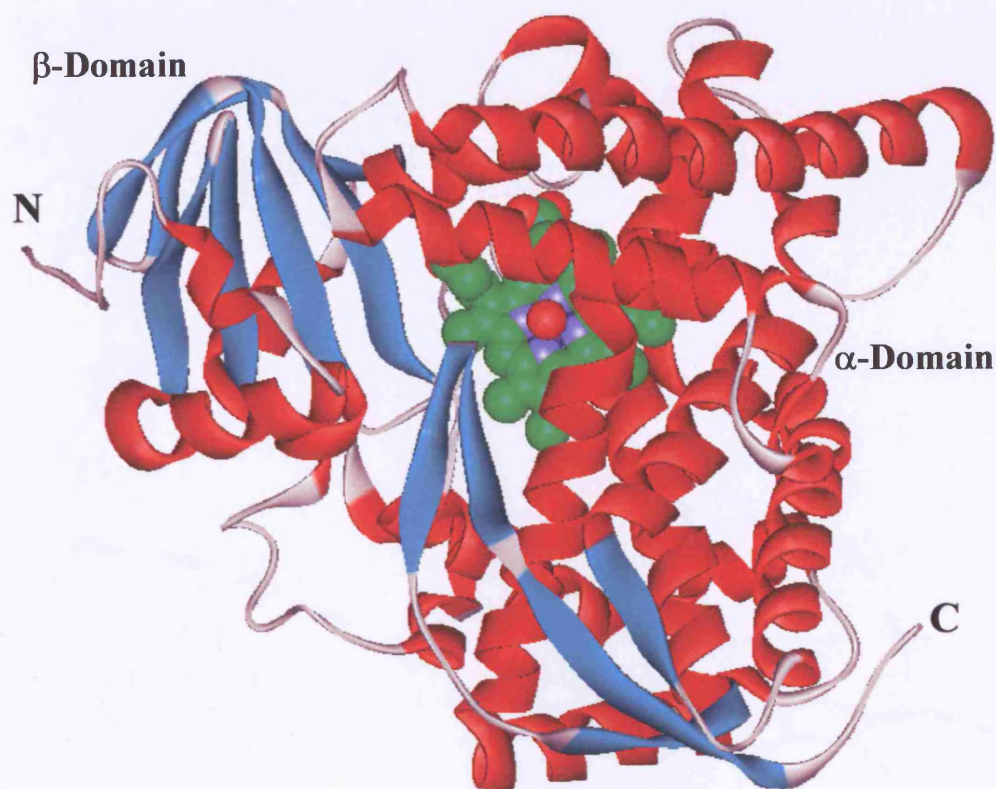
FIGURE 1.7

Crystal structure of the haem domain of cytochrome P450 BM3. The structure used was taken from Protein Data Bank (PDB), entry 1BU7 and and the picture is produced using WLViewerPro. v.3.5. software.
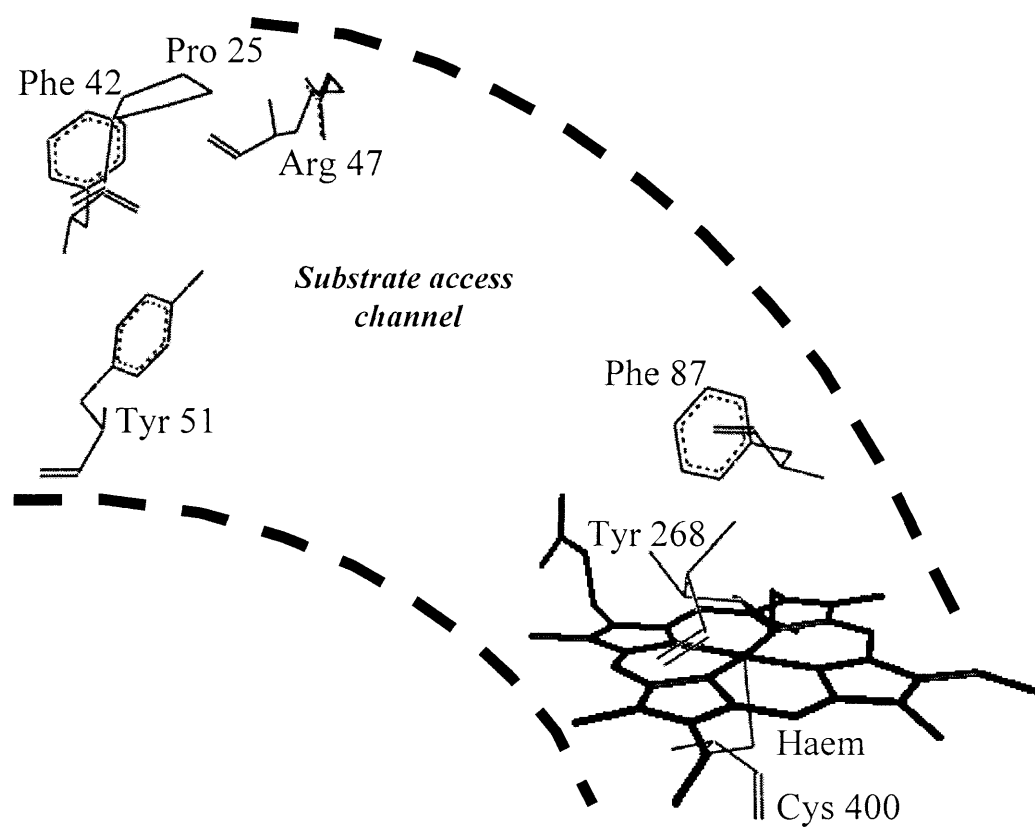
FIGURE 1.8

Schematic representation of crystal structure of substrate free P450 BM3; showing the relative position of important residues together with the substrate access channel, the roles of residues are discussed in the text.
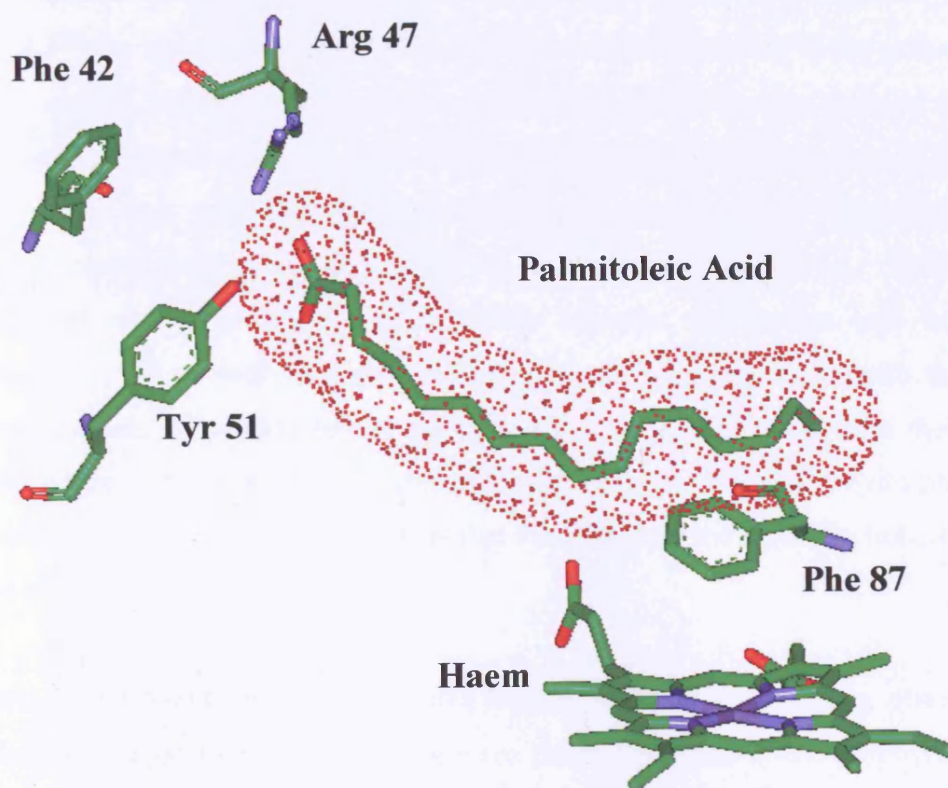
FIGURE 1.9

Representation of the relative position of residues in the active site of substrate (palmitoleic acid)-bound P450 BM3. Residues Arg 47, Tyr 51, and Phe 42 are located at the 'mouth' of the hydrophobic channel. Arg 47 and Tyr 51 offer potential interaction with the carboxyl group of the fatty acids, and Phe 42 caps the active site. Phe 87 lies above the haem ring and interacts with the ω-terminus of fatty acids substrates. The dots around palmitoleic acid indicates its van der waals surface. The structure used was taken from Protein Data Bank (PDB), entry 1FAG.

Initially, the structure has provided an opportunity to compare the "open" and "closed" conformations of a P450 enzyme. In the structure of the substrate-free P450 haem domain,[132] the phenyl side chain of Phe42 lies close to the mouth of the active site at the protein surface. However, in the substrate bound form[135] the side chain is repositioned and 'caps' the mouth of binding site, effectively protecting the substrate in its hydrophobic environment and probably also strengthening the electrostatic interaction between substrate carboxylate group and Arg47 by excluding solvent water. The study also highlighted some interesting contact points between the protein and substrate: in particular, Tyr51 as well as Arg47 is able to form hydrogen bonds with the substrate carboxylate ion. The alkyl tail of the substrate curls up and away from the iron haem moiety where it can make contact with residues Leu75 and Val78 in a hydrophobic patch. Part of the reason for a substrate curl is that Phe87 blocks the substrate from approaching closer to the haem.

In fact, the phenylalanine residue rotates from a perpendicular position, observed in the substrate-free crystal structure,[132] to a more parallel position to the porphyrin plane,[135] which more effectively blocks the ω-terminal methyl group of the substrate from approaching the haem. An unusual feature in the P450 BM3 active site is that the distance between the substrate palmitoleic acid and the iron is quite considerable compared to the situation with substrates in P450$_{cam}$. In P450$_{cam}$, the substrate carbon atom which is hydroxylated is located 4.2 Å from the iron, while the closest palmitoleic acid atom in the P450 BM3 complex is 7.5-7.9 Å from the iron. NMR studies have shown similar distances, 7.6-7.8 Å using lauric acid in P450 BM3.[136] The structure has also revealed that when the haem domain is reduced the substrate moves ~ 6 Å closer to the haem iron, positioning it correctly for hydroxylation.[137]

Mutagenesis studies have investigated the role of specific residues within the active site of P450 BM3, particularly those which have been postulated to be key to the activity of P450 BM3. For example, the R47A and R47G variants show that the electrostatic interaction between the Arg 47 guanidinium group and the fatty acid carboxyl group is involved in both initial binding and transition-state stabilization.[138] Similarly, the Y51F variant showed that the hydrogen bonding interaction between hydroxyl group of Tyr 51 and the fatty acid carboxyl group is important only for initial binding. In fact, the major purpose of the interaction between the fatty acid carboxylate group and Arg 47/Tyr51 is likely to

be in the correct positioning of the substrate to promote efficient active site dehydration and the accompanying haem iron spin state conversion that is critical for catalysis.[139] An exhaustive discussion of all variants of P450 is not possible in this Chapter, but it is noted that Phe87, Thr268, Glu267 and Pro25 have all been examined and the reader is referred to the original papers for further information.[134,138,140,141]

1.3 POLYMERIC AMINO ACIDS

Asymmetric oxidation reactions performed using synthetic or natural polypeptides are of considerable interest, since these can be considered as simplified models of enzymatic reactions.[142] The aim of this section is to expand substrate diversity of these catalysts to incorporate organic sulphides. In particular, we were interested in examining whether or not polymeric amino acid catalysts could be used for the asymmetric oxidation of alkyl aryl sulphides, as has been previously shown for the corresponding epoxidation reactions.[143,144]

The use of polymeric amino acids in oxidation reaction will be reviewed and discussed in Chapter 5.

1.4 AIMS OF THIS THESIS

The aims of this thesis are multi-fold. In a global context, one of the more wide-reaching aims is to understand in more detail the structural and functional relationships that exists between the haem protein ascorbate peroxidase and cytochrome P450 BM3, and to explore the use of these proteins in organic synthesis and their various reactivities. These reactivities will be compared and contrasted with the synthetic enzyme, poly-L-leucine.

Chapter 2 is aimed at investigation of the kinetics and mechanism of APX-catalysed oxidation of *p*-cresol and to identify the products of the reaction. The work will provide important information on the use of APX-catalysed reactions in a wider context and will provide a platform upon which more complex catalytic chemistry involving APX can be launched.

Chapter 3 is aimed at incorporation of enantioselective sulphoxidation activity into the active site of ascorbate peroxidase by site-directed mutagenesis. In particular, the effect of replacement of an active site tryptophan residue (Trp41) with an alanine (W41A) on the enantioselectivity of the reaction will be examined. Using structure-based molecular modelling techniques, the stereoselectivities of both wild type APX and the variant will be quantitatively rationalized.

In Chapter 4, the unique characteristics of P450 BM3 suggest that it may have important and exciting applications in synthetic chemistry. Therefore the aim of this chapter is to expand the substrate diversity of this enzyme to incorporate organic sulphides. The objective is to determine whether various alkyl aryl sulphides are oxidised to their corresponding sulphoxides and to determine the enantioselectivity. The results from such research will highlight the potential P450 BM3 has in synthetic chemistry. Using structure-based molecular modelling techniques, the stereoselectivities of cytochrome P450 BM3 will be quantitatively rationalized.

In Chapter 5, the diversity of substrate oxidation by various polymeric amino acids has been highlighted in terms of both reactivity, enantioselectivity and mechanism. The aim of this Chapter is to expand the substrate diversity of poly-L-leucine to incorporate organic sulphides, since there are no reports of poly-L-leucine catalysed enantioselective

sulphoxidation in the literature. Specifically, it was of interest to examine whether or not poly-L-leucine can be used for the asymmetric oxidation of alkyl aryl sulphides. In a wider context, comparison is made between natural and unnatural enzymes.

1.5 REFERENCES

1   Turner, N. J., *Curr. Org. Chem.*, 1997, **1**, 21.

2   van Deurzen, M. P. J., van Rantwijk, F. and Sheldon, R. A., *Tetrahedron*, 1997, **53**, 13183.

3   Ortiz de Montellano, P. R., *Cytochrome P450*, Plenum Press, New York 1995.

4   Dunford, H. B., *Heme Peroxidases*, John Wiley, New York 1999.

5   Dunford, H. B., *Adv. Inorg. Biochem.*, 1982, **4**, 41.

6   Dawson, J. H., *Science*, 1988, 433.

7   English, A. M. and Tsaprailis, G., *Adv. Inorg. Chem.*, 1995, **43**, 79.

8   Filizola, M. and Loew, G. H., *J. Am. Chem. Soc.*, 2000, **122**, 3599.

9   Frew, J. E. and Jones, P., in *Adv. Inorg. Bioinorg. Mech.*, *Vol. 3*, Sykes, A. G. (Ed.): Academic Press, London 1984, p. 175.

10   Li, H. and Poulos, T. L., *Curr. Opin. Chem. Biol.*, 1994, **2**, 461.

11   Ortiz de Montellano, P. R., *Annu. Rev.Pharmacol. Toxicol.*, 1992, **32**, 89.

12   Poulos, T. L., *Curr. Opin. Biotech*, 1993, **4**, 484.

13   Smith, A. T. and Veitch, N. C., *Curr. Opin. Chem. Biol.*, 1998, **2**, 269.

14   Baciocchi, E., Lanzalunga, O. and Malandrucca, S., *J. Am. Chem. Soc.*, 1996, **118**, 8973.

15   Keilin, D. and Mann, T., *Proc. Roy. Soc. (London)*, 1937, **112B**, 119.

16   Timkovich, R. and Bondoc, L. L., *Adv. Biophys. Chem.*, 1990, **1**, 203.

17   Dunford, H. B., in *Peroxidases in Chemistry and Biology*, *Vol. 2*, Everse, J., Everse, K. E. and Grisham, M. B. (Eds.): CRC Press, Boca Raton 1991, p. 1.

18   Erman, J. E. and Vitello, L. B., *J. Biochem. Mol. Biol.*, 1998, **31**, 307.

19   Campa, A., in *Peroxidases in Chemistry and Biology*, *Vol. II*, Everse, J., Everse, K. E.and Grisham, M. B. (Eds.): CRC Press, Boca Raton 1991, p. 25.

20   Welinder, K. G., *Curr. Opin. Struct. Biol.*, 1992, **2**, 388.

21   Chance, B., *J. Biol. Chem.*, 1943, **151**, 553.

22   Dunford, H. B. and Stillman, J. S., *Coord. Chem. Rev.*, 1976, **19**, 187.

23   Yonetani, T., in *The Enzymes*, *Vol. 13*, Boyer, P. D. (Ed.): Academic Press, New York 1972, p. 345.

24   Dolphin, D. and Felton, R. H., *Acc. Chem. Res.*, 1974, **7**, 26.

25   Erman, J. E., Vitello, L. B., Mauro, J. M., and Kraut, J., *Biochemistry*, 1989, **28**, 7992.

26   Scholes, C. P., Liu, Y., Fishel, L. A., Farnum, M. F., Mauro, J. M. and Kraut, J., *Israel J. Chem.*, 1989, **29**, 85.

27   Sivaraja, M., Goodin, D. B., Smith, M. and Hoffman, B. M., *Science*, 1989, **245**, 738.

28   Harris, R. Z., Newmyer, S. L. and Ortiz de Montellano, P. R., *J. Biol. Chem.*, 1993, **268**, 1637.

29   Fruton, J. S., *Molecules and Life: Historical Assays on the Interplay of Chemistry and Biology*, Wiley-Interscience, New York 1972.

30   Kelly, G. and Latzko, E., *Naturewissenschaften*, 1979, **66**, 617.

31   Groden, D. and Beck, E., *Biochim. Biophys. Acta*, 1979, **546**, 426.

32   Bach, A. and Chodat, R., *Ber*, 1903, **36**, 600.

33   Altschul, A., Abrams, R. and Hogness, T., *J. Biol. Chem.*, 1940, **136**, 777.

34   Dalton, D. A., Hanus, F. J., Russell, S. A. and Evans, H. J., *Plant Physiol.*, 1987, **83**, 789.

35   Mittler, R. and Zilinskas, B. A., *Plant Physiol.*, 1991, **97**, 962.

36   Dalton, D. A., Diaz del Castillo, L., Kahn, M. L., Joyner, S. L. and Chatfield, J. M., *Arch. Biochem. Biophys.*, 1996, **328**, 1.

37   Patterson, W. R. and Poulos, T. L., *Biochemistry*, 1995, **34**, 4331.

38   Dalton, D. A., in *Peroxidases in Chemistry and Biology, Vol. 2*, Everse, J., Everse, K. E. and Grisham, M. B. (Eds.): CRC Press, Boca Raton 1991, p. 139.

39   Raven, E., *Sub- Biochem.*, 2000, **36**, 318.

40   Gallagher, P. H., *Biochem.J*, 1923, **17**, 515.

41   Baciocchi, E., Gerini, M. F., Harvey, P., Lanzalunga, O. and Mancinelli, S., *Eur. J. Biochem.*, 2000, **267**, 2705.

42   Burner, U. and Obinger, C., *FEBS Lett.*, 1997, **411**, 269.

43   Colonna, S., Gaggero, N., Carrea, G. and Pasta, P., *Chem. Commun.*, 1992, 357.

44   Colonna, S., Gaggero, N., Casella, L., Carrea, G. and Pasta, P., *Tetrahedron-Asymm.*, 1992, **3**, 95.

45   Colonna, S., Gaggero, N., Pasta, P. and Ottolina, G., *Chem. Commun.*, 1996, 2303.

46   Holland, H. L., *Organic Synthesis with Oxidative Enzymes*, VCH, New York 1992.

47   ten Brink, H. B., Tuynman, A., Dekker, H. L., Hemrika, W., Izumi, Y., Oshiro, T., Schoemaker, H. E. and Waver, R., *Inorg. Chem.*, 1998, **37**, 6780.

48   Vargas, R. R., Bechara, E. J. H., Marzorati, L. and Wladislaw, B., *Tetrahedron-Asymm.*, 1999, **10**, 3219.

49   Corbett, M. D. and Corbett, B. R., *Biochem. Arch.*, 1985, **1**, 115.

50   Dexter, A. F., Lakner, F. J., Campbell, R. A. and Hager, L. P., *J. Am. Chem. Soc.*, 1995, **117**, 6412.

51   Hu, S. and Hager, L. P., *Tetrahedron Lett.*, 1998, **40**, 1641.

52   Jarvie, A. W. P., Overton, N. and St Pourcain, C. B., *Chem. Commun.*, 1998, 177.

53   Manoj, K. M., Yi, X., Rai, G. P. and Hager, L. P., *Biochem. Biophys. Res. Comm.*, 1999, **266**, 301.

54   Miller, V. P., DePillis, G. D., Ferrer, J. C., Mauk, A. G. and Ortiz de Montellano, P. R., *J. Biol. Chem.*, 1992, **267**, 8936.

55   Ozaki, S.-i. and Ortiz de Montellano, P. R., *J. Am. Chem. Soc.*, 1995, **117**, 7056.

56   Ozaki, S.-I., Matsui, T. and Watanabe, Y., *J. Am. Chem. Soc.*, 1997, **119**, 6666.

57   Zaks, A. and Doddds, D. R., *J. Am. Chem. Soc.*, 1995, **117**, 10419.

58   Geigert, J., Dalietos, D. J., Neidleman, S. L., Lee, T. D. and Wadsworth, J., *Biochem. Biophys. Res. Comm.*, 1983, **114**, 1104.

59   Thomas, J. A., Morris, D. R. and Hager, P. L., *J. Biol. Chem.*, 1970, **245**, 3129.

60   Corbett, M. D. and Chipco, B. R., *Biochem.J*, 1979, **183**, 269.

61   Dalton, D. A., Russell, S. A., Hanus, F. J., Pascoe, G. A. and Evans, H. J., *Proc. Natl. Acad. Sci.*, 1986, **83**, 3811.

62   Jespersen, H. M., Kjaersgard, I. V. H., Ostergaard, L. and Welinder, K. G., *Biochem.J*, 1997, **326**, 305.

63   Caldwell, C. R., Turano, F. J. and McMahon, M. B., *Planta*, 1998, **204**, 120.

64   Chatfield, M. and A, D. D., *Plant Physiol.*, 1993, **103**, 661.

65   Webb, R. P. and Allen, R. D., *Plant Physiol.*, 1995, **108**, 64.

66   Kubo, A., Saji, H., Tanaka, K. and Kondo, N., *Plant Mol. Biol.*, 1992, **18**, 691.

67   Lopez, F., Vansuyt, G., CasseDelbart, F. and Fourcroy, P., *Physiologia Plantarum*, 1996, **97**, 13.

68   Vanbreusegem, F., Villarroel, R., Vanmontagu, M. and Inze, D., *Plant Physiol.*, 1995, **107**, 649.

69   Orvar, B. L. and Ellis, B. E., *Plant Physiol.*, 1995, **108**, 839.

70   Morita, S., Kaminaka, H., Yokoi, H., Masumura, T. and Tanaka, K., *Plant Physiol.*, 1997, **114**, 437.

71   Kim, I. J. and Chung, W. I., *Plant Sci.*, 1998, **133**, 69.

72   Newman, T., De Bruijin, F. J., Green, P., Keegstra, K., Kende, H., McIntish, L., Ohlrogge, J., Raikhel, N., Somerville, S., Thomashow, M., Retzel, E. and Somerville, C., *Plant Physiol.*, 1996, **106**, 1241.

73   Ishikawa, T., Sakai, K., Yoshimura, K., Takeda, T. and Shigeoka, S., *FEBS Lett.*, 1996, **384**, 289.

74   Mano, S., Yamaguchi, K., Hayashi, M. and Nishimura, M., *FEBS Lett.*, 1997, **413**, 21.

75   Yamaguchi, K., Hayashi, M. and Nishimura, M., *Plant. Cell. Physiol.*, 1996, **37**, 405.

76   Zhang, H., Wang, J., Nickel, U., Allen, R. D. and Goodman, H. M., *Plant Mol. Biol.*, 1997, **34**, 967.

77   Ishikawa, T., Sakai, K., Takeda, T. and Shigeoka, S., *FEBS Lett.*, 1995, **367**, 28.

78   Poulos, T. L., Freer, S. T., Alden, R. A., Edwards, S. L., Skogland, U., Takio, K., Eriksson, B., Xuong, N. H., Yonetani, T. and Kraut, J., *J. Biol. Chem.*, 1980, **255**, 575.

79   Choinowski, T., Bloding, W., Winterhalter, K. H. and Piontek, K., *J. Mol. Biol.*, 1999, **286**, 809.

80   Poulos, T. L. and Edwards, S. L., *J. Biol. Chem.*, 1993, **268**, 4429.

81   Edwards, S. L., Raag, R., Wariishi, H., Gold, M. H. and Poulos, T. L., *Proc. Natl. Acad. Sci. USA*, 1993, **90**, 750.

82   Sundaramoorthy, M., Kishis, K., Golds, M. H. and Poulos, T. L., *J. Biol. Chem.*, 1997, **272**, 17574.

83   Sundaramoorthy, M., Terner, J. and Poulos, T. L., *Structure*, 1995, **3**, 1367.

84   Kunishima, N., Fukuyama, K., Matsubara, H., Hatanaka, H., Shibano, Y. and Amachi, T., *J. Mol. Biol.*, 1994, **235**, 331.

85   Schuller, D. J., Ban, N., van Huystee, R. B., McPherson, A. and Poulos, T. L., *Structure*, 1996, **4**, 311.

86   Gajhede, M., Schuller, D. J., Henricksen, A., Smith, A. T. and Poulos, T. L., *Nature Struct. Biol.*, 1997, **4**, 1032.

87   Poulos, T. L. and Kraut, J., *J. Biol. Chem.*, 1980, **255**, 8199.

88   Adachi, S., Nagano, S., Ishimori, K., Watanabe, Y., Morishima, I., Egawa, T., Kitagawa, T. and Makino, R., *Biochemistry*, 1993, **32**, 241.

89   Filizola, M. and Loew, G. H., *J. Am. Chem. Soc.*, 2000, **122**, 18.

90   Newmyer, S. L. and Ortiz de Montellano, P. R., *J. Biol. Chem.*, 1995, **270**, 19430.

91   Bosshard, H. R., Anni, H. and Yonetani, T., in *Peroxidases in Chemistry and Biology, Vol. 2*, Everse, J., Everse, K. E.and Grisham, M. B. (Eds.): CRC Press, Boca Raton 1991, p. 51.

92   Veitch, N. C. and Smith, A. T., *Adv. Inorg. Chem.*, 2001, **51**, 107.

93   Gonzalez, F. J. and W, N. D., *Trends Gen.*, 1990, **6**, 182.

94   Sono, M., Roach, M. P., Coulter, E. D. and Dawson, J. H., *Chem. Rev.*, 1996, **96**, 2841.

95   Garfinkel, D., *Arch. Biochem. Biophys.*, 1958, **77**, 493.

96   Klingenberg, M., *Arch. Biochem. Biophys.*, 1958, **75**, 376.

97   Omura, T. and Sato, R., *J. Biol. Chem.*, 1964, **239**, 2370.

98   Estabrook, R. W., Y, C. D. and Rosenthal, O., *Biochem Z*, 1963, **338**, 741.

99   Cooper, D. Y., Levine, S., Narasimhulu, S., Rosenthal, O. and W, E. R., *Science*, 1965, **147**, 400.

100   Katagiri, M., Ganguli, B. N. and Gunsalus, I. C., *J. Biol. Chem.*, 1968, **243**, 3543.

101   Lu, A. Y. H. and Coon, M., *J. Biol. Chem.*, 1968, **243**, 1331.

102   Fujii-Kuriyma, Y., Mizukami, Y., Kawajiri, K., Sogawa, K. and Muramatsu, M., *Proc. Natl. Acad. Sci USA*, 1982, **79**, 2793.

103   Haniu, M., Armes, L. G., Yasunobu, K. T., Shastry, B. A. and Gunsalus, I. C., *J. Biol. Chem.*, 1982, **257**, 12664.

104   Poulos, T. L., Finzel, B., Gunsalus, I. C., Wagner, G. C. and Kraut, J., *J. Biol. Chem.*, 1985, **260**, 16122.

105   Nelson, D. R., in *Cytochrome P450: Structure, Mechanism and Biochemistry*Ortiz de Montellano, P. R. (Ed.): Plenum Press, New York 1995, p. 575.

106   Schenkman, J. B., in *Hepatic cytochrome P450 monooxygenase system*Schenkman, J. B.and D, K. (Eds.): Pergamon, New York 1982, p. 1.

107   Rein, H. and Jung, C., in *Cytochrome P450*, Schenkman, J. and Greim, H. (Eds.): SpringerVerlag, Berlin, New York 1993, p. 105.

108   Ishimura, Y., Ullrich, V. and Peterson, J. A., *Biochem. Biophys. Res. Comm.*, 1971, **42**, 140.

109   Peterson, J., Ishimura, Y. and Griffin, B., *Arch. Biochem. Biophys.*, 1972, **149**, 197.

110   Estabrook, R. W., Hildebrandt, A., Baron, J., Netter, K. and Leibman, K., *Biochem. Biophys. Res. Comm.*, 1971, **42**, 132.

111 Rein, H., Jung, C., Ristau, O. and Ruckpaul, K., in *Fundamental research in homogeneous catalysis, Vol. 2*, Shilov, A. (Ed.): Gordon and Breach, London 1986, p. 733.

112 Bonfils, C., Balny, C. and Maurel, P., *J. Biol. Chem.*, 1981, **256**, 9457.

113 Hoa, G. H., Begard, E., Debey, P. and Gunsalus, I. C., *Biochemistry*, 1978, **17**, 2835.

114 Richter, C., Azzi, A., Weser, O. and Wendel, A., *J. Biol. Chem.*, 1977, **252**, 5061.

115 Wilker, J. J., Dmochowski, I. J., Dawson, J. H., Winkler, J. R. and Gray, H. B., *Angew. Chem. Int. Ed. Engl.*, 1999, **38**, 90.

116 Schlichting, I., Berendzen, J., Chu, K., Stock, A. M., Maves, S. A., Benson, D. E., Sweet, R. M., Ringe, D., Petsko, G. A. and Sligar, S. G., *Science*, 2000, **287**, 1615.

117 Groves, J. T. and Han, Y.-Z., in *Cytochrome P450* Ortiz de Montellano, P. R. (Ed.): Plenum Press, New York 1995, p. 3.

118 Miura, Y. and Fulco, A., *Biochim. Biophys. Acta*, 1975, **388**, 305.

119 Ho, P. P. and Fulko, A. J., *Biochim. Biophys. Acta*, 1976, **431**, 249.

120 Narhi, L. O. and Fulko, A. J., *J. Biol. Chem.*, 1982, **257**, 2147.

121 Fulco, A. J., *Ann. Rev. Pharm. Toxicology*, 1991, **31**, 177.

122 Narhi, L. O. and Fulco, A. J., *J. Biol. Chem.*, 1987, **262**, 6683.

123 Porter, T. D., *TIBS*, 1991, **16**, 154.

124 Oster, T., Boddupalli, S. S. and Peterson, J. A., *J. Biol. Chem.*, 1991, **266**, 22718.

125 Sevrioukova, I. F. and Peterson, J. A., *Biochimie*, 1996, **78**, 744.

126 Sevrioukova, I. F., Shaffer, C., Ballou, D. P. and Peterson, J. A., *Biochemistry*, 1996, **35**, 7058.

127 Sevrioukova, I. F., Truan, G. and Peterson, J. A., *Arch. Biochem. Biophys.*, 1997, **340**, 231.

128 Sevrioukova, I. F., Truan, G. and Peterson, J. A., *Biochemistry*, 1996, **35**, 7528.

129 Munro, A. W., Lindsay, J. G., Coggins, J. R., Kelly, S. M. and Price, N. C., *FEBS Lett.*, 1994, **343**, 70.

130 Govindaraj, S. and Poulos, T. L., *Biochemistry*, 1995, **34**, 11221.

131 Govindaraj, S. and Poulos, T. L., *Protein Sci.*, 1996, **5**, 1389.

132 Ravichandran, K. G., Boddupalli, S. S., Hasemann, C. A., Peterson, J. A. and Deisenhofer, J., *Science*, 1993, **261**, 731.

133 Oliver, C. F., Modi, S., Sutcliffe, M. J., Primrose, W. U., Lian, L. Y. and Roberts, G. C. K., *Biochemistry*, 1997, **36**, 1567.

134 Graham-Lorence, S., Truan, G., Peterson, J. A., Falck, J. R., Wei, S., Helvig, C. and Capdevila, J. H., *J. Biol. Chem.*, 1997, **272**, 1127.

135 Li, H. and Poulos, T. L., *Nature Struct. Biol.*, 1997, **4**, 140.

136 Modi, S., Primrose, W. U., Boyle, J. M. B., Gibson, C. F., Lian, L.-Y. and Roberts, G. C. K., *Biochemistry*, 1995, **34**, 8982.

137 Modi, S., Sutcliffe, M. J., Primrose, W. U., Lian, L.-Y. and Roberts, G. C. K., *Nature Struct. Biol.*, 1996, **3**, 414.

138 Noble, M. A., Miles, C. S., Chapman, S. K., Lysek, D. A., Mackay, A. C., Reid, G. A., Hanzlik, R. P. and Munro, A. W., *Biochemistry*, 1999, **339**, 371.

139 Daff, S. N., Chapman, S. K., Turner, K. L., Holt, R. A., Gavindaraj, S. and Poulos, T. L., *Biochemistry*, 1997, **36**, 13816.

140 Maves, S. A., Yeom, H., McLean, M. A. and Sligar, S. G., *FEBS Lett.*, 1997, **414**, 213.

141 Yoem, H., Sligar, S. G., Li, H., Poulos, T. L. and Fulco, A. J., *Biochemistry*, 1995, **34**, 14733.

142 Colonna, S., Molinari, H., Banfi, S., Julia, S., Masana, J. and Alvarez, A., *Tetrahedron*, 1983, **39**, 1635.

143 Julia, S., Guixer, J., Masana, J., Rocas, J., Colonna, S., Annunziata, R. and Molinari, H., *J. Chem. Soc. Perkin Trans. 1*, 1982, 1317.

144 Julia, S., Masana, J. and Vega, J. C., *Angew. Chem. Int. Ed. Engl.*, 1980, **19**, 929.

145 Nagano, S., Tanaka, M., Ishimori, K., Watanabe, Y. and Morishima, I., *Biochemistry*, 1996, **35**, 14251.

CHAPTER TWO

Spectroscopic and Kinetic Studies on the Catalytic

Oxidation of p-Cresol by Ascorbate Peroxidase

2.1 INTRODUCTION

The generation of coloured products from the reaction of phenols with peroxidases has been known since 1900.[1] Since then, the H_2O_2-dependent catalytic oxidation of a range of phenolic and related aromatic substrates has been identified and investigated for several peroxidases.[2-10] Ascorbate peroxidase (APX) is a relative newcomer to the peroxidase area[11-15] and is also known to catalyse the oxidation of a variety of non-physiological, aromatic substrates.[16] The biological function of APX appears to be prevention of H_2O_2 accumulation and, as such, the enzyme catalyses a reaction in which ascorbate acts as a one electron donor and H_2O_2 is reduced to water, equation [2.1].

$$2 \text{ Ascorbate} + H_2O_2 + 2H^+ \rightarrow 2 \text{ Monodehydroascorbate} + 2 H_2O \qquad ...[2.1]$$

The catalytic mechanism of the enzyme is reminiscent of that for other peroxidases.[17,18] Hence, resting enzyme (in the ferric form) reacts with H_2O_2 to generate a 2-equivalent oxidized intermediate, known as Compound I, which is then subsequently reduced by ascorbate (S) in two, successive, single electron transfers,[19] equations [2.2] – [2.4].

$$APX + H_2O_2 \xrightarrow{\ k_1\ } \text{Compound I} + H_2O \qquad ...[2.2]$$

$$\text{Compound I} + HS \xrightarrow{\ k_2\ } \text{Compound II} + S^\bullet \qquad ...[2.3]$$

$$\text{Compound II} + HS \xrightarrow{\ k_3\ } APX + S^\bullet + H_2O \qquad ...[2.4]$$
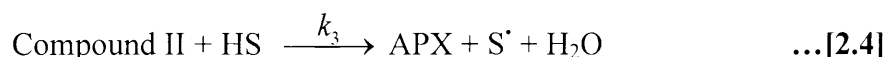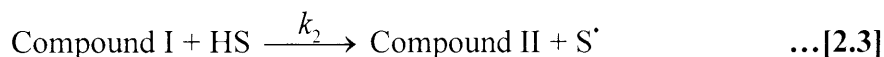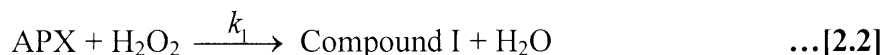
Detailed mechanistic information for oxidations of substrates other than ascorbate is not yet available for APX. Aromatic oxidations of this kind are of special significance for APX, since chemical modification combined with site-directed mutagenesis experiments[14] have recently indicated that there are likely to be *two* binding sites on APX - one for ascorbate itself and another for aromatic substrates. In this work, the kinetics and mechanism of APX-catalyzed oxidation of *p*-cresol has been investigated and the products of the reaction have been identified. The work represents the first such study for an ascorbate peroxidase and the implications of these results in the wider context of APX-catalysed aromatic oxidations are discussed.

46

2.2 RESULTS

2.2.1 Expression and Purification of Pea Cytosolic Ascorbate Peroxidase

Purification of cytosolic rAPX resulted in a 10-fold increase in specific activity and a final yield of 45%. The calculated purity number, *Rz* (A_{403}/A_{280}), for each purification steps are also shown in Table 2.1. The purified enzyme had a specific activity of 318 ± 12 μmol ascorbate oxidised /mg protein^{-1}/min^{-1}.

SDS-PAGE gel details the purification of rAPX (see Section 6.2.1). The cell-free extracts of rAPX were red-coloured, which indicated that the heme incorporation occurred *in vivo*. It has been reported that if rAPX is expressed alone and not as a fusion protein, an apo dimer that does not incorporate haem is purified.[20] Since the fusion protein behaves as a monomer upon gel filtration, it appears that linking APX to the maltose binding protein (MBP) prevents dimerisation, which in turn allows the heme to incorporate. Since cleavage of the recovered fusion protein with factor *Xa* is not effective (only partial cleavage of the fusion product was obtained) and required large quantities of the protease over long incubation periods (> a week), trypsin was used to digest the fusion protein because the factor *Xa* recognition sequence ends with Arg. The digestion products were easily removed from the holo-rAPX by amylose affinity column.

2.2.2 Electronic Absorption Spectra

The electronic spectrum of ferric APX is shown in Figure 2.1 at 298 K. Wavelength maxima were observed at 403, about 506 and about 636 nm. These results were in agreement with previously observed values and the extinction coefficient value at 403 nm was previously determined and found to be 88 ± 2 mM^{-1} cm^{-1}.[21]

2.2.3 APX-catalysed Oxidation of p-Cresol with Hydrogen Peroxide

HPLC analysis of the products of the reaction of APX and H_2O_2 with *p*-cresol (**I**, Scheme 2.1) indicated the presence of four compounds with retention times of 1.6, 3.7, and 11.4 and 18.6 minutes (Figure 2.2).

47

TABLE 2.1

Purification of rAPX showing yields and activities of each purification step

Step	Total Protein (mg)	Total Activity (μmol / min)	Specific Activity (μmol / mg/ min)	Yield (%)	Rz	Purification (-fold)
Cell-Free Extract	198	6246	34 ± 2	100	0.04	1.0
1st Amylose Column	114	6156	54 ± 10	97	0.55	1.6
2nd Amylose Column	27	Nd	nd	nd	1.53	nd
FFQ Column	8.9	2830	318 ± 12	45	2.06	9.4

nd: not determined

48
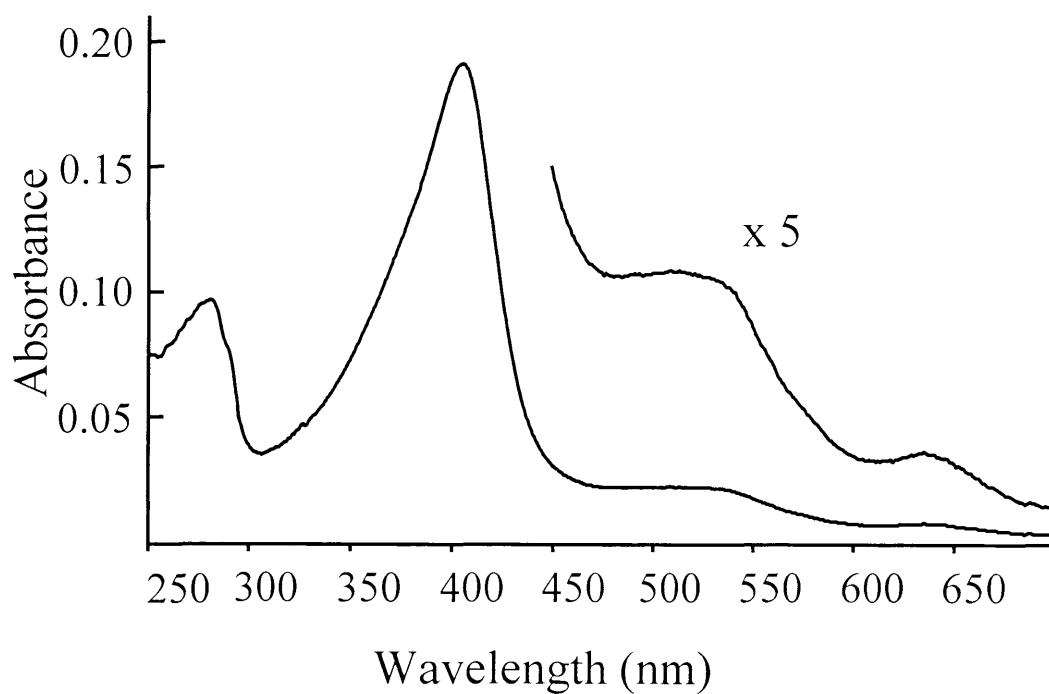
FIGURE 2.1

Electronic absorption spectra of rAPX. Absorbance readings in the visible

region have been amplified by a factor of five Conditions: sodium phosphate,

pH 7.0, μ= 0.10 M, 25 °C.
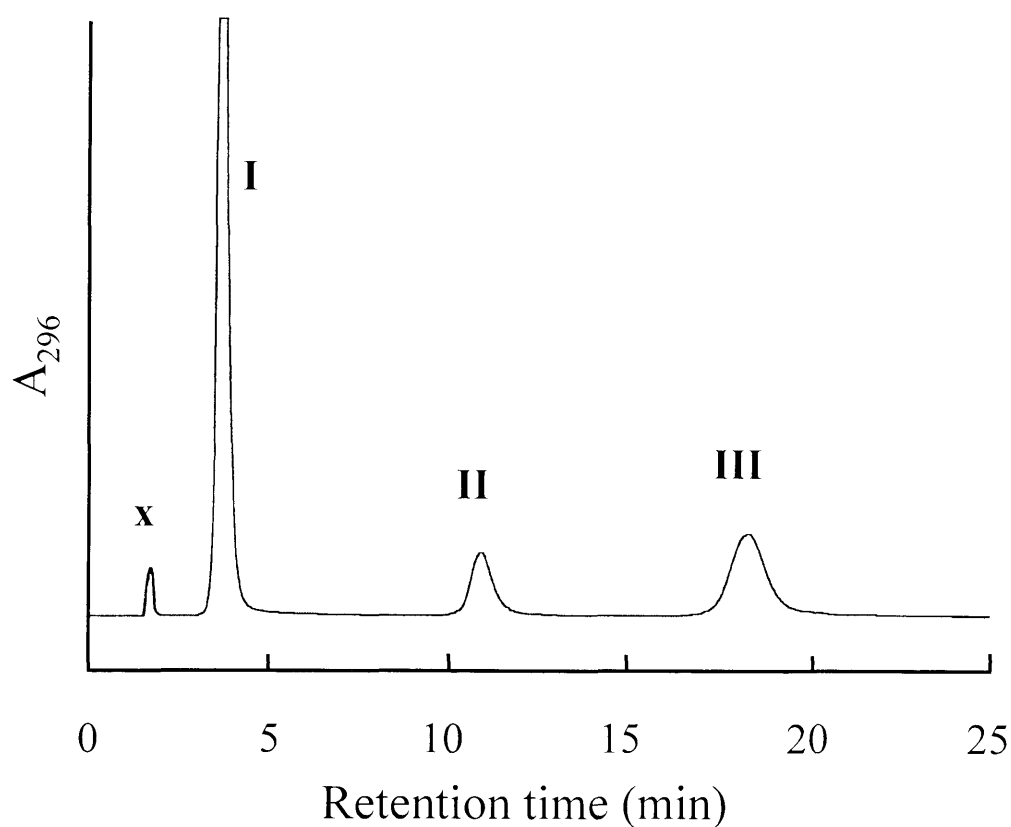
FIGURE 2.2

HPLC analysis of the products (labelled according to Scheme 1) of the reaction of p-cresol with H_2O_2 and APX. Peak **I** (Rt = 3.7 minutes): unreacted p-cresol; peak **II** (Rt =11.4 minutes): 2,2'-dihydroxy 5,5'-dimethylbiphenyl; peak **III** (Rt = 18.6 minutes): Pummerers' ketone. The peak labelled **x** (Rt = 1.6 minutes) is an impurity found in the p-cresol. Conditions: [APX] = 4.4 μM, [H_2O_2] = 1.25 mM, [p-Cresol] = 40 mM, phosphate buffer, pH 7.0, μ= 0.10 M, 25 °C).

The first two peaks were assigned as arising from unreacted starting material (**I**) and impurities in p-cresol (**x**) (determined by injection of p-cresol in the absence of APX and hydrogen peroxide). Peaks **II** and **III** were assigned as arising from the oxidation products. Further analysis of these products was carried out using GC-MS, NMR and by direct comparison with HPLC analysis of an authentic sample (see Section 6.2.3 and 6.2.6). The products with retention time 11.4 and 18.6 minutes (**II** and **III**, Scheme 2.1) were characterised as 2,2'-dihydroxy-5,5'-dimethylbiphenyl and 4a,9b-dihydro-8,9b-dimethyl-3(4H)-dibenzofuranone, known as Pummerer's ketone respectively.
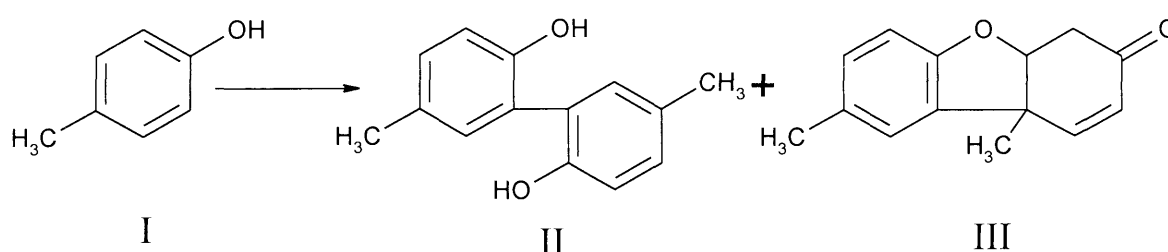
SCHEME 2.1.

Reaction scheme and products for the APX-catalysed oxidation of p-cresol (**I**) by hydrogen peroxide.

2.2.4 APX Catalyzed Oxidation of p-Cresol with Cumene Hydroperoxide

In the presence of cumene hydroperoxide (Scheme 2.2) rather than hydrogen peroxide, GC-MS analyses indicated two additional products (Figure 2.3).
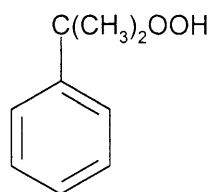
SCHEME 2.2

The peak with retention time 7.4 minutes yielded a mass spectrum consistent with the formation of 1,1-dimethyl benzyl alcohol (**IV**, Scheme 2.3), which, by analogy with the reaction of H_2O_2 releasing H_2O as product (equations [2] – [4]), is the expected product of cumene hydroperoxide reduction.
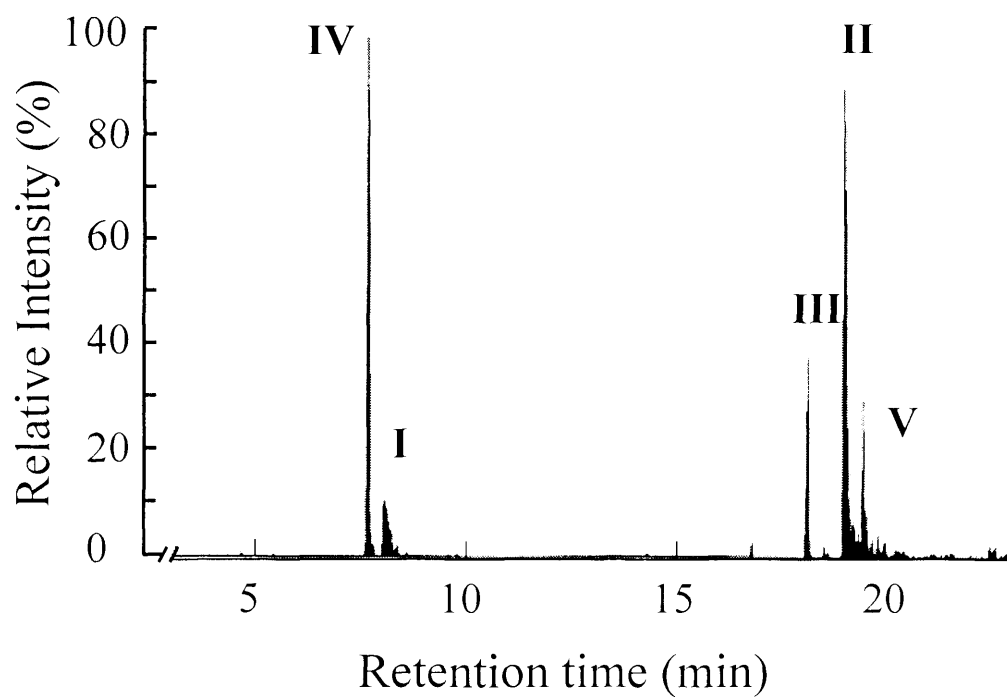
FIGURE 2.3

GC-MS analysis of the oxidation products (labelled according to Scheme 2.4) of the reaction of APX with *p*-cresol and cumene hydroperoxide. Conditions: [APX] = 4.4 μM, [Cumene hydroperoxide] = 1.25 mM, [p-Cresol] = 40 mM, phosphate buffer, pH 7.0, μ= 0.10 M, 25 °C).

The other product, with retention time 19.3 minutes, is consistent with the formation of bis-(1-methyl-1-phenyl-ethyl) peroxide (**V**, Scheme 2.3). Formation of this coupling product is probably via radical formation on benzyl alcohol. Spectroscopic and chromatographic data for Compounds **I** – **V** are given in Section 6.2.3.
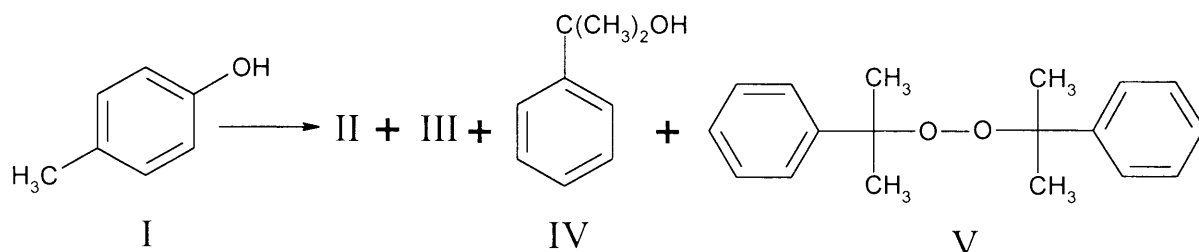
SCHEME 2.3

Reaction scheme and products for the APX-catalysed oxidation of *p*-cresol (**I**) by cumene hydroperoxide.

2.2.5 Effect of Enzyme Concentration on Product Formation

The effect of enzyme concentration on product ratio for *p*-cresol oxidation in the presence of hydrogen peroxide was determined and the results are shown in Figure 2.4. Figure 2.4 indicates that at low concentrations of enzyme Pummerer's ketone (**III**) predominates, but, as the concentration of enzyme increases, formation of the biphenyl compound (**II**) is more favourable.

2.2.6 Effect of Hydrogen Peroxide Concentration

Increases in H_2O_2 concentration had an inhibitory effect on enzyme activity (Figure 2.5): maximum activity was observed at $[H_2O_2]$ = 0.30 mM but above this concentration the activity decreased. Peroxidase inhibition at high concentrations of H_2O_2 is well known[22] and derives from the formation of Compound III. The details of these inhibition mechanisms for APX are currently under investigation[23] and were not pursued further in this work.
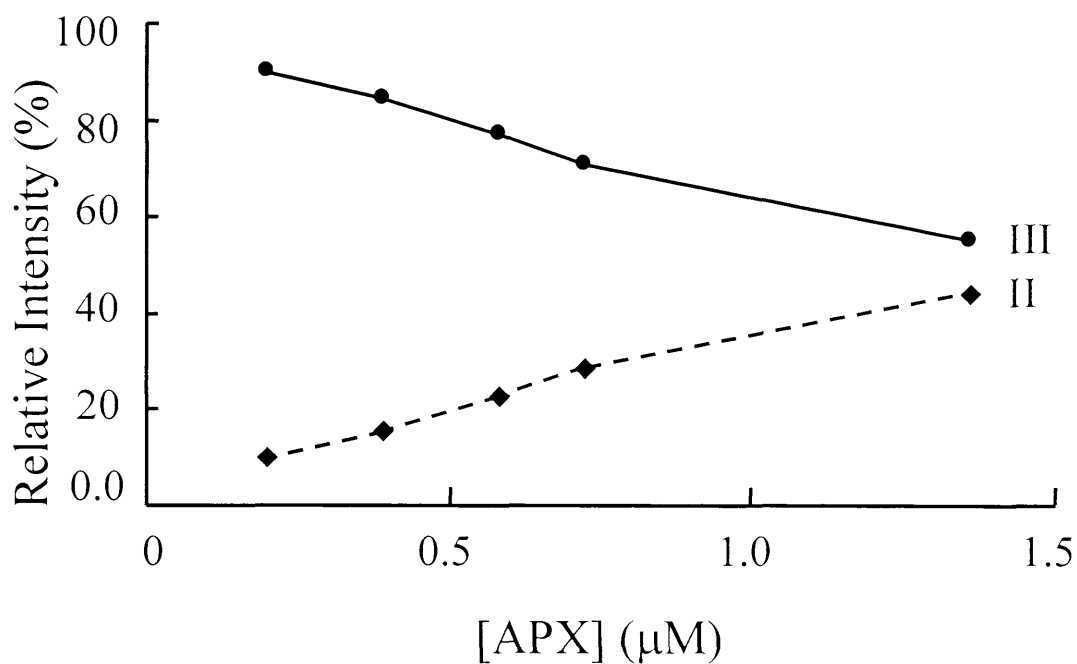
FIGURE 2.4

Effect of enzyme concentration on product ratio. Conditions: sodium

phosphate. pH 7.0. μ = 0.10 M. $[H_2O_2]$ = 1.25 mM. [p-cresol] = 0.25 mM.

room temperature.
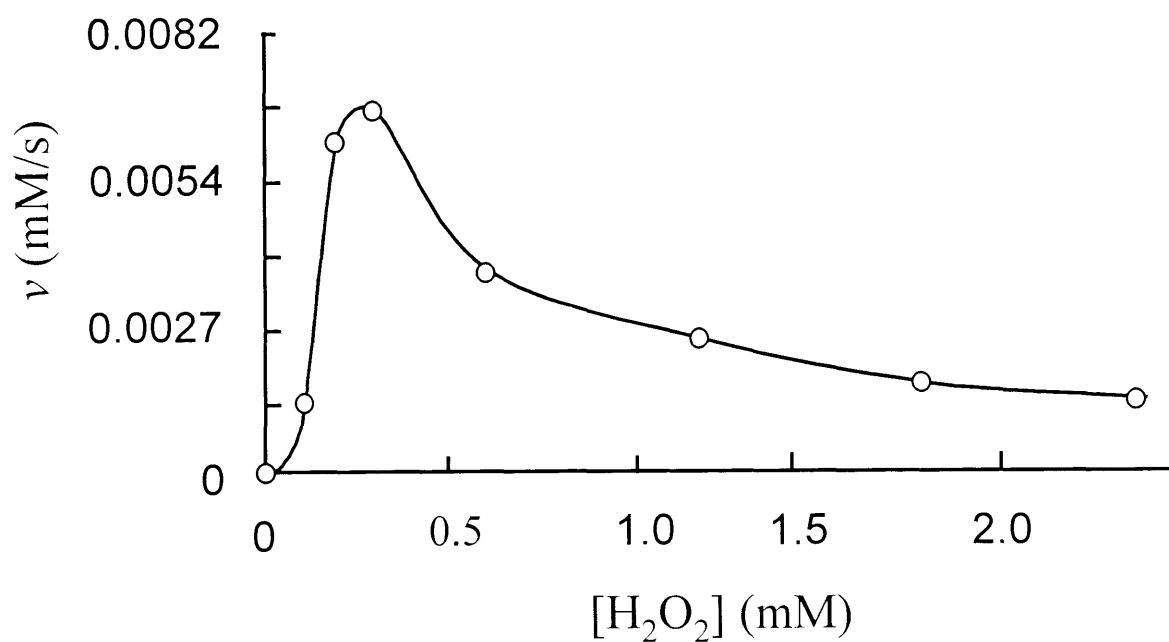
FIGURE 2.5

Effect of hydrogen peroxide concentration on reaction rate. Conditions:

[APX] = 23 nM, [H_2O_2] = 0-2.5 mM, [p-Cresol] = 18 mM, phosphate buffer,

pH 7.0, μ= 0.10 M, 25 °C.

2.2.7 Variation in Substrate Concentration

The effect of variation in substrate concentration was investigated. At > 30 mM of p-cresol, a decrease in activity was observed (Figure 2.6). Similar behaviour has been reported for chloroperoxidase[3,24] These effects are poorly understood but might be indicative of competition between H_2O_2 and p-cresol for the active site or covalent modification of the enzyme by the PC• radical[25] at high concentrations of substrate.

2.2.8 Kinetic Studies

2.2.8.1 Rapid Scan Spectra

Rapid scanning experiments were carried out to show that APX catalysis occurs via the intermediates, compound I and compound II (Figure 2.7). Under single turnover conditions, the reaction of APX with p-cresol was initially assumed to occur by the following mechanism, equations [2.5] –[2.7].

$$APX + H_2O_2 \xrightarrow{k_1} \text{Compound I} + H_2O \qquad ...[2.5$$

$$\text{Compound I} + PC \xrightarrow{k_2} \text{Compound II} + PC• \qquad ...[2.6$$

$$\text{Compound II} + PC \xrightarrow{k_3} APX + PC• + H_2O \qquad ...[2.7$$
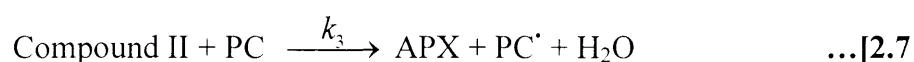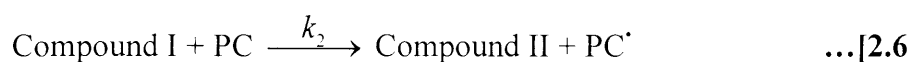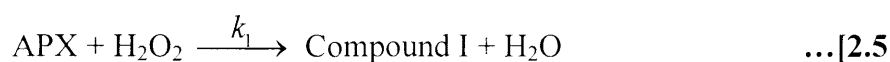
in which PC represents p-cresol and PC• represents the oxidised p-methylphenoxy radical. Direct evidence for two, successive, single electron transfers and the involvement of Compounds I and II in this mechanism, which is consistent with previous work on HRP,[2,26-28] came from the observation by rapid scanning spectrophotometry of Compound I formation from ferric enzyme and the spectra of compound II formation from Compound I. It should be noted that in the absence of reducing substrate, p-cresol, a compound II-like species, which is thought to contain a protein-based radical, forms from the spontaneous decay of Compound I,[29] but this process is much slower.
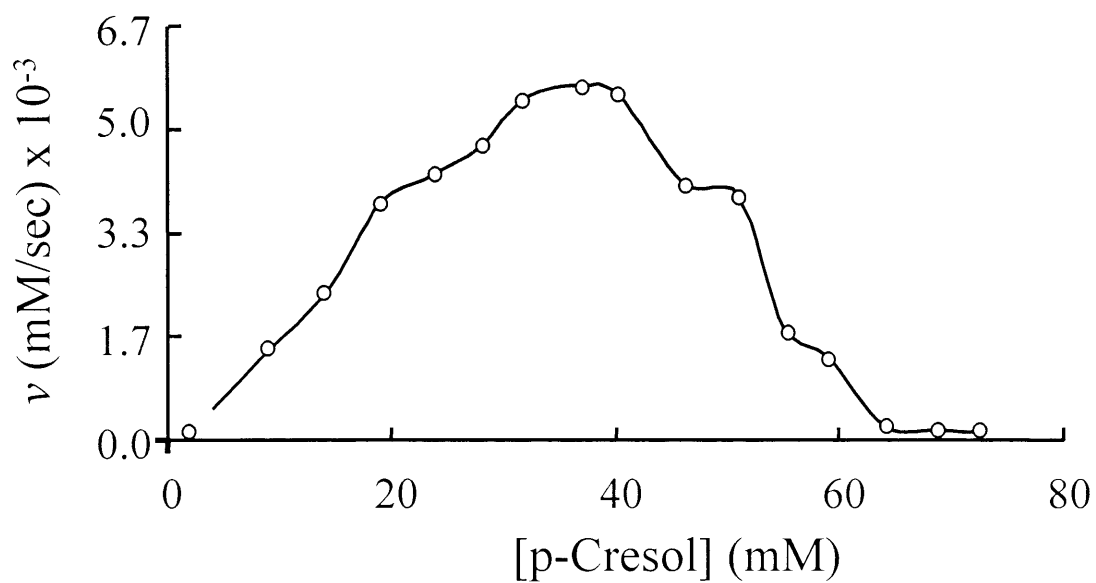
FIGURE 2.6

Effect of p-cresol concentration on reaction rate. (Conditions: [APX] = 23 nM, [H2O2] = 100 μM, [p-Cresol] = 0-73.4 mM, phosphate buffer, pH 7.0, μ= 0.10 M, 25 °C).
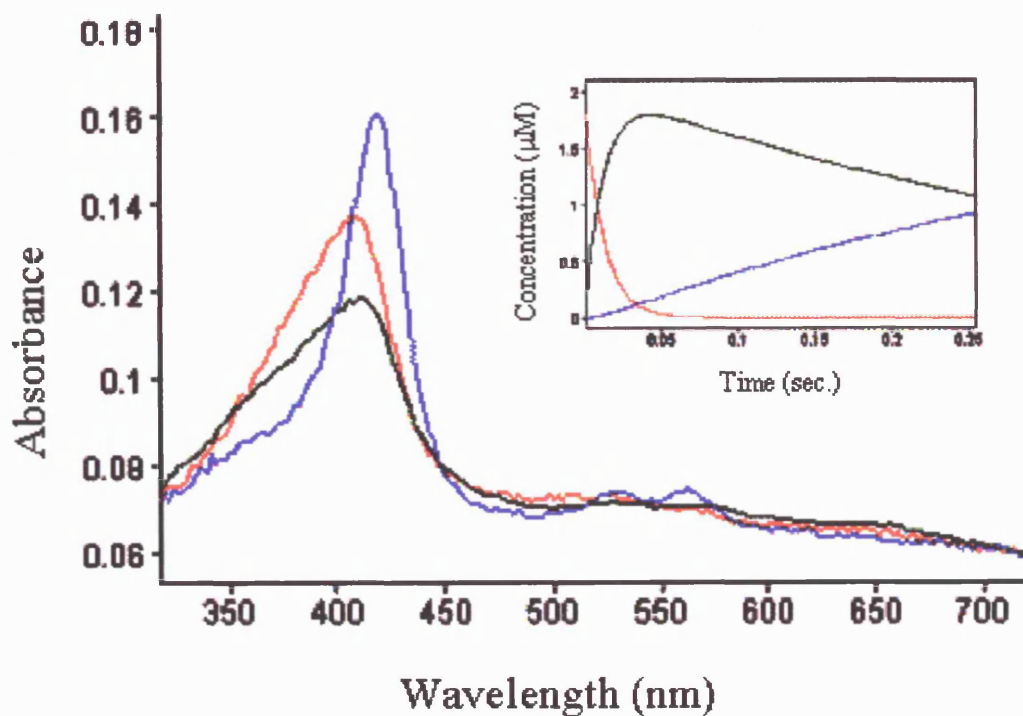
FIGURE 2.7

Experimental spectra obtained from diode array analysis of reaction of ferric

APX (-) with hydrogen peroxide to give Compound I (-) and Compound I

with p-cresol to give Compound II (-). Inset: Illustration of the decay of

ferric APX (-), formation and subsequently decay of Compound I (-), and

formation of Compound II (-). Conditions: [APX]= 2μM, [H$_2$O$_2$] = 2 μM, [p-

cresol] = 10 μM, Sodium phosphate buffer, pH 7.0, μ = 0.10 M, 5 °C. Model

used for the inset: A→B→C.

2.2.8.2 Transient-Steady State Kinetics

Kinetic evidence for the two one-electron transfer mechanism came from the concentration dependencies of the observed rate constants for equations [2.6] and [2.7]. Second order rate constants for formation of Compound I, equation [2.5], have been reported previously[14,15,30] and were not, therefore, examined in detail in this work. Pseudo-first-order rate constants, $k_{2,obs}$, for the reaction of Compound I with p-cresol showed a linear dependence on [p-cresol], Figure 2.8. A second order rate constant, k_2, derived from a linear least squares fit of the data, was found to be $(5.42 \pm 0.10) \times 10^5 \ M^{-1}s^{-1}$.

Reduction of Compound II by p-cresol, k_3, showed saturation kinetics, Figure 2.9. Behavior of this kind is consistent with the following mechanism, equations [2.8] and [2.9],

$$APX + PC \xrightleftharpoons{\quad K_a \quad} [APX - PC] \qquad \text{...[2.8}$$

$$[APX - PC] \xrightarrow{\quad k_3 \quad} APX + PC^\bullet \qquad \text{...[2.9}$$

and an expression for $k_{3,obs}$ can be derived, equation [10].

$$k_{3,obs} = \frac{k_3}{1 + K_d / [PC]} \qquad \text{...[2.10]}$$

where [PC] is defined as above and K_d is the dissociation constant of the bound complex in equation [2.8] ($K_d = 1/K_a$).

According to this expression, plots of $k_{3,obs}$ *versus* [p-cresol] are non-linear and values for k_3 and K_d can be derived from a non-linear least squares fit of the data to equation [2.10], Figure 2.9. Values were found to be $k_3 = 18.5 \pm 0.7 \ s^{-1}$ and $K_d = (1.54 \pm 0.12) \times 10^{-3} \ M$.
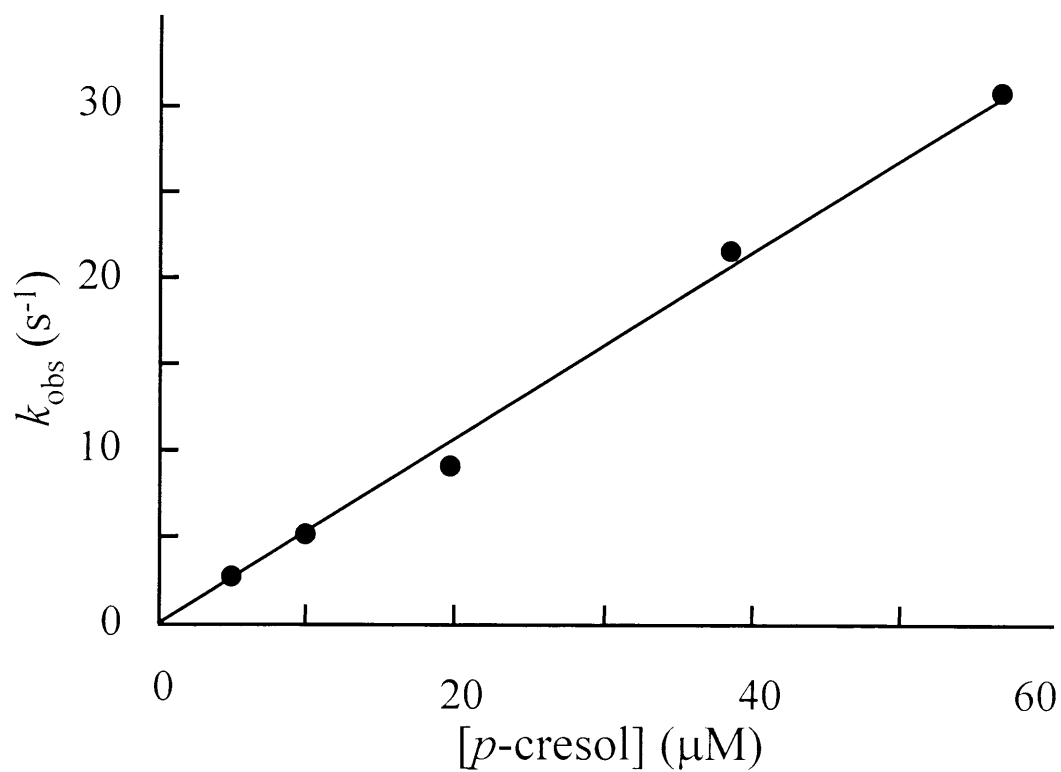
FIGURE 2.8

Dependence of $k_{2,obs}$ on [p-cresol] for reduction of Compound I. Conditions:

sodium phosphate, pH 7.0, 5.0 °C, $\mu = 0.10$ M, [APX] = 1 μM.
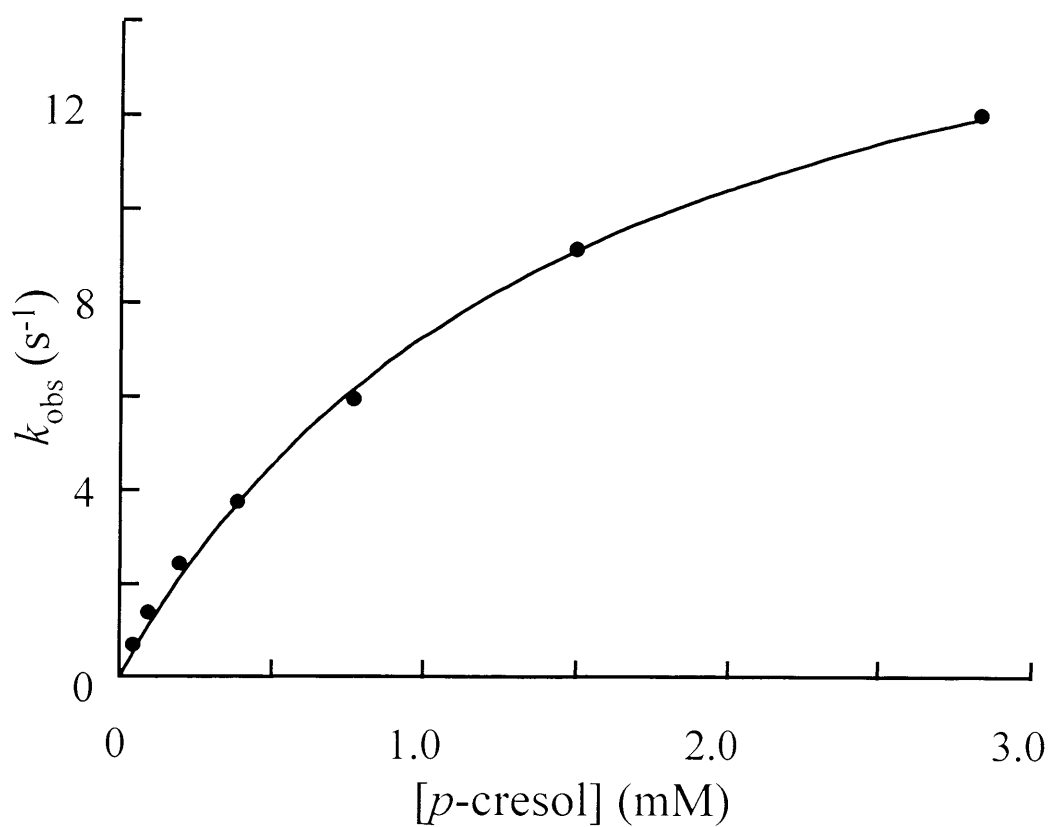
FIGURE 2.9

Dependence of $k_{3,obs}$ on [p-cresol] for reduction of Compound II. Conditions:

sodium phosphate pH 7.0, 5.0 °C, $\mu = 0.10$ M, [APX] = 1 μM.

2.2.8.3 Steady State Kinetics

Lineweaver-Burk plots of APX (1/rate against 1/[PC] for APX catalysed reaction) were non-linear and did not conform to normal Michaelis-Menten kinetics. Plots of velocity *versus* [p-cresol] showed a sigmoidal response up to [p-cresol] ≈ 30 mM ([APX] = 21 nM, 25.0 °C, sodium phosphate, pH 7.0, μ = 2.2 mM). The data were fitted to the Hill equation [2.11],

$$\frac{v}{V_{max}} = \frac{[S]^n}{K^n + [S]^n}$$

...[2.11]

where v is the initial rate, n is the number of substrate binding sites (see below), K is the substrate concentration at which the velocity is half-maximal and V_{max} is the maximum velocity. When n = 1, equation [2.1] reduces to the more usual Michaelis-Menten equation. A least squares fit of the steady state data to equation [2.11] is shown in Figure 2.10 and values for V_{max} = 4.6 ± 0.3 μMs^{-1}, K = 18.2 ± 1.4 mM and n = 2.01 ± 0.15 were derived. Equation [2.11] is consistent with two mechanisms: (a) non-allosteric behavior where n is the number of substrate binding sites for each non-interacting monomer or (b) allosteric behaviour where n is the total number of binding sites per dimer for interacting monomers of a homodimer. APX is known to exist as a homodimer[13] and non-Michaelis kinetics have been reported previously using ascorbate as a reductant.[20] To establish whether or not the sigmoidal kinetics derive from dimer formation, the same experiments were conducted at higher ionic strength where dimer formation is predicted to be unfavourable on electrostatic grounds. At μ = 0.10 and 0.50 M, the same sigmoidal response was observed and similar values for V_{max}, K and n were derived (Table 2.2).
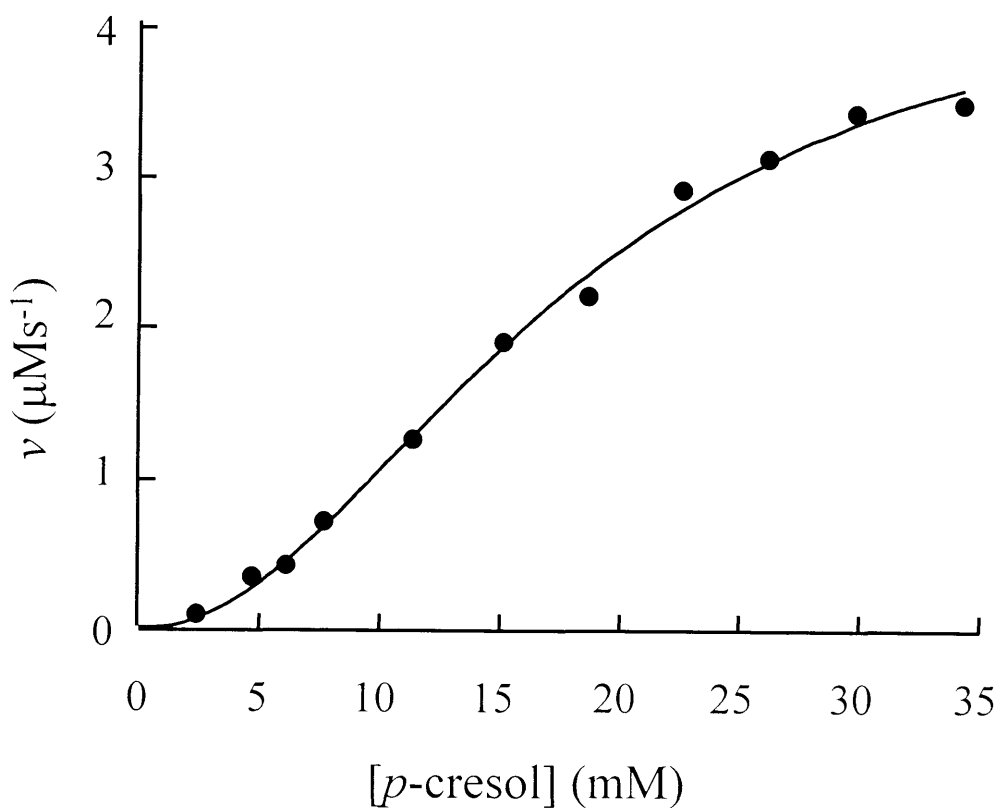
FIGURE 2.10

Steady state oxidation of p-cresol by APX. Conditions: [APX] = 21 nM, 25.0 °C, sodium phosphate, pH 7.0, μ = 2.2 mM). The solid line is a fit of the data to equation [11].

TABLE 2.2

Kinetic parameters for APX-catalysed oxidations of *p*-cresol

Ionic Strength (μ, mM)	V_{max} (μMs^{-1})	K (mM)	n
2.2	4.6 ± 0.3	18.2 ± 1.4	2.01 ± 0.15
100	6.8 ± 0.5	18.8 ± 1.7	1.97 ± 0.21
500	7.2 ± 0.5	13.5 ± 1.4	2.01 ± 0.24

2.2.9 Oxidation of 2-Naphtol

As oxidoreductases may play a central role in the biogenesis of biaryls, we studied the potential of APX for catalysing oxidative dimerisation reactions. Oxidation of 2-naphthol (in phosphate buffer, pH 7.0 and DMSO 5%) led to the corresponding biaryl (1.1'-binaphthyl-2,2'-diols) by coupling in ortho position to the hydroxy group as shown in Scheme 2.4.
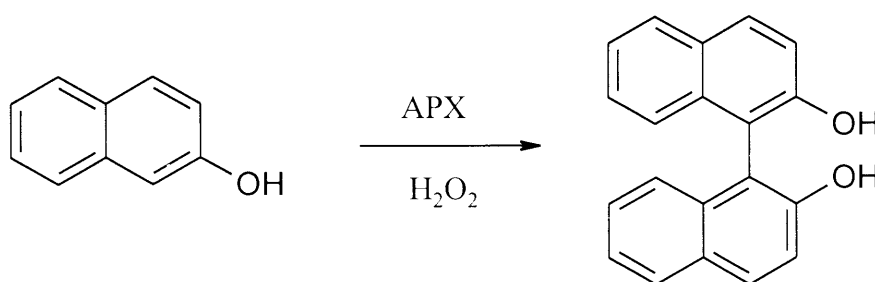
SCHEME 2.4

Oxidative dimerisation of 2-naphthol by ascorbate peroxidase catalysis

The enantiomeric excesses were not determined due to the low yields obtained. However, the possibility of having satisfactory ee values is probably quite low. Schmitt and co workers carried out similar reactions using HRP as a catalyst and found that the asymmetric induction values (ee) were less than 5 %, even though Sridhar and co workers reported otherwise (52 % e.e.).[31,32] However, the latter work seems less convincing as no report has confirmed these results in the literature.

2.2.10   Oxidation of 2,2'-Azino-di-(3-ethylbenzthiazoline-6-sulphonic Acid) (ABTS)

The oxidation of 2,2'-azino-di-(3-ethylbenzthiazoline-6-sulfonic acid), commonly known as ABTS, is a routine reaction for determining peroxidase activity. The reagent is commonly supplied as the ammonium salt of the acid. ABTS has its maximum absorbance at 340 nm. It acts as a one-electron donor to form a cation radical that absorbs strongly at 414 nm. The products generated from this reaction have already been characterised in the literature[33] (Scheme 2.5). Therefore no product characterisation was carried out here assuming that APX–catalysed oxidation generates the same products. Instead, steady-state kinetics was carried out to determine catalytic constants in order to compare APX activity with other peroxidases.

Oxidation of ABTS was shown to follow Michaelis-Menten kinetics (Figure 2.11). Unlike p-cresol oxidation no sigmoidal behaviour was observed. The kinetic parameters, K_m and k_{cat} are calculated to be 88 μM and 1.5 S^{-1} respectively. In the term of specific activity, the calculated value was 3.67 μmol ABTS oxidised /mg $protein^{-1}/min^{-1}$. This is in similar range with other ascorbate peroxidases from different sources. For example, specific activity of APX from legume root nodules has been reported to be 2.7 oxidised /mg $protein^{-1}/min^{-1}$.[34]   However, the activity is about 10-30 times less than human peroxidases.[35]
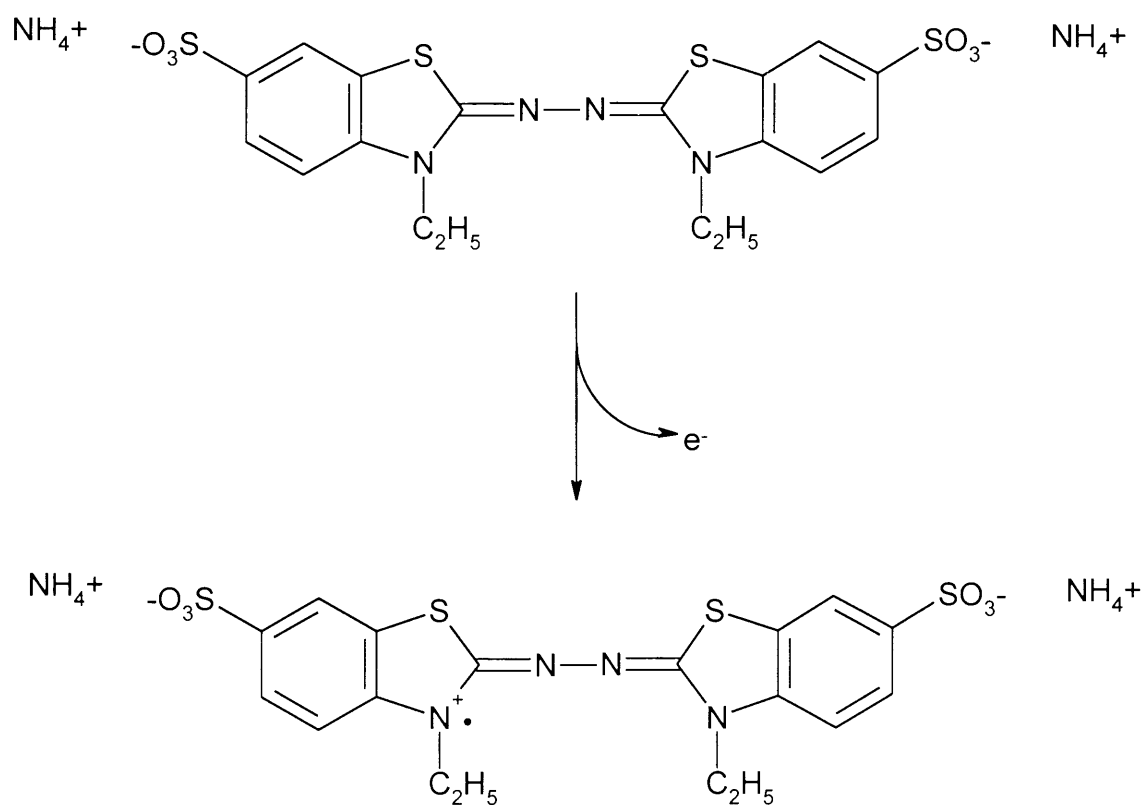
SCHEME 2.5.

2,2'-Azino-di-(3-ethylbenzthiazoline-6-sulfonic acid, (ABTS), top, and its cation radical product formed by one-electron oxidation.
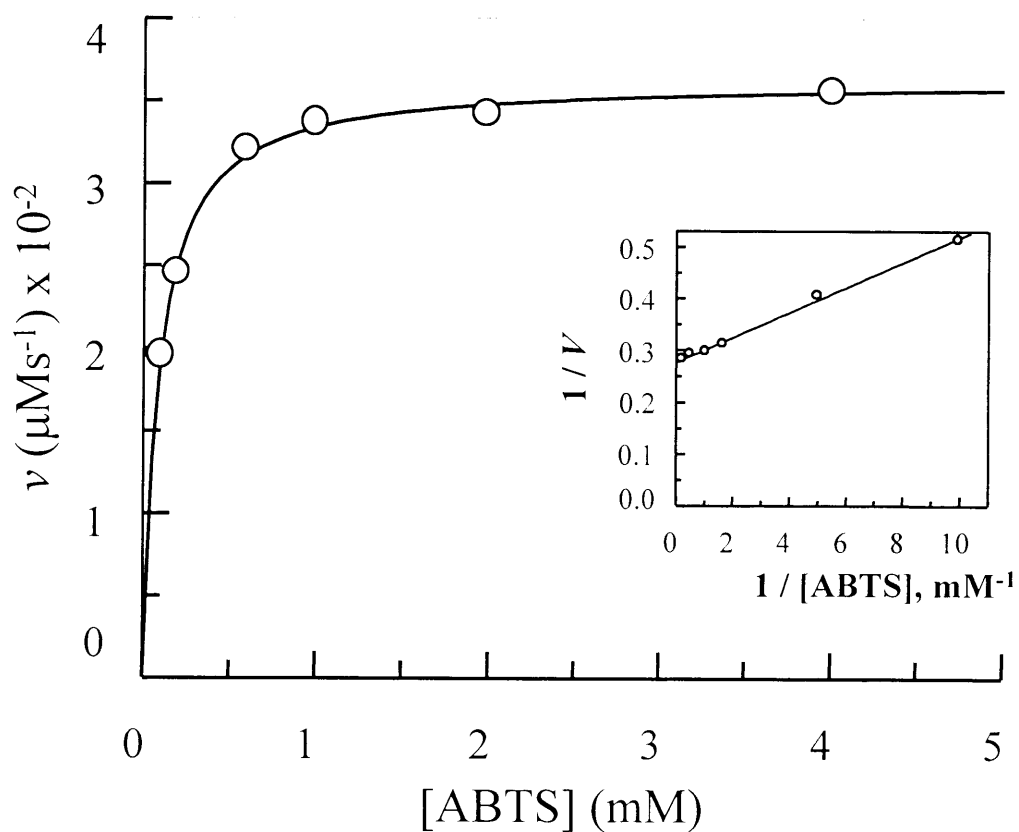
FIGURE 2.11

Steady state oxidation of ABTS by APX. Conditions: [APX] = 22.4 nM, 25.0

°C, sodium phosphate, pH 7.0, μ = 2.2 mM). The solid line is a fit of the data

to Michaelis-Menten equation. Inset: The Lineweaver-Burk plot.

2.3 DISCUSSION

The results presented in this work for the H_2O_2-dependent oxidation of p-cresol by APX are entirely consistent with a mechanism in which the oxidised Compound I intermediate of APX undergoes two, successive single electron reductions to generate, initially, the singly oxidised Compound II intermediate followed by regeneration of the ferric enzyme (equations [2.5] – [2.7]). Hence, the direct observation of a Compound II species during the catalytic cycle provides convincing evidence for the proposed mechanism. The observed products of the reaction, Scheme 2.1, which are derived from reactions of the p-methylphenoxy radical (PC•), can be accommodated from the known chemistry of the radical products.[2,4] Similarly, the observation that the exact product ratio (II:III) shows a dependence on enzyme concentration, Figure 2.4, can be sensibly rationalized using equations [2.5]-[2.7]. Hence, when [APX] is low, [PC•] will be correspondingly low compared to [PC] ([PC] in large excess over [APX] during the experiment) and most of the radical species will react with the excess PC to give Pummerer's ketone (PC• + PC → III). As [APX] increases, [PC•] increases and dimerisation of the radical (PC• + PC• → II) becomes more favourable.

Most interestingly, the results of the steady state experiments revealed a sigmoidal dependence on substrate concentration. Non-Michaelis kinetics have been observed previously for the oxidation of ascorbate[20] and the homodimeric structure of the APX enzyme[13] has been put forward as a possible explanation of the unusual concentration dependence. Our data for p-cresol oxidation do not appear to be consistent with this hypothesis, since almost identical kinetic behaviour was observed under high ionic strength conditions (500 mM) which would be expected to disrupt the salt bridges known to be involved in the monomer-dimer electrostatic interaction. Similar conclusions have recently been derived from site-directed mutagenesis experiments on APX,[14,15] in which the removal of charged residues at the dimer interface had no effect on the (non-Michaelis) steady state oxidation of ascorbate. In fact, the absence of an ionic strength dependence for p-cresol oxidation is consistent with the hydrophobic nature of the substrate and our data at all ionic strengths fit to a model in which two redox-active binding sites are involved in p-cresol oxidation. Interestingly, single turnover experiments on APX revealed no evidence for multiple binding sites which suggests that, under the conditions of these experiments,

only one binding site is utilised.

The possible existence of a second binding site for p-cresol is curious but not altogether unexpected. In fact, a consensus of data for APX is beginning to appear that is suggestive of a binding interaction with certain substrates which is more complex than the expected 1:1 ratio. For example, NMR data for binding of ascorbate to APX are consistent with the existence of two binding sites for the substrate[21] and experiments on site-directed variants and chemically modified derivatives of APX have established that the enzyme is likely to utilise different sites for aromatic and non-aromatic substrates.[14] When viewed more generally in the context of other peroxidases, the existence of a second binding site is not unprecedented. Hence, the cytochrome c/cytochrome c peroxidase[36] and, more recently, manganese peroxidase[37] binding interactions are, under certain conditions, known to involve more than one binding site. Very recently, discrete binding sites have been proposed for substrate binding in lignin peroxidase.[38] In general, however, the kinetic competence of these multiple sites is more difficult to establish in an unambiguous manner and, for APX, remains unclear.

2.3.1 Mechanism of p-Cresol Oxidation

One of the major features of the chemistry of phenols is the stabilization of the phenoxide ion (and the phenoxy radical) by the adjacent aromatic π-electron system and this results in the facile removal of the hydroxyl hydrogen (either as a proton or as a radical).

One-electron oxidation of phenoxide ions gives phenoxy radicals which may undergo coupling reactions. Oxidative coupling is an extremely important biosynthetic process but many *in vitro* examples are also known. It is rare for two phenoxy radicals to give a peroxide dimer; much more common is dimerisation by way of C-C bond formation. Both symmetrical and unsymmetrical dimers are obtainable, but these may themselves be highly reactive and undergo further transformation.[39]

One electron abstraction from p-cresol forms a p-cresol radical, of which there are three resonance forms which can be written as **a**, **b**, **c** in Scheme 2.6.
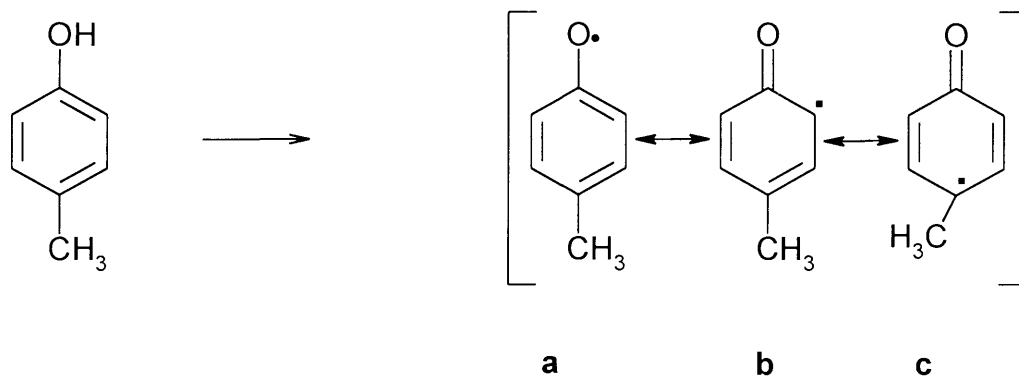
SCHEME 2.6

From these resonance forms, there are three coupling reactions possible. First, the form of b, in which an electron stays on *ortho* position of phenyl ring will couple with another b to form a biphenol coupling product (Scheme 2.7).
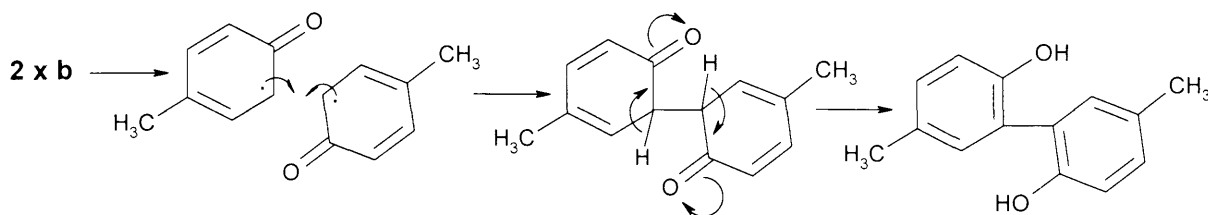
SCHEME 2.7

Second, the resonance form of **a**, in which the unpaired electron stays on oxygen atom of the radical molecule and b can undergo coupling reaction to form another coupling product (Scheme 2.8).
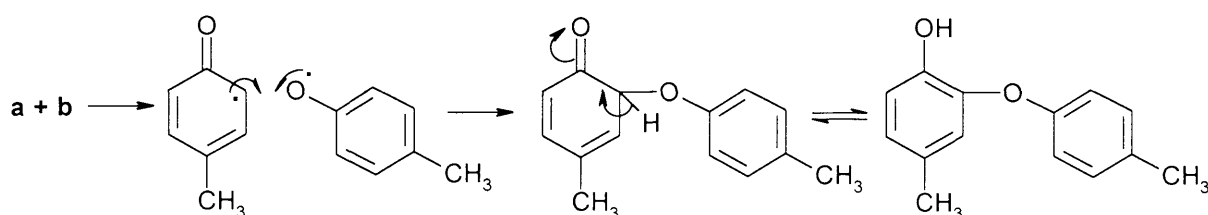
SCHEME 2.8

Third, the resonance form of **b**, and **c**, in which an unpaired electron stays on the *para* position of phenyl ring can undergo a coupling reaction to form Pummerres' ketone (Scheme 2.9).
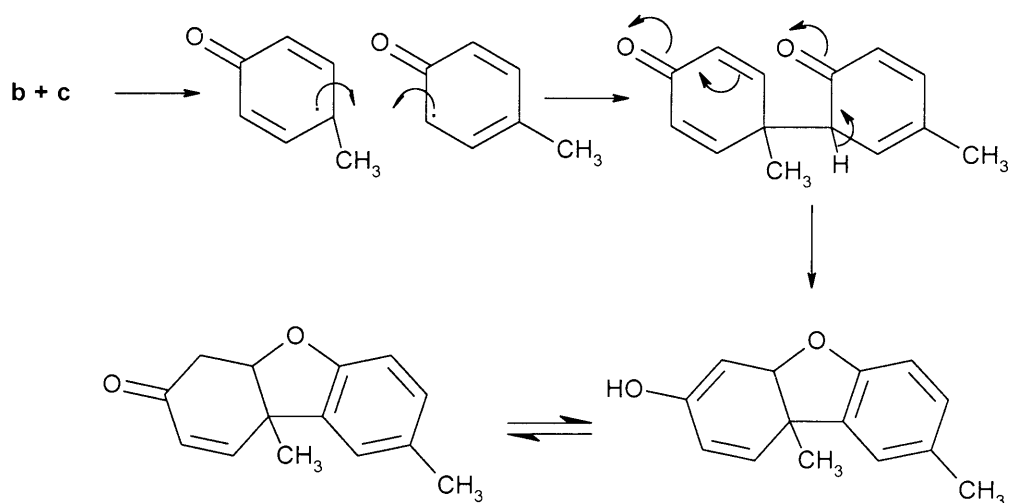
SCHEME 2.9

This is not the only mechanism for formation of Pummerer's ketone, however. It can also be formed by coupling of a phenoxy radical with *p*-cresol itself (Scheme 2.10). Evidence for this would come from the effects of enzyme concentration on product formation mentioned before.

Although it is rare for two phenoxy radicals to give a peroxide dimer, using cumene hydroperoxide instead of hydrogen peroxide yielded 1,1-dimethyl benzyl alcohol, which is equivalent to water formation from hydrogen peroxide. Interestingly this alcohol can behave as a substrate, since peroxide dimer formation along with other coupling products mentioned previously is observed (Scheme 2.11).
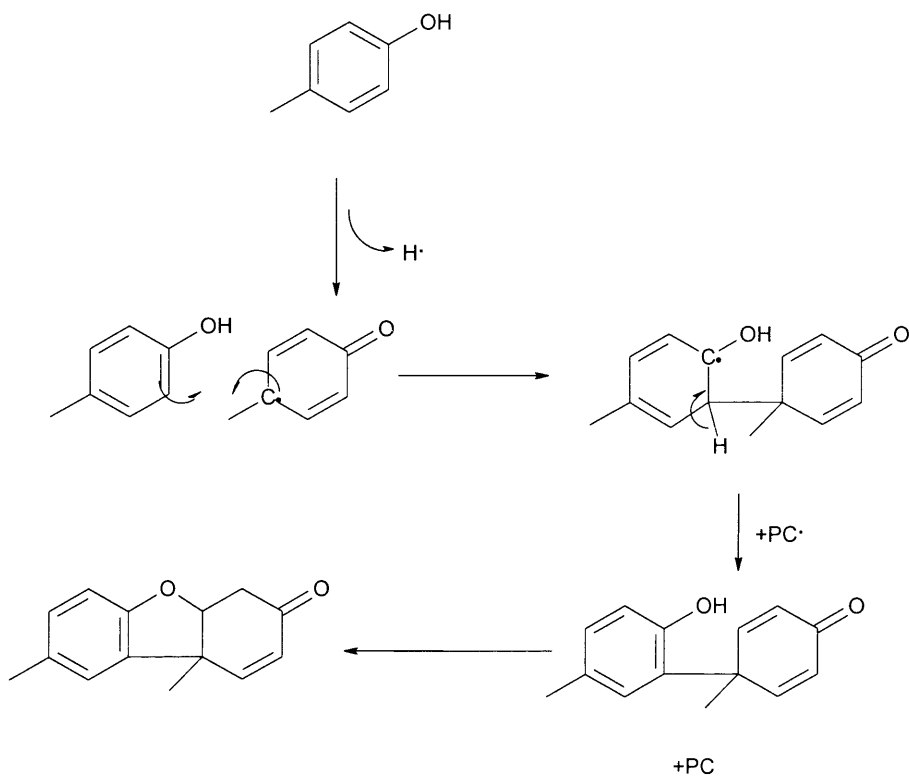
SCHEME 2.10
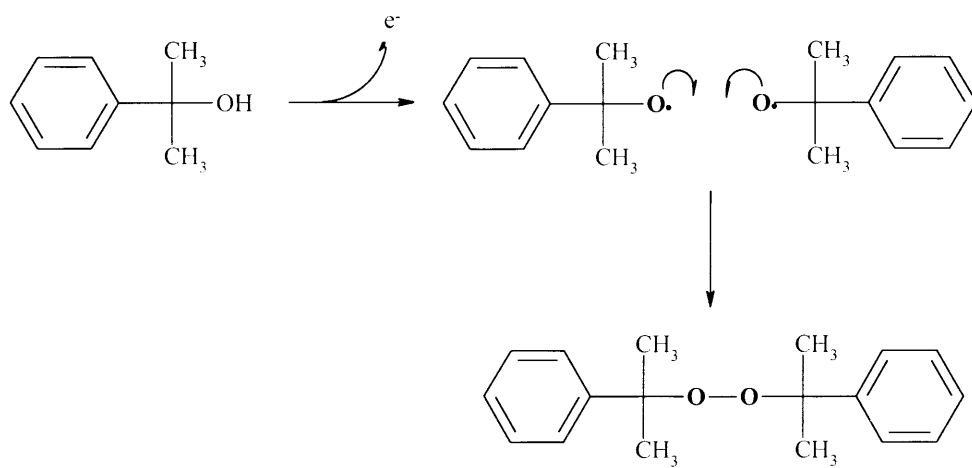
SCHEME 2.11

Formation of bis-(1-methyl-1-phenyl-ethyl) peroxide

2.4 REFERENCES

1   Saunders, B. C., Holmes-Siedle, A. G. and Stark, B. P., *Peroxidase: the properties and uses of a versatile enzyme and of some related catalysts*, Butterworths, London 1964.

2   Hewson, W. D. and Dunford, H. B., *J. Biol. Chem.*, 1976, **251**, 6036.

3   Casella, L., Monzani, E., Gullotti, M., Santelli, E., Poli, S. and Beringhelli, T., *Gaz. Chim. Ital.*, 1996, **126**, 121.

4   Hewson, W. D. and Dunford, H. B., *J. Biol. Chem.*, 1976, **251**, 6043.

5   Joshi, D. K. and Gold, M. H., *Eur. J. Biochem.*, 1996, **237**, 45.

6   Chung, N. and Aust, S. D., *Arch. Biochem. Biophys.*, 1995, **316**, 851.

7   Wariishi, H., Dunford, H. B., MacDonald, I. D. and Gold, M. H., *J. Biol. Chem.*, 1989, **264**, 3335.

8   Popp, J. L. and Kirk, T. K., *Arch. Biochem. Biophys.*, 1991, **288**, 145.

9   Chung, N. and Aust, S. D., *Arch. Biochem. Biophys.*, 1995, **316**, 733.

10   Koduri, R. S., Whitwam, R. E., Barr, D., Aust, S. D. and Tien, M., *Arch. Biochem. Biophys.*, 1996, **326**, 261.

11   Patterson, W. R., Poulos, T. L. and Goodin, D. B., *Biochemistry*, 1995, **34**, 4342.

12   Patterson, W. R. and Poulos, T. L., *J. Biol. Chem.*, 1994, **269**, 17020.

13   Patterson, W. R. and Poulos, T. L., *Biochemistry*, 1995, **34**, 4331.

14   Mandelman, D., Jamal, J. and Poulos, T. L., *Biochemistry*, 1998, **37**, 17610.

15   Mandelman, D., Schwarz, F. P., Li, H. and Poulos, T. L., *Protein Science*, 1998, **7**, 2089.

16   Dalton, D. A., in *Peroxidases in Chemistry and Biology, Vol. 2*, Everse, J., Everse, K. E. and Grisham, M. B. (Eds.): CRC Press, Boca Raton 1991, p. 139.

17   Bosshard, H. R., Anni, H. and Yonetani, T., in *Peroxidases in Chemistry and Biology, Vol. 2*, Everse, J., Everse, K. E. and Grisham, M. B. (Eds.): CRC Press, Boca Raton 1991, p. 51.

18   Dunford, H. B., in *Peroxidases in Chemistry and Biology, Vol. 2*, Everse, J., Everse, K. E. and Grisham, M. B. (Eds.): CRC Press, Boca Raton 1991, p. 1.

19   Marquez, L. A., Quitoriano, M., Zilinskas, B. A. and Dunford, H. B., *FEBS Lett.*, 1996, **389**, 153.

20   Mittler, R. and Zilinskas, B. A., *Plant Physiol.*, 1991, **97**, 962.

21   Hill, A. P., Modi, S., Sutcliffe, M. J., Turner, D. D., Gilfoyle, D. J., Smith, A. T.,

Tam, B. M. and Lloyd, E., *Eur. J. Biochem.*, 1997, **248**, 347.

22 Howiler, M., Zenzer, H. and Kohler, H., *Eur. J. Biochem.*, 1986, **158**, 609.

23 Hiner, A. N. P., Rodríguez-López, J. N., Arnao, M. B., Raven, E. L., García-Cánovas, F. and Acosta, M., *Biochem.J*, 2000, **348**, 321.

24 Casella, L., Poli, S., Gullotti, M., Selvaggini, C., Beringhelli, T. and Marchesini, A., *Biochemistry*, 1994, **33**, 6377.

25 Divi, R. L. and Doerge, D. R., *Biochemistry*, 1994, **33**, 9668.

26 Chance, B., *Arch. Biochem. Biophys.*, 1952, **41**, 416.

27 George, P., *Nature*, 1952, **169**, 612.

28 George, P., *Biochem.J*, 1953, **54**, 267.

29 Rodríguez-López, J. N., Martínez, J. I., Arnao, M. B., Acosta, M., Turner, D. D. and Raven, E. L., *Submitted to Eur. J. Biochem.*, .

30 Pappa, H., Patterson, W. R. and Poulos, T. L., *J. Biol. Chem.*, 1996, **1**, 61.

31 Schmitt, M. M., Schuler, E., Braun, M., Haring, D. and Schreier, P., *Tetrahedron Lett.*, 1998, **39**, 2945.

32 Sridhar, M., Vadivel, S. K. and Bhalerao, U. T., *Tetrahedron Lett.*, 1997, **38**, 5695.

33 Dunford, H. B., *Heme Peroxidases*, John Wiley, New York 1999.

34 Dalton, D. A., Hanus, F. J., Russell, S. A. and Evans, H. J., *Plant Physiol.*, 1987, **83**, 789.

35 Pruitt, K. M., Kamau, D. N., Miller, K., Mansson-Rahemtulla, B. and Rahemtulla, F., *Anal. Biochem.*, 1990, **191**, 278.

36 Erman, J. E. and Vitello, L. B., *J. Biochem. Mol. Biol.*, 1998, **31**, 307.

37 Mauk, M. R., Kishi, K., Gold, M. H. and Mauk, A. G., *Biochemistry*, 1998, **37**, 6767.

38 Doyle, W. A., Bloding, W., Veitch, N. C., Piontek, K. and Smith, A. T., *Biochemistry*, 1998, **37**, 15097.

39 Streitwieser, A. (JR) and Heathcock, C.H., *Introduction to Organic Chemistry*, 3rd Ed., Macmillan Pub.Com., London, 1989.

CHAPTER THREE

Alkyl Aryl Sulphide Oxidation Catalysed by Ascorbate Peroxidase and the W41A variant

3.1 INTRODUCTION

Haem peroxidases constitute a class of enzymes that catalyse the H_2O_2-dependent oxidation of a substrate using a two-equivalent oxidised intermediate known as Compound I.[1-3] The mechanistic aspects of haem peroxidase catalysis and the role of key active site amino acids are clearly defined, largely as a result of extensive kinetic studies on a number of site-directed variants of cytochrome *c* peroxidase and, subsequently, horseradish peroxidase (reviewed in[2,4,5] and briefly discussed in Chapter 1). This mechanistic data, combined with high-resolution crystallographic information for a number of peroxidase enzymes[6-16] has allowed detailed rationalisation of the catalytic and substrate binding properties of these enzymes and has provided a mechanistic framework that can be both experimentally tested and manipulated. Of particular interest has been to understand in a more general sense the diversity of function exhibited by haem proteins and the way in which these differences in reactivity are controlled.[17-19] Indeed, one of the most intriguing aspects of haem chemistry and function that has yet to be fully resolved is the relationship between the peroxidase and cytochrome P450 classes of enzymes.[20,21] Hence, whilst P450s are thought to utilise a similarly transient two-equivalent oxidised intermediate (which has only very recently been detected,[22,23] they are not only able to catalyse the insertion of one mole of oxygen into substrate – a reaction which peroxidases, with a few exceptions (*vide infra*), are unable to support - but also to achieve this in a enantioselective manner. The molecular basis for these differences in reactivities is not completely understood but is likely to derive, at least partially, from variations in the axial ligation to the haem and the access of the substrate to the oxidised ferryl species.[17-19]

3.1.1 Aims of This Work

As mentioned above, whilst peroxidases are unable to support true monoxygenase activity, they are capable of sulphide oxidation, Scheme 3.1. Hence, oxidations of this kind have been reported for a number of peroxidase enzymes,[24-37] although in all cases the results are presented as empirical observations with no attempt at rational catalytic redesign. The first enantioselective sulphoxidation catalysed by a peroxidase, CPO, was reported by Kobayashi in 1987,[32,38] and was followed by Colonna and co-workers.[28,39] Subsequently, in 1992, horseradish peroxidase was also shown to catalyse the enantioselective

sulphoxidation of various alky aryl sulphides.[40] With various degrees of enantioselectivity and yield, other peroxidases have been reported as being capable of sulphoxidation, including lactoperoxidase,[38,41] cytochrome c peroxidase,[42] *Coprinus cinereus* peroxidase,[34] myeloperoxidase and manganese peroxidase,[43,44] and vanadium peroxidases.[26] However, examples in which enhancements of the enantioselectivity of the sulphoxidation reaction have been successfully engineered have been far fewer[42,45-47] and a fully quantitative, structure-based molecular modelling rationalisation of the enantiomeric ratios has not been performed previously (although this has been attempted for cytochrome P450).[48-52]

In this chapter, we have embarked upon a series of experiments aimed at incorporating enantioselective sulphoxidation activity into the active site of recombinant pea cytosolic ascorbate peroxidase (rAPX). Studies by De Montellano and co workers on CcP and HRP [42,45-47] and our preliminary molecular modelling work indicated that the distal tryptophan residue at position 41 in rAPX may partially hinder access of the substrate to the haem and may control the enantiomeric ratios of products. Hence, a site-directed variant of rAPX in which Trp41 has been replaced with an alanine has been prepared and the effect of this alteration on the enantioselectivity of the reaction has been examined in detail. These experiments provide the first detailed analysis of sulphoxidation chemistry in APX and have established not only that specific enhancements in enantioselectivity can indeed be incorporated into the molecule, but also that structure-based molecular modelling techniques can provide a fully quantitative rationalisation of the stereoselectivities of rAPX and W41A.

3.2 RESULTS

The sulphides used in this study are shown in Scheme 3.1.

Sulphide → *R*-Sulphoxide + *S*-Sulphoxide
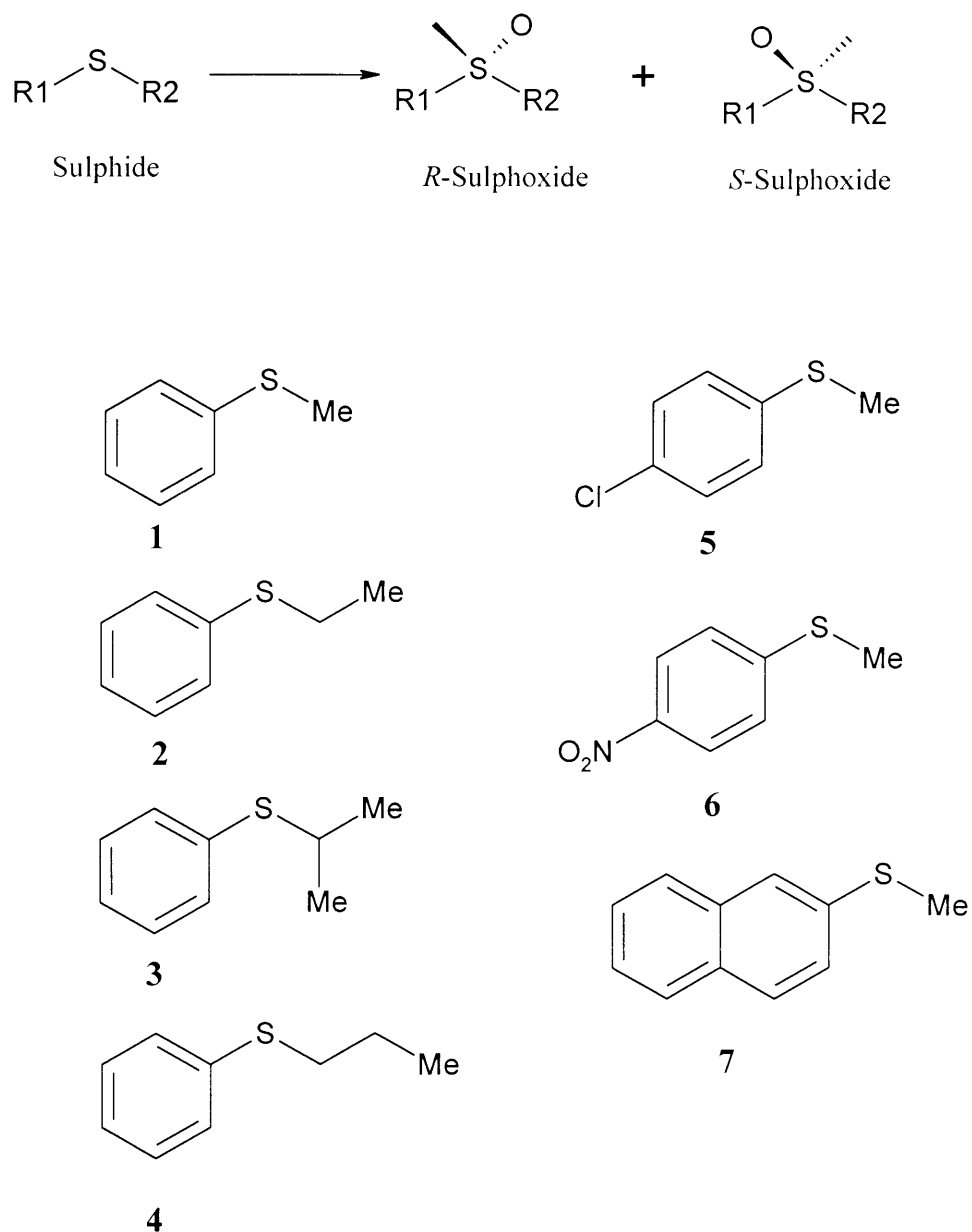
SCHEME 3.1.

Structures and stereochemistry of the sulphides studied in this work. In each case, R1 is the aromatic group and R2 is the alkyl group.

78

3.2.1 Characterisation of the APX W41A Mutant

3.2.1.1 Electronic Absorption Spectra of W41A

Wavelength maxima for the ferric derivative of the W41A variant (λ_{max}/nm (ε/mM^{-1}cm^{-1}) = 411 (125), 534, 560, 632) were found to be slightly different from those of rAPX,[53,54] Figure 3.1, and the red-shifted Soret band of W41A is indicative of an increased proportion of 6-coordinate, high-spin and/or 6-coordinate, low-spin haem. The electronic spectrum of the ferric derivative of the variant was altered in the presence of excess cyanide, indicative of the formation of a low-spin haem species (λ_{max}/nm (ε/mM^{-1}cm^{-1}) = 416.5 (118), 540) similar to that observed for rAPX (λ_{max}/nm = 419, 539). The spectrum of ferric W41A was, on the other hand, unaffected by the addition of either azide or fluoride, suggesting that these (weak field) ligands do not bind to the haem under these conditions (Table 3.1).

TABLE 3.1

Wavelength maxima (nm) and, in parenthesis, absorption coefficients (mM^{-1} cm^{-1}) for various ferric derivatives of W41A variant (Conditions: sodium phosphate, pH 7.0, μ = 0.10 M, 25.0 °C).

Derivative of W41A variant	Wavelength maxima, λ_{max}/nm (ε/mM^{-1}cm^{-1})
Fe(III)	411 (125), 534 (13), 560 (11), 632 (5)
Fe(III)-CN$^-$	416 (118), 540 (14)
Fe(III)-F$^-$	412 (124), 535 (13), 559 (11), 630 (5)
Fe(III)-N$_3^-$	411 (125), 534 (13), 563 (11), 629 (5)

3.2.1.2 Enzyme Activity

The specific activity of W41A for ascorbate (14.9 ± 0.6 units/mg enzyme) was approximately 20-fold less than the corresponding value for rAPX (320 ± 10 units/mg enzyme). On the other hand, the specific activity for oxidation of ABTS by W41A (4.75 ± 0.04 units/mg enzyme) was approximately the same as the corresponding value for rAPX (4.25 ± 0.1 units/mg enzyme).

79
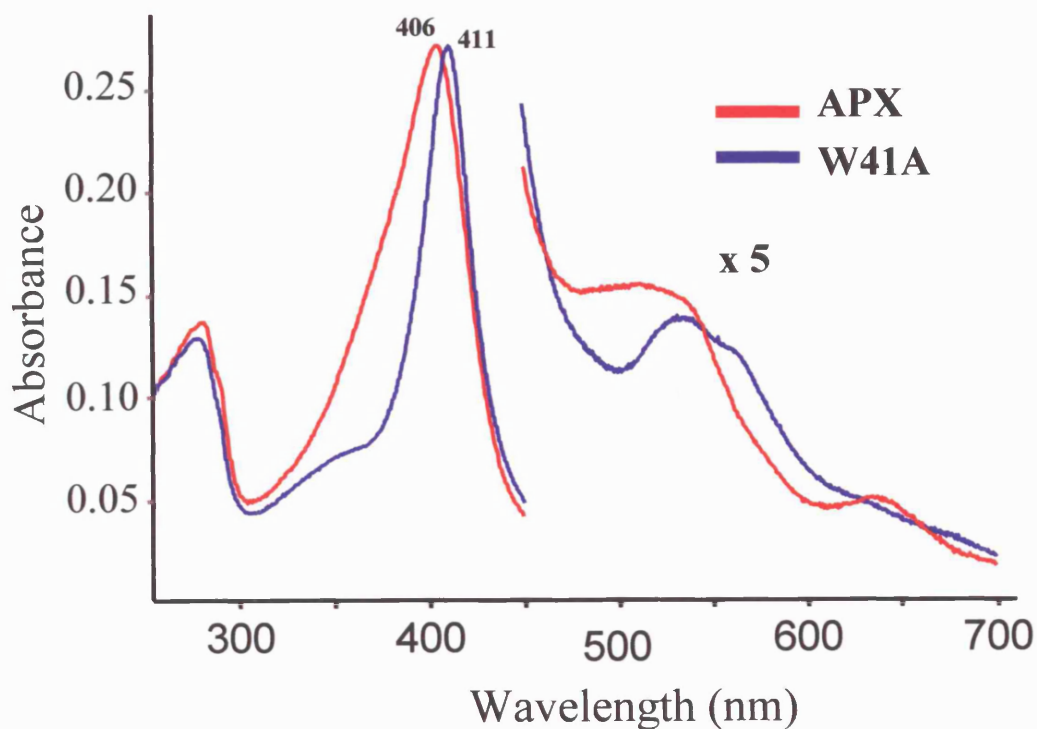
FIGURE 3.1

Ultraviolet-visible spectrum of APX (red) and W41A (blue). Absorbance reading in the 450-700 nm range have been amplified by a factor of five. Absorbance maxima are indicated. (Condition: sodium phosphate, pH 7.0, μ = 0.10 M, 25.0 ºC).

3.2.2 Oxidation of Sulphides

The oxidation of various sulphides (Scheme 3.1) catalysed by ascorbate peroxidase and the mutant (W41A) leads to the formation of the corresponding sulphoxides (Figure 3.2). The structures of the sulphoxide products were established by HPLC, NMR and GC-MS comparison with authentic samples of the sulphoxide standards. No products other than the sulphoxides were detected with all sulphides examined. Analysis of the sulphoxide products by chiral HPLC shows that the two enantiomers are produced. A significant degree of enantioselectivity was observed during catalytic sulphide oxidation to sulphoxide. Experimentally-derived enantiomeric ratios for sulphide oxidation are presented in Table 3.2. For rAPX, essentially racemic mixtures of *R*- and *S*-sulphoxides were obtained in all cases. In contrast, the W41A variant shows substantial enhancements in enantioselectivity for all sulphides, with the best results obtained for sulphide **6** (*R:S* = 85:15).

3.2.2.1 Oxygen Labelling Study

Confirmation that substrate oxidation is occurring by an oxo-transfer mechanism from the ferryl haem to the substrate comes from labelling experiments with [^{18}O] H_2O_2. Incubation of ethyl phenyl sulphide **2** with rAPX or W41A and [^{18}O] H_2O_2 showed that 95% (rAPX) and 96% (W41A) of the sulphoxide oxygen comes from the peroxide.
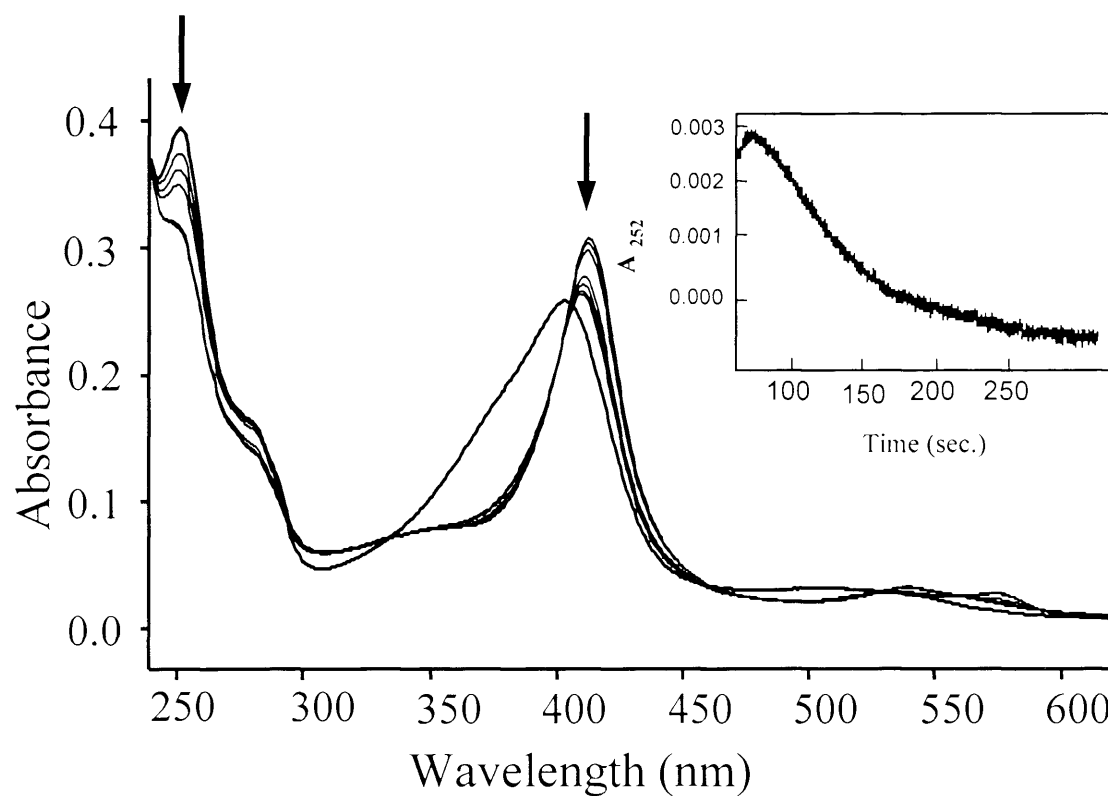
FIGURE 3.2

Time-dependent spectra of the enzyme intermediates of APX in the oxidation sulphide. Hereafter the enzyme started to return to the native (ferric) state. Inset: The decrease in absorbance at 252 nm., which is a measure of sulphoxide formation, is displayed. (Conditions: $[Pr^nPhS]$ = 50 µM, [APX] = 1.17 µM and $[H_2O_2]$ = 100 µM, sodium phosphate buffer, pH 7.0, μ = 0.10 M, 25.0 °C).

TABLE 3.2

Experimentally-derived enantiomeric ratios for sulphide oxidation

Sulphide	RAPX (*R:S*)	W41A (*R:S*)
1	51:49	63:37
2	49:51	80:20
3	50:50	64:36
4	50:50	63:37
5	49:51	65:35
6	48:52	85:15
7	48:52	53:47

3.2.3 Kinetic Studies

Steady state oxidation of sulphides **1 – 7** obeyed Michaelis-Menton kinetics. A typical plot of rate *versus* substrate concentration is shown in Figure 3.3. Steady state parameters, k_{cat} and K_m, for oxidation of sulphides **1 – 7** are given in Table 3.3. For sulphides **1 – 4**, values for k_{cat} are approximately 10-fold higher for the W41A variant than for rAPX. For sulphides **5** and **6**, no rate enhancements are observed; in contrast, sulphide **7** shows a >100-fold enhancement in rate. With the possible exception of sulphide **1**, values for K_m are largely unaffected by the replacement of Trp41.

3.2.4 Computational Studies

Computational work was carried out in collaboration with Dr M J Sutcliffe (University of Leicester). A comparison of the experimental and modelled enantiomeric product ratios for the seven different sulphides is given in Table 3.4. To check if 20 dockings were sufficient, a total of 50 dockings were generated for sulphide **4** in W41A. The 50 dockings resulted in an enantiomeric *R:S* ratio of 61:39; analysis of the first 20 dockings produced a ratio of 60:40. Thus, given the negligible difference between these ratios, the results generated for 20 dockings were used as the basis for further analysis of the experimental data.

The modelled results for both rAPX and W41A suggest that all seven sulphide compounds can be accommodated in the active site — this is consistent with the experimental observations (above) that ^{18}O-labelled product is produced when labelled $[^{18}O]H_2O_2$ is used as the source of oxidising equivalents. However, there are large discrepancies (Table 3.4) between the experimental (column 2) and modelled (column 3) values for the enantiomeric product ratios in rAPX, with an overestimation of the *R-* enantiomer in all cases. Reorientation of the sidechain of Arg38 in rAPX, such that access to the haem iron is much less restricted, produces modelled results that more closely match the experimental data (Table 3. 4 column 4 and Figure 3.4).
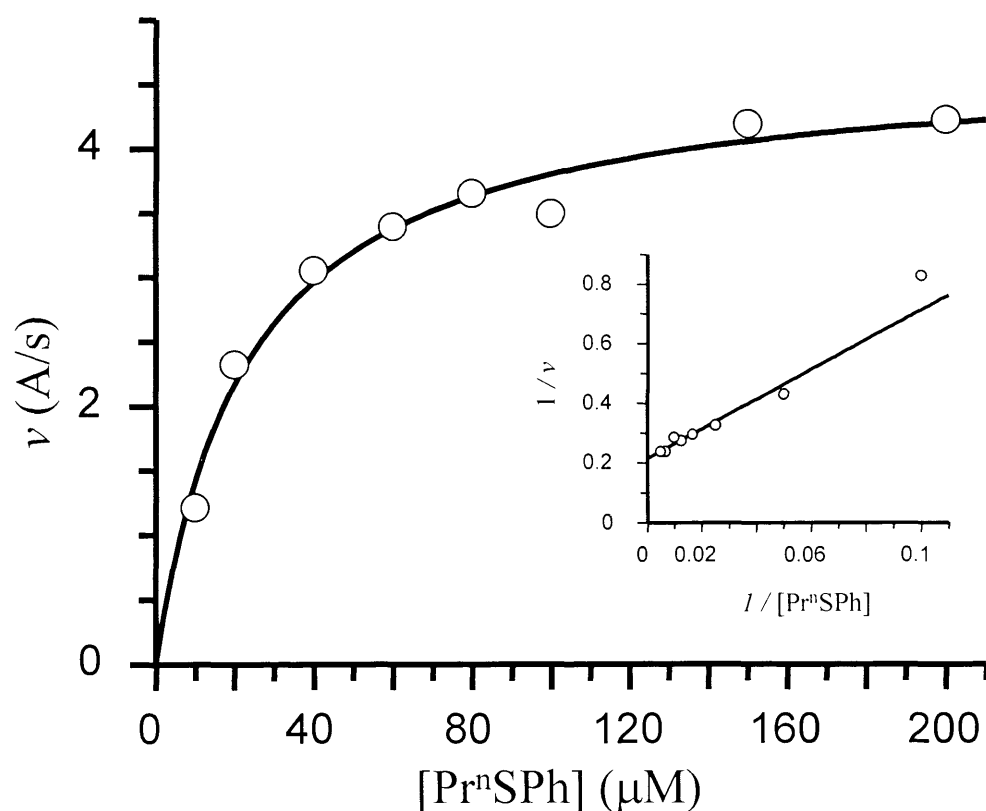
FIGURE 3.3

A typical Michaelis-Menten curve for APX-catalysed a sulphide oxidation.

Inset: Lineweaver-Burk plot. (Conditions: $[Pr^nSPh] = 0\text{-}200$ μM, $[APX] =$

1.17 μM, $[H_2O_2] = 100$ μM, sodium phosphate buffer, pH 7.0, $\mu = 0.10$ M,

$25.0\ ^\circ$C).

TABLE 3.3

Steady state parameters for oxidation of various sulphides by rAPX and W41A

(pH 7.0, μ = 0.10 M, 25.0 °C).

Sulphide	rAPX		W41A	
	K_m (μM)	k_{cat} (min^{-1})	K_m (μM)	k_{cat} (min^{-1})
1	27	1.0	80	18
2	17	2.7	16	47
3	23	2.6	31	34
4	24	0.4	28	15
5	120	8.1	150	13
6	7.5	0.9	27	1.1
7	6.3	0.3	8.7	37

TABLE 3.4

Experimental and modelled enantiomeric ratios (R:S) for oxidation of sulphides **1 – 7** by rAPX and W41A.

Sulphide	rAPX Experimental	rAPX[a] Modelled	rAPX[b] Modelled	W41A Experimental	W41A[a] Modelled	W41A[b] Modelled
1	51:49	100:0	50:50	63:37	75:25	63:37
2	49:51	100:0	50:50	80:20	78:22	75:25
3	50:50	100:0	55:45	64:36	80:20	75:25
4	50:50	100:0	55:45	63:37	60:40	70:30
5	49:51	100:0	53:47	65:35	100:0	63:37
6	48:52	100:0	53:47	85:15	80:20	80:20
7	48:52	100:0	53:47	53:47	75:25	53:47

[a] Sidechain of arginine 38 residue located as in crystal structure [9]

[b] Sidechain conformation of arginine 38 modified.

FIGURE 3.4

The orientation of sulphide **6** docked into the active site of rAPX. (**a**) Arg38 orientation as identified in the crystal structure: the pro-*R* lone pair (indicated) is poised for attack by the ferryl oxygen and (**b**) Arg38 orientation modified: both the pro-*R* (indicated) and pro-*S* lone pairs are poised for attack by the ferryl oxygen.

The discrepancy between the experimental (Table 3.4, column 5) and modelled (Table 3.4, column 6) values for the enantiomeric product ratios in W41A is much less, and in some cases there is a very good agreement. Where there is a large discrepancy (sulphides **3**, **5** and **7**), there is again an overestimation of the *R*- enantiomer. As with rAPX, reorientation of the sidechain of Arg38 produces modelled results that closely match the experimental data (Table 3.4 column 7 and Figure 3.5). Analysis of all of the docked conformations reveals that each sulphide adopts either one or three discrete clusters. When the sidechain of Arg38 is oriented as in the crystal structure, the aryl ring packs against the hydrophobic part of Arg38 and a single cluster is generated for all 7 sulphides, yielding 100% of the *R*-enantiomer. In this cluster, all the aryl rings are effectively overlayed on each other; there is a small amount of movement of the alkyl chain, but this is not large enough to affect the enantioselectivity. When the sidechain conformation of Arg38 is modified from that observed in the crystal structure, three discrete clusters are observed for all sulphides: the first cluster has the pro-*R* and the pro-*S* lone pair approximately equidistant from the ferryl oxygen (*e.g.* Figure 3.4b); the second and third clusters have either the pro-*R* (*e.g.* Figure 3.4a) or the pro-*S* lone pair, respectively, poised for attack by the ferryl oxygen. In all cases, the most highly populated cluster is that in which the pro-*R* lone pair is poised for attack. In each cluster, the aryl ring occupies a distinct position and is effectively overlayed in each conformation within a cluster. Furthermore, for the cluster yielding the *R*-enantiomer, the position of the aryl ring is essentially the same as that observed when Arg38 is oriented as in the crystal structure.

When the sidechain of Arg38 is oriented as in the crystal structure of rAPX in the modelled structure for W41A, there are two major observations. First, for sulphides **1-4** and **6-7**, there are two discrete clusters - in which either the pro-*R* or the pro-*S* lone pair is poised for attack by the ferryl oxygen - and, in all cases, the most highly populated cluster is that in which the pro-*R* lone pair is poised for attack. The aryl ring occupies a distinct position in each cluster and in a given cluster the aryl ring and alkyl group are overlayed. Two clusters are observed in these cases, rather than one as seen in rAPX, because the mutation W41A creates additional free volume in the active site, which can be occupied by the alkyl group to form the second cluster. Second, for substrate **5**, there is a single cluster with the pro-*R* lone pair poised for attack: this results in products which are 100% *R* (Figure 3.5a).
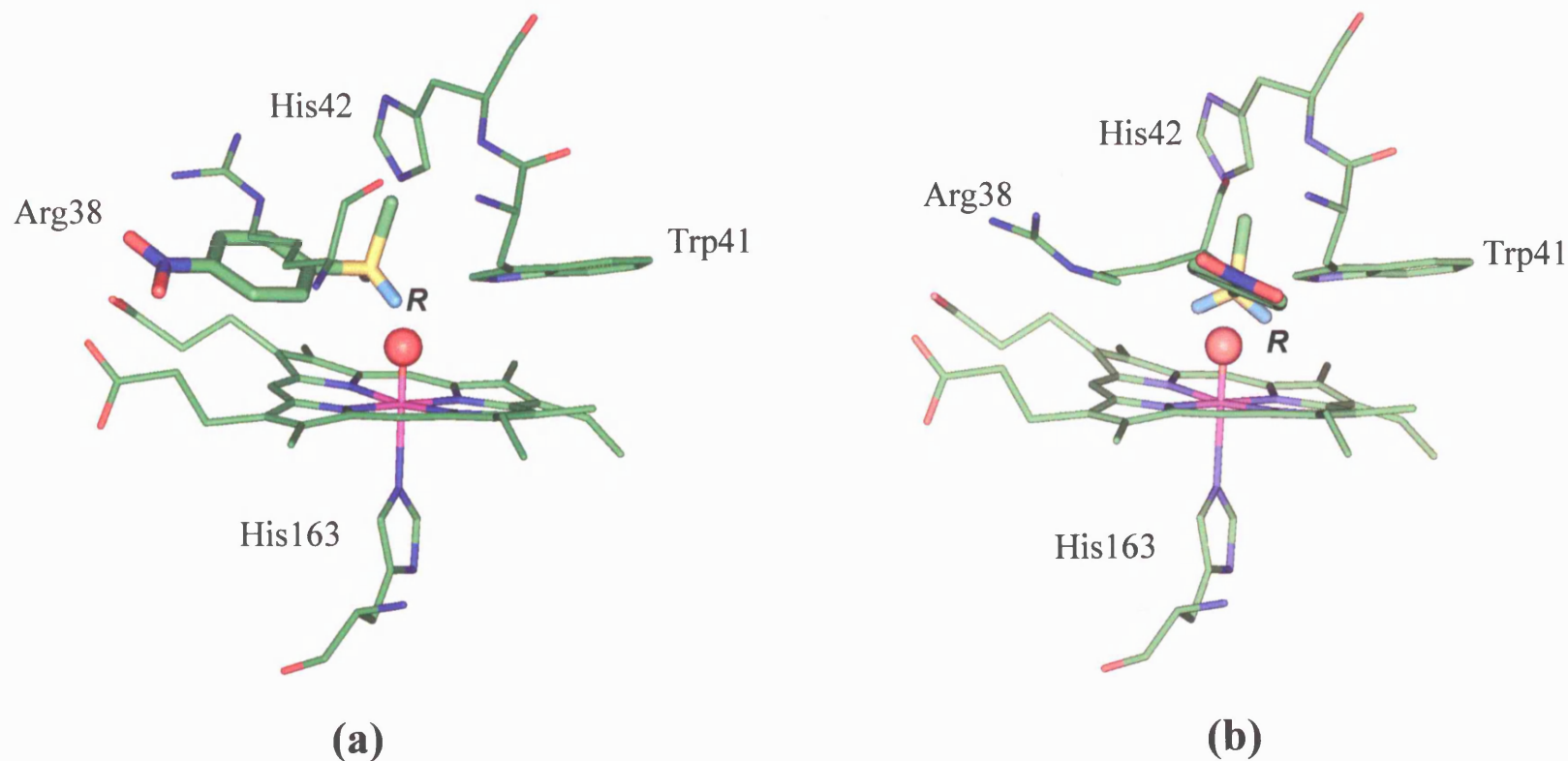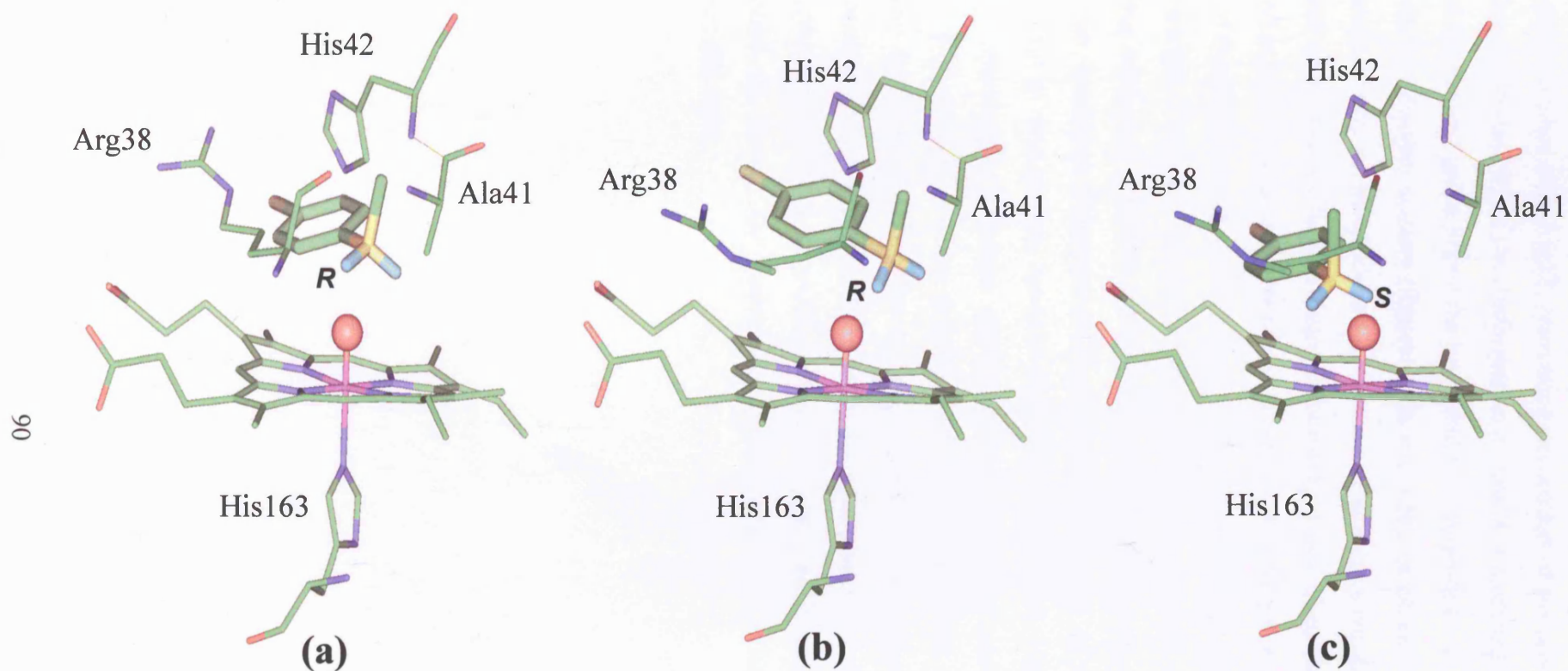
FIGURE 3.5

The orientation sulphide **5** docked into the active site of W41A. (**a**) Arg38 orientation as identified in the crystal structure: the pro-*R* lone pair (indicated) is poised for attack by the ferryl oxygen, (**b**) Arg 38 orientation modified: the pro-*R* lone pair (indicated) is poised for attack by the ferryl oxygen and (**c**) Arg 38 orientation modified: in a minority of cases the pro-*S* lone pair (indicated) is poised for attack by the ferryl oxygen.

This dominance of the *R*-enantiomer arises because the chloride substituent of sulphide **5** clashes sterically (due to its relatively large van der Waals radius) with the haem and the alkyl group clashes with Arg38, preventing occupation of the second cluster observed for the other substrates. When the conformation of Arg38 is modified in W41A, more space is created for the aryl group above the haem and all 7 sulphides – now including of sulphide **5** - form two discrete clusters (Figures 3.5b and 3.5c), in which the pro-*R* and pro-*S* lone pair, respectively, is poised for attack. These two clusters have the aryl ring in a slightly different orientation to the two clusters observed formed when the sidechain of Arg38 is oriented as in the crystal structure of rAPX (above). Sulphide **5** is now included as a direct result of the W41A mutation, since steric hindrance of the alkyl group of this sulphide has been relieved. Thus, two orientations of the sulphide are formed: each orientation has the aryl ring occupying a distinct position and, within each cluster, the aryl ring and alkyl group are overlayed. Attempts to directly assess the role of Arg38, by site-specific replacement of this residue, have, so far, been unsuccessful. Hence, removal of Arg38 leads to apo-enzyme formation during bacterial expression: reconstitution of the apo-enzyme with exogenous haem generates electronic spectra that are inconsistent with a high-spin iron and activities for ascorbate which are very low. Similarly anomalous spectroscopic and catalytic properties have also been observed in this laboratory for other (non-active site) variants of rAPX in which apo-enzyme is generated during bacterial expression. (E. Raven, The University of Leicester). These effects were not examined further in this work.

3.3 DISCUSSION

Initial examination of the crystal structure[9] of recombinant pea cytosolic APX revealed that Trp41 – which lines the active site and is approximately 55% solvent accesible – may partially hinder access of substrate to the haem and, hence, may account for the poor peroxygenase activity of rAPX. Furthermore, our original modelling studies indicated that efficient conversion of rAPX into a stereoselective oxidising agent for sulphides could be achieved by replacement of this residue by alanine (W41A). Hence, whilst rAPX produces a racemic mixture of products with all compounds studied, the W41A variant was initially predicted to produce products with R:S ratios as high as 4:1. As indicated in Table 3.4, these predictions were subsequently validated experimentally.

Site-specific replacement of Trp41 by alanine yields an enzyme with spectroscopic properties that differ slightly from rAPX. Hence, examination of the electronic spectrum of the ferric derivative of W41A reveal a wavelength maximum that is red-shifted compared to rAPX, suggesting the presence of increased quantities of either 6-coordinate, high-spin or 6-coordinate, low-spin haem (or both). Indeed, resonance Raman experiments[54] have shown that rAPX itself exists as a mixture of spin and coordination states in the ferric form and, whilst the exact quantities of each may vary slightly from sample to sample, there is currently no evidence to suggest that these variations affect catalytic activity in any way and we have not embarked upon a detailed rationalisation of the origin of this red shift for the W41A variant.

Although rAPX exhibited no enantioselectivity for any of the sulphides examined, experiments with labelled [^{18}O]H$_2$O$_2$ established that efficient (95% for sulphide **2**) transfer of peroxide oxygen to the substrate was occurring for rAPX, clearly indicating that the haem is partially accessible to the substrate even in the absence of a Trp41Ala mutation. These data are consistent with the results of the modelling experiments on rAPX – which clearly show that all seven sulphides can be accommodated in the pocket – and with previous work on horseradish peroxidase[25,27,38] in which transfer of oxygen from the ferryl species to the substrate has been established. With the exception of sulphides **5** and **6**, k_{cat} values for oxidation of all sulphides to the corresponding sulphoxide by W41A were found to be significantly faster than for rAPX (Table 3.3), which probably reflects a more favourable binding orientation in the haem pocket.

A systematic mechanistic study of the sulphoxidation reaction was beyond the scope of this thesis, although the source of the oxygen atom incorporated during sulphoxide formation from the corresponding sulphides was established (Section 3.2.2.1). The mechanism is likely to involve both one-electron oxidation of the substrate (discussed in Chapter 1) or direct, two-electron oxidation. Both mechanisms have been reported previously for other peroxidases,[32] and are referred to as the oxene and oxygen-rebound mechanism, Figure 3.6.

In the oxene mechanism, compound I directly transfers its oxygen to the sulphide and returns to the native state via this process, which is the accepted mechanism for CPO.[24] In the oxygen-rebound mechanism, the sulphide is first oxidised by compound I via one-electron oxidation to a sulphide radical cation, creating Compound II and a radical cation intermediate, possibly existing as a bound complex.[34] Subsequently, the oxygen is transferred from compound II to the sulphide and the enzyme returns to the native (ferric) state. Both processes may take place in or near the active site, since considerable enantioselectivity is observed. At high H_2O_2 concentration a third enzyme intermediate, compound III, can be formed (Figure 3.6). In most reactions this intermediate is believed to be a catalytic inactive, mostly a dead-end species leading to inactivated enzyme for most peroxidases, even though otherwise stated for some peroxidases.[55] In this work, a detailed mechanistic analysis has not been carried out, and we are not able to comment on whether or not the reaction proceeds by an oxygen rebound or oxene mechanism.

More interestingly, replacement of Trp41 with an alanine residue improves the stereoselectivity of the reaction for all seven sulphides, as was initially predicted by the preliminary modelling studies. However, whilst an improvement in the $R:S$ ratio is an empirically satisfying result, we sought to obtain a more quantitative rationalisation of our data based on the published structure for the enzyme.[9] Detailed analysis of all of the docking conformations for rAPX with all of the sulphides indicates that a single cluster of substrate binding conformations is observed when the sidechain of Arg38 is located as in the crystal structure. The absolute orientation of the lone pairs of the sulphide is determined by packing constraints between its aryl ring and the hydrophobic part of Arg38 and leads to modelled data that predict complete dominance of the R-isomer – in direct contrast to the experimental results.

Oxene Mechanism

$$O = \overset{\overset{\displaystyle R_1}{|}}{S} - R_2$$

$$\overset{\overset{\displaystyle R_1}{|}}{S} - R_2$$

$$H_2O_2 \qquad H_2O$$

$$-\!\!\!-\ Fe^{3+}\ -\!\!\!-$$
Native

$$\overset{\displaystyle O}{\underset{\displaystyle ||}{}}$$
$$-\!\!\!-\ Fe^{4+}\ \underline{\quad}\ ^{\bullet +}$$
Compound I

Oxygen Rebound Mechanism

$$O = \overset{\overset{\displaystyle R_1}{|}}{S} - R_2$$

$$\overset{\overset{\displaystyle R_1}{|}}{S} - R_2$$

$$\overset{\overset{\displaystyle R_1}{|}}{\overset{\displaystyle +}{\cdot}S - R_2}$$

$$\overset{\displaystyle O}{\underset{\displaystyle ||}{}}$$
$$-\!\!\!-\ Fe^{4+}\ -\!\!\!-\quad \textit{Compound II complex}$$

Excess H_2O_2

$$\overset{\displaystyle O^{\cdot\cdot}}{\underset{\displaystyle O}{\diagdown}}$$

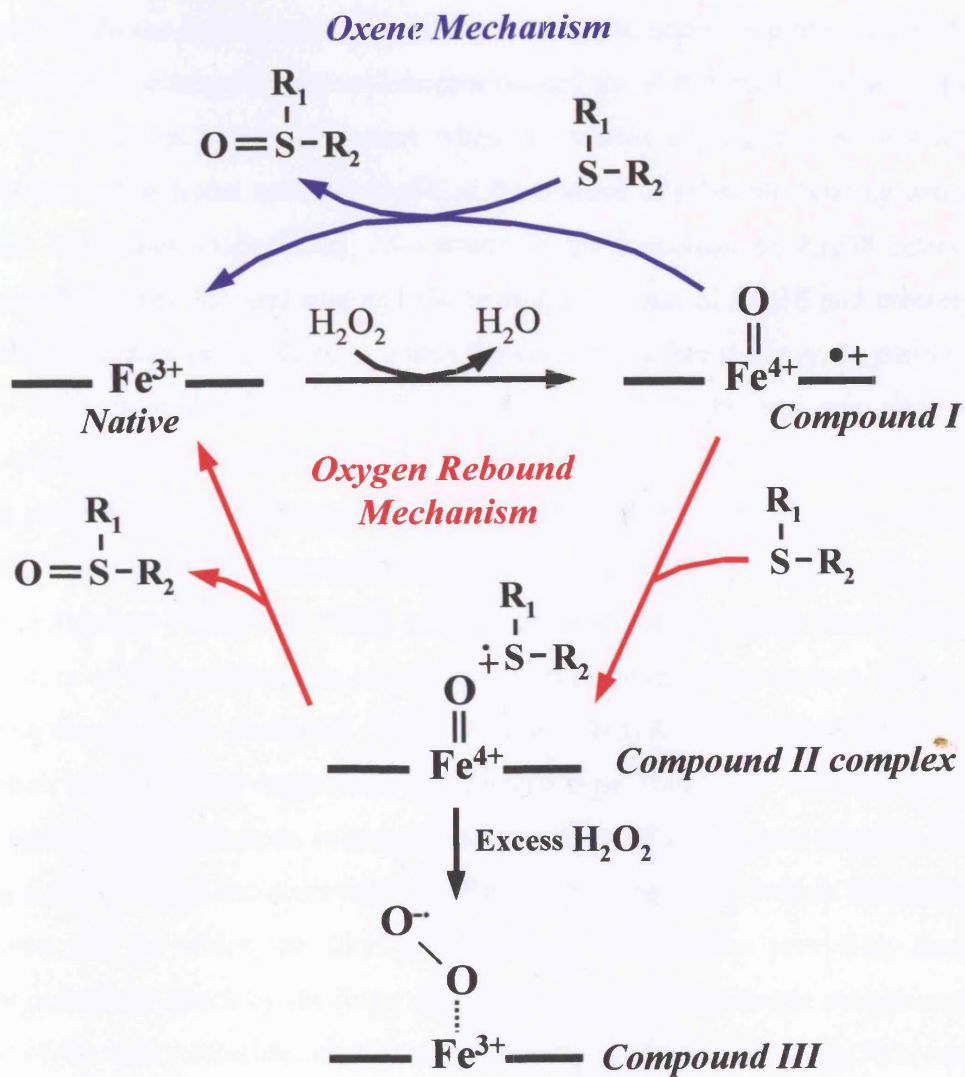$$-\!\!\!-\ Fe^{3+}\ -\!\!\!-\quad \textit{Compound III}$$

FIGURE 3.6

Oxene and oxygen rebound mechanisms for oxygen transfer to sulphides. Compound III formation under a large excess of H_2O_2 is also shown.

Precise correlation with the experimentally-determined $R:S$ ratios could only be achieved for rAPX when the sidechain of Arg38 was reoriented in response to binding of the substrate within the haem pocket. Whilst the discrepancies between the modelled data and the experimental observations were less pronounced for W41A than for rAPX, the data for W41A also showed better agreement when movement of Arg38 was included in the analysis and a functional role for Arg38 in the control of substrate binding orientation is therefore implicated (vide infra). Movement of the sidechain of Arg38 relieves steric interactions between the aryl ring and the hydrophobic part of Arg38 and creates a cavity above the distal face of the haem in which the substrate is free to move. In particular, three discrete clusters of the docked conformations – in which the aryl and alkyl rings are effectively overlaid – are observed for all sulphides: one of these clusters places the pro-R and the pro-S lone pair approximately equidistant from the ferryl oxygen, and the others place either the pro-R or the pro-S lone pairs close to the ferryl oxygen. As a result, the predicted absolute enantioselectivity reflects the populations within each cluster. Thus, modification of the conformation of Arg38, whilst retaining R-dominance, allows some of the S-enantiomer to be produced (Table 3.4). For W41A, the location of Arg38 is also influential, but to a lesser extent than for the wild type. Hence, for W41A, when Arg38 is in the same conformation as in the crystal structure of rAPX, two discrete clusters of binding conformations are observed - in which either the pro-R (which dominates) or the pro-S lone pair (in which the alkyl group occupies the volume previously occupied by W41) is poised for attack by the ferryl oxygen (sulphide 5 is the single exception to this on account of the bulky chloride substituent). When the conformation of Arg38 is modified in W41A, the results closely match the experimental data. Clearly, site-specific replacement of Arg38 will provide a more detailed assessment of the exact role of this residue in sulphide oxidation. Unfortunately, replacement of Arg38 in rAPX leads to apo-protein formation and reconstitution protocols using exogenous haem failed to generate active enzyme, as assessed by electronic spectroscopic and activity measurements (E Raven, The University of Leicester). These difficulties are currently being addressed using an alternative expression vector for rAPX. Reorientation of Arg38 and a possible functional role in the control of substrate binding and orientation, as indicated above, is interesting. In fact, large structural rearrangements of this kind are not unprecedented in both the chemistry of peroxidases and of the globins: movement of the corresponding arginine group (Arg48) has been identified for ligand-bound derivatives of cytochrome c peroxidase[56,57] and a functional, mobile Arg residue close to the haem has also been

established for *Aplysia* myoglobin[58,59] Indeed, Arg38 has also been suggested[60] to have a catalytic role in horseradish peroxidase-catalysed oxidation of ferulic acid. As mentioned above, the exact role of Arg38 in sulphide oxidation by APX can only be assessed directly by site-specific replacement and this was not considered further in this work.

3.4 REFERENCES

1   Dunford, H. B., *Heme Peroxidases*, John Wiley, New York 1999.

2   English, A. M. and Tsaprailis, G., *Adv. Inorg. Chem.*, 1995, **43**, 79.

3   Everse, J., Everse, K. E. and Grisham, M. B., *Peroxidases in Chemistry and Biology*, CRC Press, Boca Raton, Florida 1991.

4   Bosshard, H. R., Anni, H. and Yonetani, T., in *Peroxidases in Chemistry and Biology, Vol. 2*, Everse, J., Everse, K. E. and Grisham, M. B. (Eds.): CRC Press, Boca Raton 1991, p. 51.

5   Smith, A. T. and Veitch, N. C., *Curr. Opin. Chem. Biol.*, 1998, **2**, 269.

6   Gajhede, M., Schuller, D. J., Henricksen, A., Smith, A. T. and Poulos, T. L., *Nature Struct. Biol.*, 1997, **4**, 1032.

7   Henriksen, A., Welinder, K. G. and Gajhede, M., *J. Biol. Chem.*, 1998, **273**, 2241.

8   Sundaramoorthy, M., Terner, J. and Poulos, T. L., *Structure*, 1995, **3**, 1367.

9   Patterson, W. R. and Poulos, T. L., *Biochemistry*, 1995, **34**, 4331.

10   Choinowski, T., Bloding, W., Winterhalter, K. H. and Piontek, K., *J. Mol. Biol.*, 1999, **286**, 809.

11   Kunishima, N., Fukuyama, K., Matsubara, H., Hatanaka, H., Shibano, Y. and Amachi, T., *J. Mol. Biol.*, 1994, **235**, 331.

12   Edwards, S. L., Raag, R., Wariishi, H., Gold, M. H. and Poulos, T. L., *Proc. Natl. Acad. Sci. USA*, 1993, **90**, 750.

13   Finzel, B. C., Poulos, T. L. and Kraut, J., *J. Biol. Chem.*, 1984, **259**, 13027.

14   Sundaramoorthy, M., Kishi, K., Gold, M. H. and Poulos, T. L., *J. Biol. Chem.*, 1994, **269**, 32759.

15   Petersen, J. F. W., Kadziola, A. and Larsen, S., *FEBS Lett.*, 1994, **339**, 291.

16   Zeng, J. and Fenna, R. E., *J. Mol. Biol.*, 1992, **266**, 185.

17   Dawson, J. H., *Science*, 1988, 433.

18   Ortiz de Montellano, P. R., *Annu. Rev.Pharmacol. Toxicol.*, 1992, **32**, 89.

19   Ortiz de Montellano, P. R., *Acc. Chem. Res.*, 1987, **20**, 289.

20   Ortiz de Montellano, P. R., *Cytochrome P450*, Plenum Press, New York 1995.

21   Lewis, D. F. V., *Cytochromes P450*, Taylor and Francis, London 1996.

22   Schlichting, I., Berendzen, J., Chu, K., Stock, A. M., Maves, S. A., Benson, D. E., Sweet, R. M., Ringe, D., Petsko, G. A. and Sligar, S. G., *Science*, 2000, **287**, 1615.

23   Wilker, J. J., Dmochowski, I. J., Dawson, J. H., Winkler, J. R. and Gray, H. B., *Angew. Chem. Int. Ed. Engl.*, 1999, **38**, 90.

24   Baciocchi, E., Lanzalunga, O. and Malandrucca, S., *J. Am. Chem. Soc.*, 1996, **118**, 8973.

25   Harris, R. Z., Newmyer, S. L. and Ortiz de Montellano, P. R., *J. Biol. Chem.*, 1993, **268**, 1637.

26   ten Brink, H. B., Tuynman, A., Dekker, H. L., Hemrika, W., Izumi, Y., Oshiro, T., Schoemaker, H. E. and Waver, R., *Inorg. Chem.*, 1998, **37**, 6780.

27   Doerge, D. R., Cooray, N. M. and Brewster, M. E., *Biochemistry*, 1991, **30**, 8960.

28   Colonna, S., Gaggero, N., Manfredi, A., Casella, L., Gullotti, M., Carrea, G. and Pasta, P., *Biochemistry*, 1990, **29**, 10465.

29   Burner, U. and Obinger, C., *FEBS Lett.*, 1997, **411**, 269.

30   Perez, U. and Dunford, H. B., *Biochemistry*, 1990, **29**, 2757.

31   van Deurzen, M. P. J., van Rantwijk, F. and Sheldon, R. A., *Tetrahedron*, 1997, **53**, 13183.

32   Kobayashi, S., Nakano, M., Kimura, T. and Schaap, A. P., *Biochemistry*, 1987, **26**, 5019.

33   Goto, Y., Matsui, T., Ozaki, S.-i., Watanabe, Y. and Fukuzumi, S., *J. Am. Chem. Soc.*, 1999, **121**, 9497.

34   Tuynman, A., Vink, M. K. S., Dekker, H. L., Schoemaker, H. E. and Wever, R., *Eur. J. Biochem.*, 1998, **258**, 906.

35   Burner, U., Jantschko, W. and Obinger, C., *FEBS Lett.*, 1999, **443**, 290.

36   Casella, L., Gullotti, M., Ghezzi, R., Poli, S., Beringhelli, T., Colonna, S. and Carrea, G., *Biochemistry*, 1992, **31**, 9451.

37   Zaks, A. and Doddds, D. R., *J. Am. Chem. Soc.*, 1995, **117**, 10419.

38   Kobayashi, S., Nakano, M., Goto, T., Kimura, T. and Schaap, A. P., *Biochem. Biophys. Res. Comm.*, 1986, **135**, 166.

39   Colonna, S., Gaggero, N., Casella, L., Carrea, G. and Pasta, P., *Tetrahedron-Asymm.*, 1992, **3**, 95.

40   Colonna, S., Gaggero, N., Carrea, G. and Pasta, P., *Chem. Commun.*, 1992, 357.

41   Doerge, D. R., *Arch. Biochem. Biophys.*, 1986, **244**, 678.

42   Miller, V. P., DePillis, G. D., Ferrer, J. C., Mauk, A. G. and Ortiz de Montellano, P. R., *J. Biol. Chem.*, 1992, **267**, 8936.

43   Tuynman, A., Spelberg, J. L., Kooter, I. M., Schoemaker, H. E. and Wever, R., *J. Biol. Chem.*, 2000, **275**, 3025.

44   Tuynman, A., Schoemaker, Hans E and Wever, R., *Monatshefte fur Chemie*, 2000, **131**, 687.

45   Ozaki, S.-i. and Ortiz de Montellano, P. R., *J. Am. Chem. Soc.*, 1995, **117**, 7056.

46   Ozaki, S.-I. and Ortiz de Montellano, P. R., *J. Am. Chem. Soc.*, 1994, **116**, 4487.

47   Savenkova, M. I. and Ortiz de Monyellano, P. R., *Arch. Biochem. Biophys.*, 1998, **351**, 286.

48   De Voss, J. J., Sibbesen, O., Zhang, Z. and Ortiz de Montellano, P. R., *J. Am. Chem. Soc.*, 1997, **119**, 5489.

49   De Voss, J. J. and Ortiz de Montellano, P. R., *J. Am. Chem. Soc.*, 1995, **117**, 4185.

50   Ortiz de Montellano, P. R., Fruetel, J. A., Collins, J. R., Camper, D. L. and Loew, G. H., *J. Am. Chem. Soc.*, 1991, **113**, 3195.

51   Fruetel, J., Chang, Y.-T., Collins, J. R., Loew, G. L. and Ortiz de Montellano, P. R., *J. Am. Chem. Soc.*, 1994, **116**, 11643.

52   Fruetel, J. A., Collins, J. R., Camper, D. L., Loew, G. L. and Ortiz de Montellano, P. R., *J. Am. Chem. Soc.*, 1992, **114**, 6987.

53   Hill, A. P., Modi, S., Sutcliffe, M. J., Turner, D. D., Gilfoyle, D. J., Smith, A. T., Tam, B. M. and Lloyd, E., *Eur. J. Biochem.*, 1997, **248**, 347.

54   Nissum, M., Neri, F., Mandelman, D., Poulos, T. L. and Smulevich, G., *Biochemistry*, 1998, **37**, 8080.

55   Howiler, M., Zenzer, H. and Kohler, H., *Eur. J. Biochem.*, 1986, **158**, 609.

56   Edwards, S. L., Poulos, T. L. and Kraut, J., *J. Biol. Chem.*, 1984, **259**, 12984.

57   Edwards, S. L. and Poulos, T. L., *J. Biol. Chem.*, 1990, **265**, 2588.

58   Qin, J., La Mar, G. N., Ascoli, F., Bolognesi, M. and Brunori, M., *J. Mol. Biol.*, 1992, 891.

59   Conti, E., Moser, C., Rizzi, M., Mattevi, A., Lionetti, C., Coda, A., Ascenzi, P., Brunori, M. and Bolognesi, M., *J. Mol. Biol.*, 1993, **233**, 498.

60   Henriksen, A., Smith, A. T. and Gajhede, M., *J. Biol. Chem.*, 1999, **274**, 35005.

CHAPTER FOUR

*Sulphide Oxidation Catalysed by Cytochrome P450 BM3*

4.1 INTRODUCTION

Cytochrome P450s are an important class of enzymes. They present in all types of living cells (discussed in Chapter 1) and play vital role in biological systems, involved in the detoxification of the living organism (detoxifications mostly start with the oxygenation of lipophilic *xenobiotics*, that are subsequently conjugated with glycosides, gluthatione or sulphates to become water soluble, extractable metabolites). They have therefore been most thoroughly studied in mammalians.[1-7] Eventually, studies on this class of enzymes may lead to utilise P450s not only *in vivo* but *in vitro* applications. The use of cytochrome P450s in organic synthesis is now expanding dramatically, since there are many reactions in organic synthesis which it is either impossible or difficult to perform and often require environmentally hazardous substances (e.g. heavy metals).

Cytochrome P450 enzymes are related to peroxidases, since there are many similarities between peroxidases and cytochrome P450 enzymes in terms of prosthetic group and catalytic mechanism. However, there are also important differences in three - dimensional structure, interactions with other proteins and the reactions catalysed. The focus of this study will be on the reaction catalysed by both enzymes, in particular enantioselective sulphoxidation of simple pro-chiral sulphides. The use of haem peroxidases in sulphoxidation reactions is discussed in Chapter 3. In here, however, an involvement of cytochrome P450 enzymes in the oxidation of alkyl aryl sulphides will be discussed.

4.1.1 Enantioselective Sulphoxidation

One of the most remarkable reactions of biocatalysis is sulphoxidation, the formation of a chiral sulphoxide by oxidation of a prochiral sulphide[8] (Scheme 4.1).
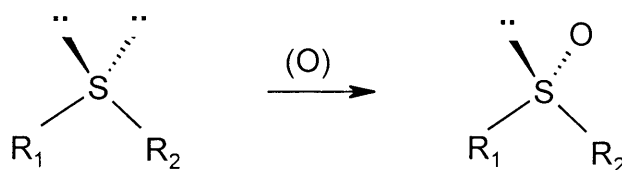
SCHEME 4.1

101

One of the biological approaches to the preparation of chiral sulphoxides with high regio- and setereoselectivity is to use of either microorganisms or isolated oxidative enzymes. The first use of microorganisms for such reactions can be traced back as early as 1960s. One of the first discoveries, reported by Dadson and co-workers in 1962,[9] was the use of a fungus, *Aspergillus niger* to oxidize benzyl phenyl sulphide to the corresponding sulphoxide with a reasonable degree of enantioselectivity (40% ee) (Scheme 4.2).

SCHEME 4.2

Subsequently, a systematic study of fungal oxidation of a series of unsymmetrical substituted organic sulphides was carried out in the laboratories of Professor Henbest.[10,11] In the last decades, there were more microorganism-catalysed sulphoxidation reaction discovered and reported, such as *Mortierella isabellina*[12] and *Helminthosporium species.*[13] Bacteria have also been discovered to be capable of enantioselective oxidation of organic sulphides, examples including, *Streptomyces* species,[14] *Corynebacterium equi,*[15-17] and *Pseudomonas.*[18,19]

Although the isolation and usage of oxidative enzymes in sulphoxidation reactions took a long time to discover and develop, cytochrome P450-dependent monooxygenases have been intensively studied in recent years.[8] Walsh and co workers[20] have described the synthesis of both enantiomers of ethyl *p*-toly sulphoxide by the use of purified monooxygenase from dog liver microsomes (*R*-sulphoxide, A) or cyclohexanone monooxygenase (*S*-sulphoxide, B) from *Acinetobacter* (Scheme 4.3).

Subsequently, the investigation was extended by Carrea and co-workers[21] to the other sulphoxides using the same species. Additionally, sulphoxidation catalysed by cytochrome P450 enzymes have been further studied using rat liver microsomes[22,23] or enzymes from microbial origin.[24]
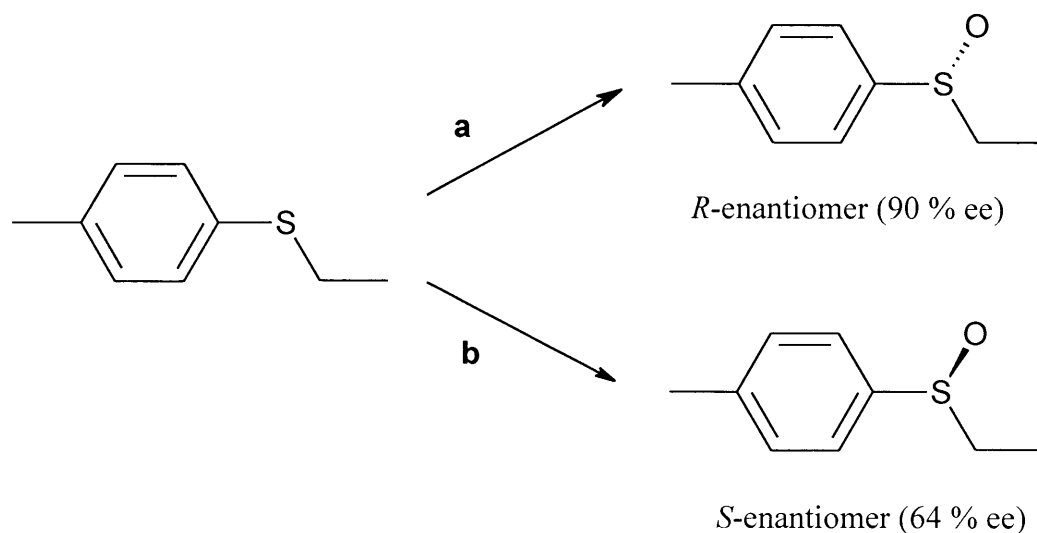
SCHEME 4.3

Chiral *p*-toly sulphoxide formation from oxidation of *p*-toly sulphide using (**a**) dog liver microsomes and (**b**) cyclohexanone monooxygenase.

The most recent work has been carried out using the cytochrome P450$_{cam}$ enzyme from *Pseudomonas putida*, the best-studied enzyme in this family.[25] Frutel and co-workers[26] have shown that P450$_{cam}$ is capable of catalysing the sulphoxidation of phenyl methyl sulphides and *p*-methyl phenyl sulphide to the corresponding sulphoxide with moderate degree of enantioselectivity (44 % ee and 4 % ee) (Scheme 4.4).
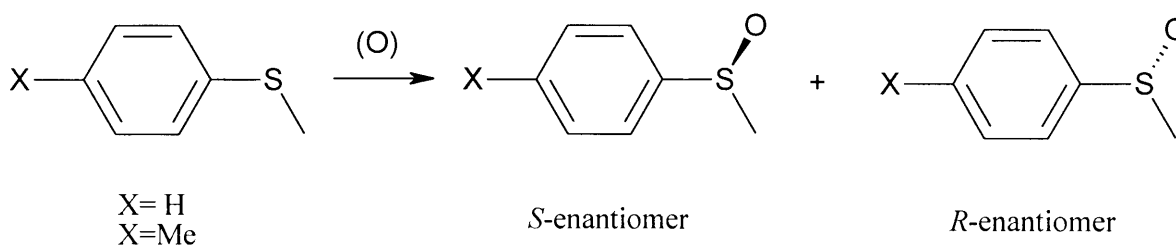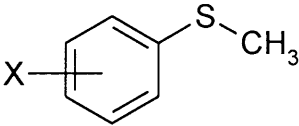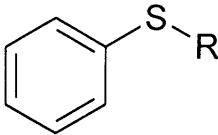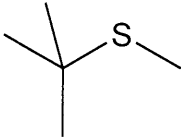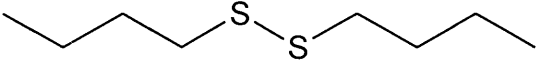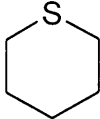
SCHEME 4.4

A large number of studies on cytochrome P450 enzyme-catalysed oxidation of sulphides have been reported and it is not possible to mention each of them individually, instead an indication of the diversity of substrate structure tolerated by cytochrome P450 monooxygenases is given in Table 4.1, in which yields and enantiomeric excesses for a representative sample of substrates are summarized.

TABLE 4.1

Yields and enantiomeric excesses for the catalytic oxidation of various substrates.

Substrate	Yield (%)	Asymmetric induction (%e.e.)	References
X = p-F, o-CH$_3$, m-CH$_3$, p-CH$_3$, o-Cl , p-Cl, o-CH$_3$O, p-CH$_3$O	35-94	32-92	21,26
R = Me, Et, Pro^i	88,86,93	99,47,3	21,26
	98	99	21
	85	32	21
	NG	NG	20

4.1.2 Binding of Sulphide Substrates to Cytochrome P450

The absence of studies of substrate binding between cytochrome P450 and sulphides limits the understanding of this substrate – enzyme interaction. Instead, more information can be obtained by direct comparison between various monooxygenases and their substrates, which naturally occur in metabolism. The correlations that exist between the hydrophobic character of the substrate and its oxidation feature (both the rate of substrate oxidation and substrate induced spectral changes in the enzyme) suggest that hydrophobic interactions play an important role in the binding of cytochrome P450 substrates.[1] The observation by Fukushima and co-workers[27] and, Waxman and co-workers[28] suggested that the oxidation of sulphides to corresponding sulphoxides is most efficient in terms of overall yield when the substrate carries large hydrophobic substituents, and is least efficient when the substrate carries polar groups (e.g., NO_2). On the basis of this observation, the hydrophobic binding interaction between the enzyme and substrate and the direction of oxygenation at either of a pro-S or pro-R sulphur position (determined by the three dimensional relationship between the bound substrate and the haem moiety) is responsible for the enantioselective formation of sulphoxide. (Figure 4.1).

Directions of Oxidation

Pro-S Pro-R
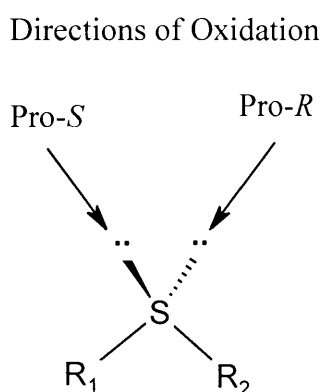
FIGURE 4.1

Stereoselectivity in enzymatic sulphide oxidation provided that R_1 is the aryl (e.g. phenyl) group and R_2 is the alkyl group (e.g. methyl).

There are however, many enzymes that catalyse sulphoxidation reaction with little or no stereoselectivity. The possible explanation for such an observation could either be an enzyme operating with non-specific substrate binding followed by a specific direction of

oxidation or a non-specific direction of oxidation (where the two lone pairs on the sulphur atom are equidistant from the oxidising species) following specific substrate binding.

4.1.3 Mechanism of Oxidation of Sulphides

The oxidizing species reacting with the sulphur in the sulphide substrates is formed within the catalytic cycle by which all cytochrome P450 monooxygenases function, the Fe-O intermediate (Scheme 4.5). The true nature of the oxidizing species is not fully characterized, but studies in this area agree that a ferryl species is the most likely reactive intermediate.[1,2]
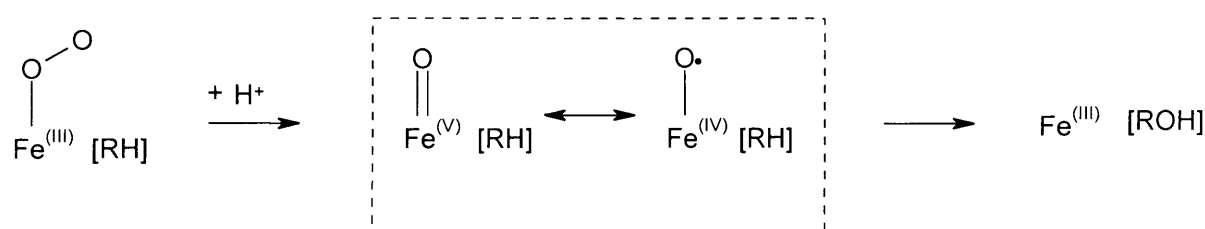
SCHEME 4.5

Although an intensive mechanistic study has been carried out for the hydroxylation at a saturated carbon,[13] there is no comparable mechanistic study available for sulphoxidation. However, since sulphur and carbon are both oxidized by the same enzyme it is assumed that the oxidizing species in a sulphoxidation reaction is the same as that for a carbon centred hydroxylation, which involves the nonconcerted radical – rebound mechanism outlined in Scheme 4.6.
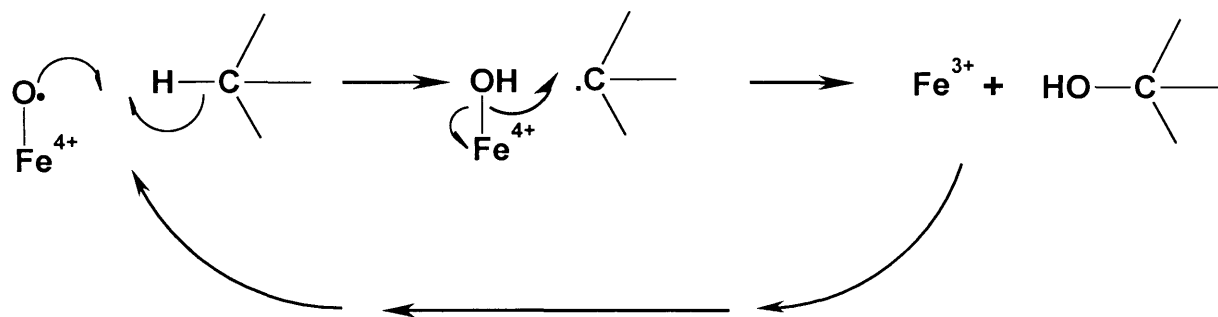
SCHEME 4.6

Hydroxylation reaction of cytochrome P450 monooxygenases

Thus, taking Fe-O˙ as the oxidizing intermediate, there are two possible routes, which differ in the initial electron demand from sulphur, for sulphoxidation to occur (Scheme 4.7).[29] These involve initially either a one-electron abstraction (route A), analogous to the radical mechanism for hydroxylation, or a direct two-electron oxidation (route B), analogous to a concerted oxygen insertion into a C-H bond. Distinguishing between the two routes using Hammett ρ values for the oxidation of series of *p*-substituted phenyl methyl sulphides as a parameter will be further discussed in Section 4.2.1.
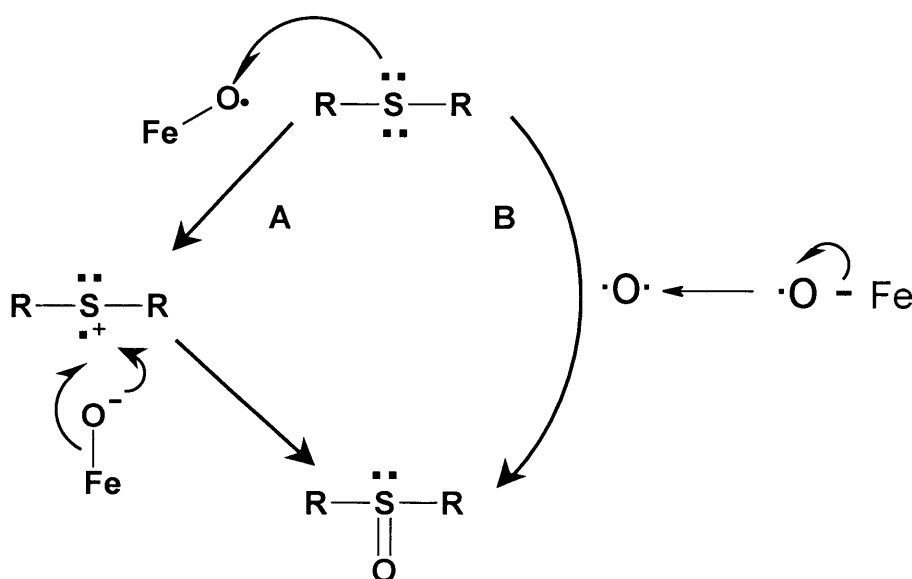
SCHEME 4.7

One and two-electron routes for sulphoxidation by Cytochrome P450 monooxygenases.

4.1.4 Sulphoxidation Studies with P450 BM3

Although a large number of publications about cytochrome P450 BM3-catalysed hydroxylation of fatty acids have appeared, there have been no published sulphoxidation studies, except for the study carried out by Avery[30] (University of Leicester). In this study, rather than using simple alkyl aryl sulphides, mimics of fatty acids containing sulphur atoms were studied. For instance, the sulphide selected as a substrate for oxidation studies was 11-phenylsulpanylundecanoic acid (Scheme 4.8). The criterion of a substrate selection was to make close derivatives of fatty acids, which are known to be good substrates for cytochrome P450 BM3.

107
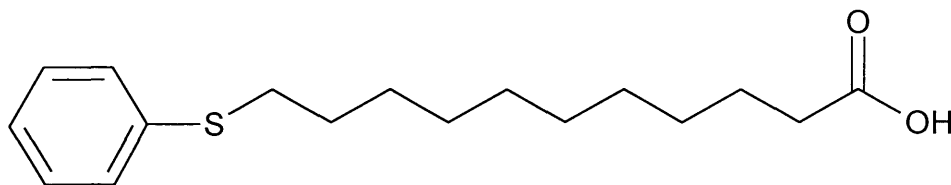
SCHEME 4.8

The length of the substrate is comparable to the that of myristic acid (14 carbon chain length) and the carboxylic acid functional group has been maintained for anchorage to the arginine amino acid residue at the entrance to the P450 BM3 active site. There may be preference for the pro-*R* or pro-*S* lone pairs on the sulphur leading to enantiodiscrimination if the substrate is bound in a fixed orientation in the active site of P450 BM3 (Scheme 4.9).

The reported enantioselectivity is almost racemic. The catalytic constants for this reaction were K_m = 78.8 μM and k_{cat} = 3204 min^{-1}. The oxidation of the thiophenoxy derivative was highly regioselective but the oxidation of the sulphur centre has occurred with a lack of stereoselectivity. Although there is no enantiodiscrimination observed in this study, we have considerable interest in the potential for P450 BM3 to catalyse enantioselective sulphoxidation. This will be tested by using simple sulphides in this chapter.

S-enantiomer

R-enantiomer
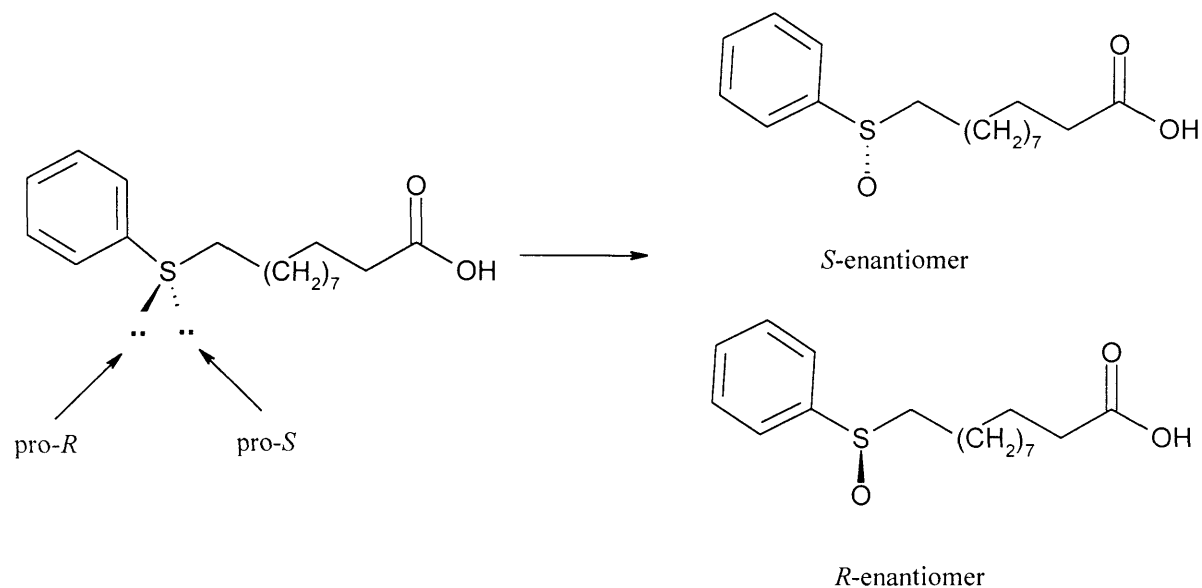
SCHEME 4.9

4.1.5 Aims of This Work

In the above discussion, the diversity of substrate oxidation by various cytochrome P450 enzymes has been highlighted in terms of both reactivity, enantioselectivity and mechanism. The aim of this chapter is to expand the knowledge of the substrate diversity of these enzymes to incorporate organic sulphides, since there are no reports of cytochrome P45 BM3-catalysed enantioselective sulphoxidation of simple organic sulphides in the literature. Specifically, we are interested in examining whether or not cytochrome P45 BM3 can be used for the asymmetric oxidation of alkyl aryl sulphides. The results from this study and from Chapter 3 also provide very useful information for comparison of ascorbate peroxidase and cytochrome P450 BM3 catalytic oxidation of sulphides in terms of mechanism, enantiodiscrimination and catalytic parameters.

4.2 RESULTS AND DISCUSSION

We report on a systematic study of the stereochemistry of oxidation at sulphur by cytochrome P450 from *Bacillus megaterium*, using several alkyl aryl sulphides as the substrate. We found that the sulphide structure dramatically influenced not only the magnitude of the enantioselectivity but also the nature of the enantiopreference of the enzyme from *S*-configuration to *R*-configuration. The sulphides used in this study are shown in Scheme 4.10, and are divided into two groups, namely *p*-substituted phenyl methyl sulphides (Group A) and alkyl phenyl sulphides(Group B), in order to show various effects arise from sulphide structure on the P450 BM3 enzyme catalysis.

(A)   **(B)**
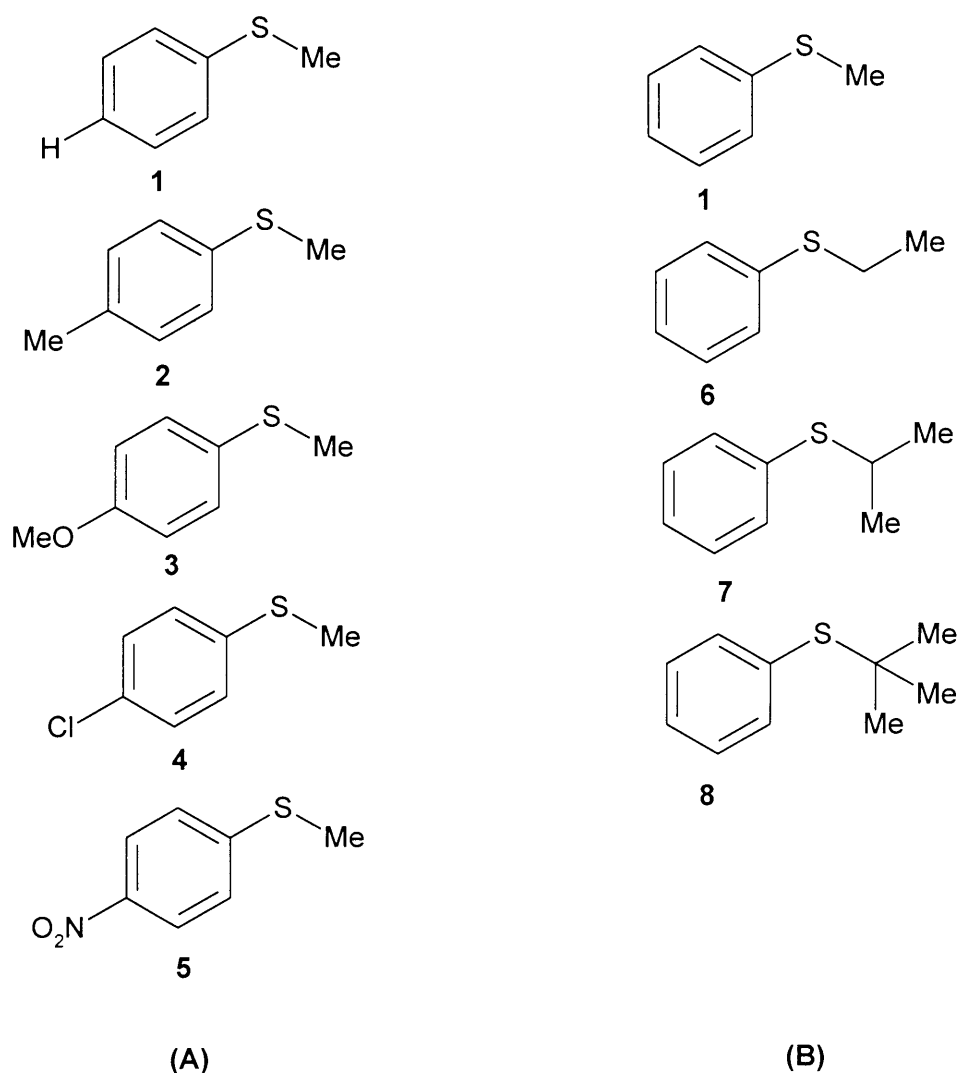
SCHEME 4.10

Structures of the sulphides studied in this work. (**A**) *p*-Substituted phenyl methyl sulphides and (**B**) alky phenyl sulphides.

4.2.1 Oxidation of p-Substituted Phenyl Methyl Sulphides (A)

Phenyl methyl sulphide (**1**), and, *p*-substituted phenyl methyl sulphides (**2 - 5**) are oxidized by cytochrome P450 BM3 system to the corresponding sulphoxides (Scheme 4.11). The structures of the sulphoxide products were established by HPLC, NMR and GC-MS comparison with authentic samples of the sulphoxide standards. No products other than the sulphoxides were detected with all.

R-enantiomer   *S*-enantiomer
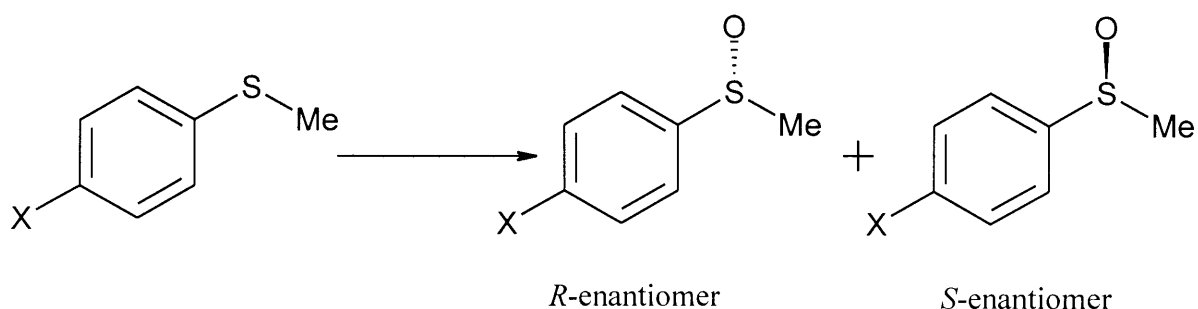
SCHEME 4.11

4.2.1.1 Stereochemistry of the Products from the Oxidation of p-Substituted Phenyl Methyl Sulphides

The HPLC trace of thioanisole as an example is shown in Figure 4.2. Analysis of the sulphoxide products by chiral HPLC shows that the two enantiomers are produced from the sulphides (Figure 4.2, Table 4.2). A significant degree of enantioselectivity was observed during catalytic sulphide oxidation to sulphoxide. In the case of sulphides **1,2** and **5**, the *S*-sulphoxide enantiomer was the major product. In the case of sulphide **3** and **4**, the absolute configuration of the corresponding sulphoxide was the *R* - enantiomer. The best enantioselectivity was observed with sulphide **5**. The dominant *S* - enantiomer formation for sulphide **1,2** and **5** and, *R* - enantiomer formation for sulphide **4** and **5** argues strongly for a specific binding pocket for each substrate, with oxidation predominantly but not exclusively from one direction.
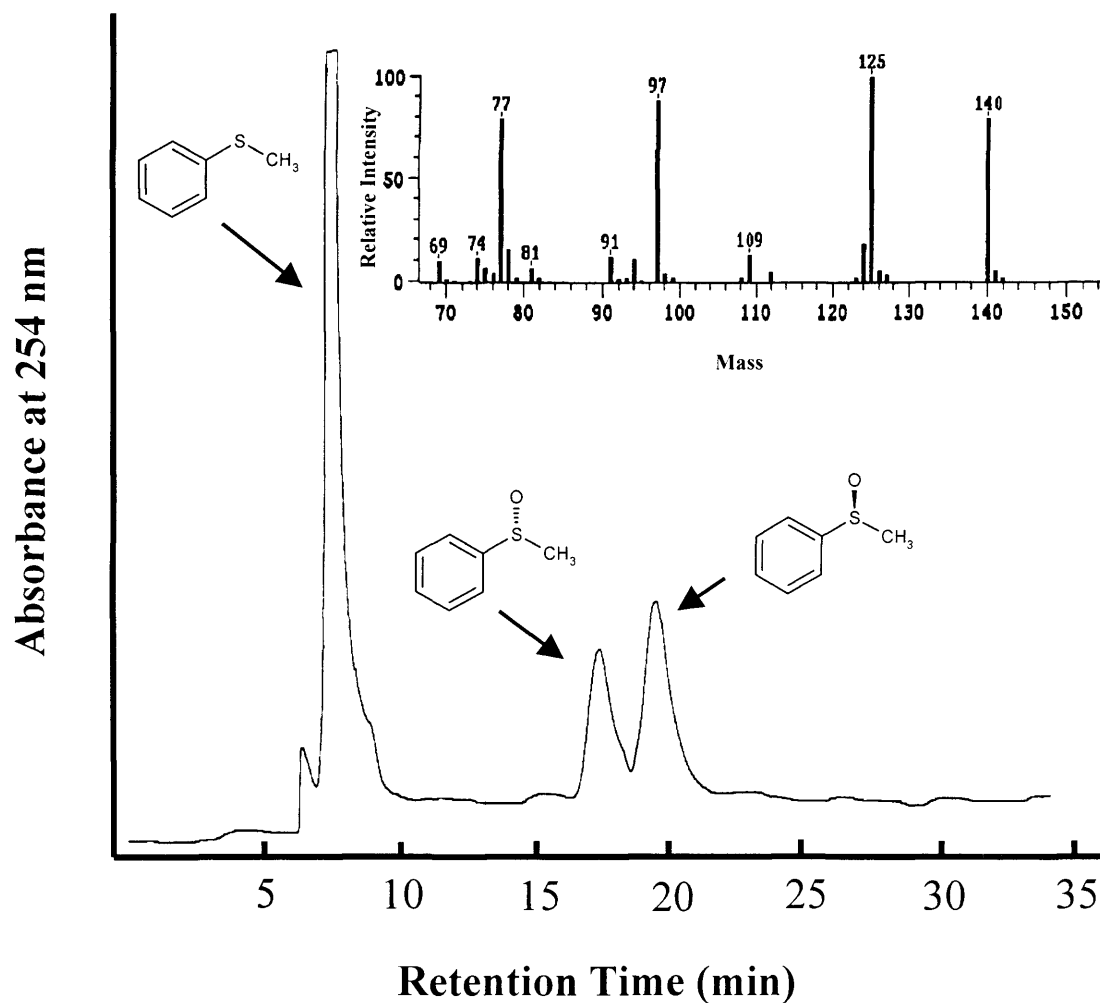
FIGURE 4.2

Chiral HPLC analysis of the enantioselectivity of the oxidation of thioanisole by cytochrome P450 BM3. The HPLC conditions are given in the experimental chapter. **Inset**: Mass spectrometry analysis of methyl phenyl sulphoxide obtained from oxidation of thioanisole by cytochrome P450 BM3. The MS conditions are given in the experimental chapter.

TABLE 4.2

Experimental absolute configurations for oxidation of sulphides 1-5 by cytochrome P450 BM3.

Sulphides	R-enantiomer (%)	S-enantiomer (%)
1	39	61
2	47	53
3	56	44
4	55	45
5	28	72

4.2.1.2 Kinetic Studies of the Oxidation of p-Substituted Phenyl Methyl Sulphides, and Hammett Analysis

Steady state parameters were measured under standard condition following the procedure of Matson *et al.*[31] with small modifications. Sulphides **1-5** were all shown to be substrates for cytochrome P450 BM3. The kinetic measurements used a substrate concentration range of 10-500 µM. The only exception was sulphide **5**, with a concentration range of 1 — 150 µM. The oxidation of sulphides to sulphoxides was determined spectrophotometrically by monitoring NADPH consumption at 340 nm. The rates were calculated from the linear part of the graph. The kinetic parameters with errors were obtained using the Michaelis-Menten equation and are shown in Table 4.3. These kinetic values show that the sulphides are good substrates for cytochrome P450 BM3 since both K_m and k_{cat} of the sulphides are in a similar range to those observed with myristate, a well known cytochrome P450 BM3 substrate ($K_m = 8$ µM and $k_{cat} = 3127$ min^{-1}).[32]

Minor changes or substitutions in the structure of substrates can have profound effects on reaction kinetics. The effects of substituents on the phenyl ring of sulphides **1-5** can be understood through the use of semi-quantitative empirical correlations such as the Hammett relation. Hammett's relationship utilizes the electronic properties as the descriptors of structures. Hammett plots of the logarithm k_{cat}/K_m *vs.* σ_p and σ^+_p were examined for sulphides **1-5**. Using the data from Table 4.3, plot of log k_{cat}/K_m *versus* the Hammett constant,[33] σ_p and σ^+_p shows a linear free energy relationship (Figure 4.3). A good correlation vs σ_p ($\rho = + 0.66$, r = 0.920) and a relatively poor correlation vs. σ^+_p ($\rho = +0.47$, r = 0.876) were obtained for the P450 BM3 - dependent sulphur oxygenation. The value of ρ and ρ^+ was calculated from Figure 4.3, according to the equation [4.1].

$$\text{Log}(k_{cat} / K_m) = \rho\sigma_p \qquad \qquad ...[4.1]$$

TABLE 4.3.

Steady state parameters with error in parenthesis for oxidation of sulphides **1-5** by cytochrome P450 BM3.

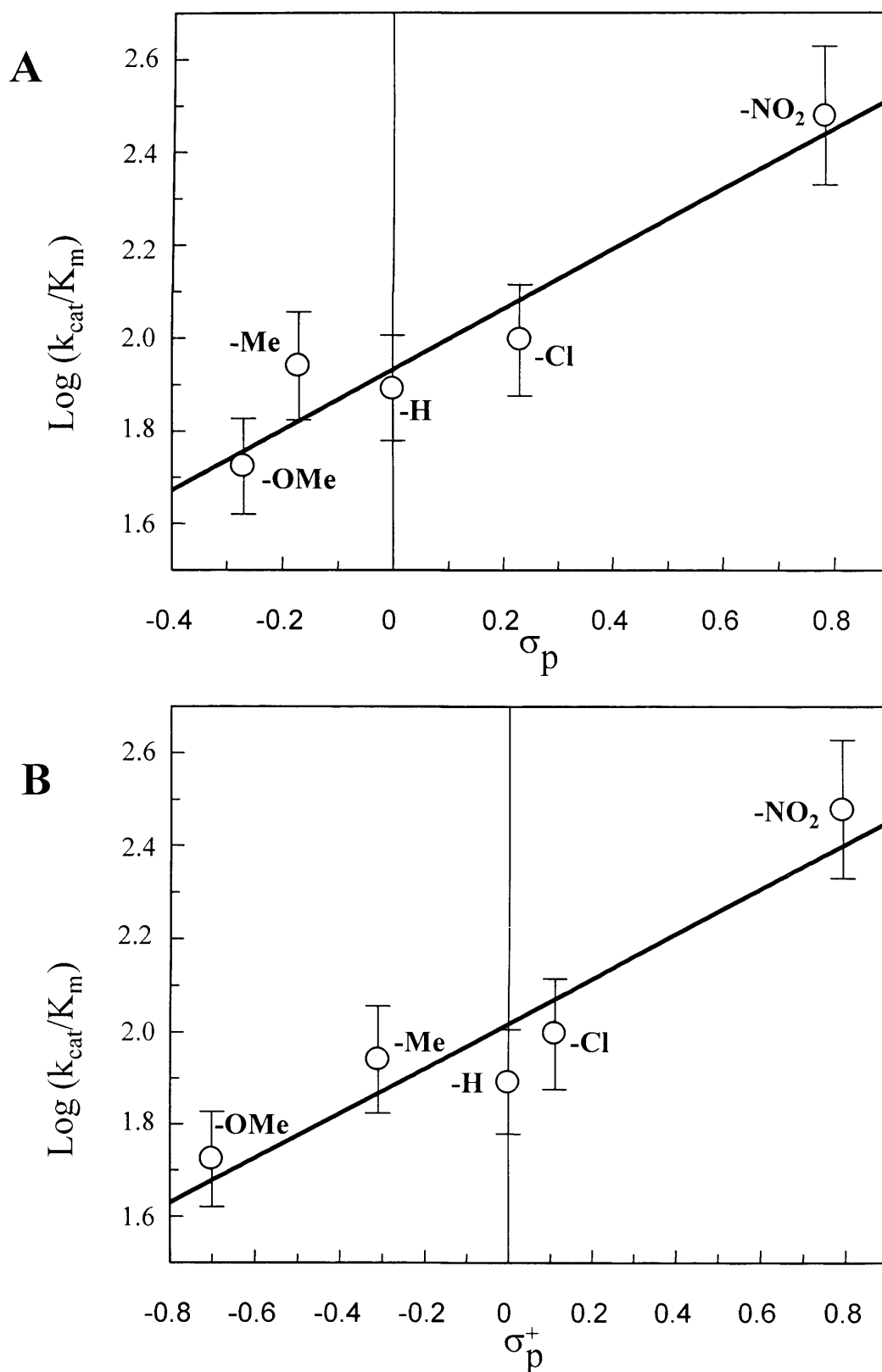| Sulphides	K_m (μM)	k_{cat} (min^{-1})	k_{cat}/K_m (μM^{-1} min^{-1})
1	28.4±6.9	2218±136	78
2	11.2±2.0	968±48	87
3	29.6±6.8	1564±103	53
4	10.7±3.7	1063±59	99
5	4.9±0.8	1528±76	309

FIGURE 4.3

(A) Hammett plot of the logarithm of catalytic efficiencies for sulphoxidation of para-substituted thioanisoles vs. σ_p parameters and (B) Hammett plot of the logarithm of catalytic efficiencies for sulphoxidation of para-substituted thioanisoles vs. σ^+ parameters. Substituents constants taken from Hansch (1979).

A correlation of this type is clear evidence that the changes in structure produce proportional changes in the activation energy. This would be evidence that there is an electronic contribution to the affinity of the p-substituents (Figure 4.3). As shown in Table 4.3, there is a clear trend in the series in the fact that going from a strongly electron donating group to a strongly electron withdrawing group improves affinity (K_m, provided that the rate limiting step is the turnover of enzyme - substrate complex to enzyme – product complex). As a result of this, the catalytic efficiency (k_{cat}/K_m) is improved. A change in the substituent from p-OMe (sulphide **3**) to p-NO$_2$ (sulphide **5**) ($\Delta\sigma_p \sim 0.7$) is accompanied by a six-fold change in catalytic efficiency. However, it should be noted that the $\Delta\sigma_p$ (~ 0.7) is a small change in comparison with other enzymes and it is largely from the K_m of sulphide **5.** It can be argued that the enzymatic reaction rates in the above studies were determined only by monitoring NADPH consumption thus may not reflect the real rate effects caused by variation of substrate structure. The answer would be that under the same condition, sulphides **1-5** are catalytically oxidised to corresponding sulphoxides and the rate of these reactions are relative to one to another.

The correlation of the logarithm k_{cat}/K_m with the substituent constants values (σ_p or σ_p^+) could be used to identify the reaction mechanism. As the sign of ρ and ρ^+ are positive, the electron withdrawing groups stabilizes the transition state complex or energetically close intermediate. But, the reported ρ value for sulphoxidation catalysed by enzyme from rabbit liver is negative, and the proposed mechanism was one electron transfer (Route A, Scheme 4.7).[29] Because a negative value is indicative of the transient involvement of a sulphur radical species bearing a significant amount of positive charge. Our results, however, suggests the opposite. The possible explanation for these surprising, but not totally unexpected, either cytochrome P450 BM3-catalysed sulphide oxidation may differ from the reported mechanism by following the direct oxygen transfer mechanism (Route B, Scheme 4.7) or that, as mentioned above, measuring the NADPH-consumption rather that sulphoxide accumulation may not provide enough information to identify the true reaction mechanism. Nevertheless, a relatively recent study by Goto and co-workers shows that direct oxygen transfer is also possible.[34] Although there is a clear linear relationship between Hammett constants and the catalytic efficiency of sulphoxidation, we believe that different methods are required to support the direct oxygen transfer mechanism for sulphoxidation. A study that is more detailed is beyond the scope of this thesis.

4.2.2 Oxidation of Phenyl Alkyl Sulphides (B)

Alkyl aryl sulphides (sulphides **6** and **7**) are oxidized by cytochrome P450 BM3 system to the corresponding sulphoxides, except *t*-butyl phenyl sulphide (sulphide **8**) (Scheme 4.12). All attempts to oxidise of sulphide **8** showed only the starting sulphide.

R-enantiomer   *S*-enantiomer
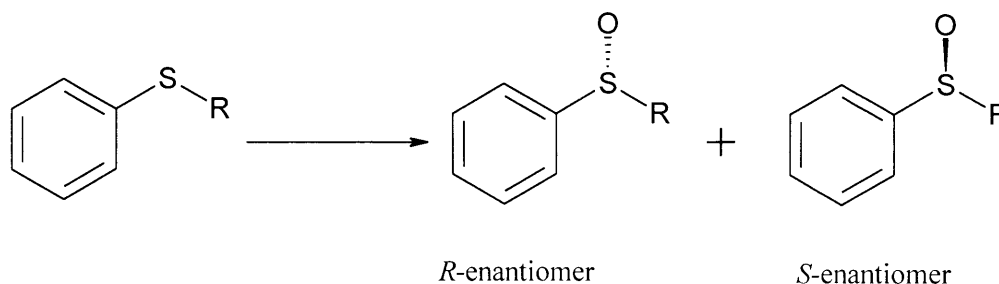
SCHEME 4.12

4.2.2.1 Stereochemistry of the Products from Oxidation of Phenyl Alkyl Sulphides

The structures of the sulphoxide products were established by HPLC, NMR and GC-MS comparison with authentic samples of the sulphoxide standards. The HPLC trace of ethyl phenyl sulphide (sulphide **6**) as an example is shown in Figure 4.4. A significant degree of enantioselectivity was observed during catalytic sulphide oxidation to sulphoxide. Analysis of the sulphoxide products by chiral HPLC shows that the two enantiomers are produced from the sulphides (Figure 4.4, Table 4.4). In the case of sulphide **6**, the *S*-sulphoxide enantiomer was the major product as determined by chiral HPLC. In the case of sulphide **7**, the absolute configuration of the corresponding sulphoxide was *R*. In the case of sulphide **8**, there is no sulphoxide formation observed, the starting material was recovered in all attempts.
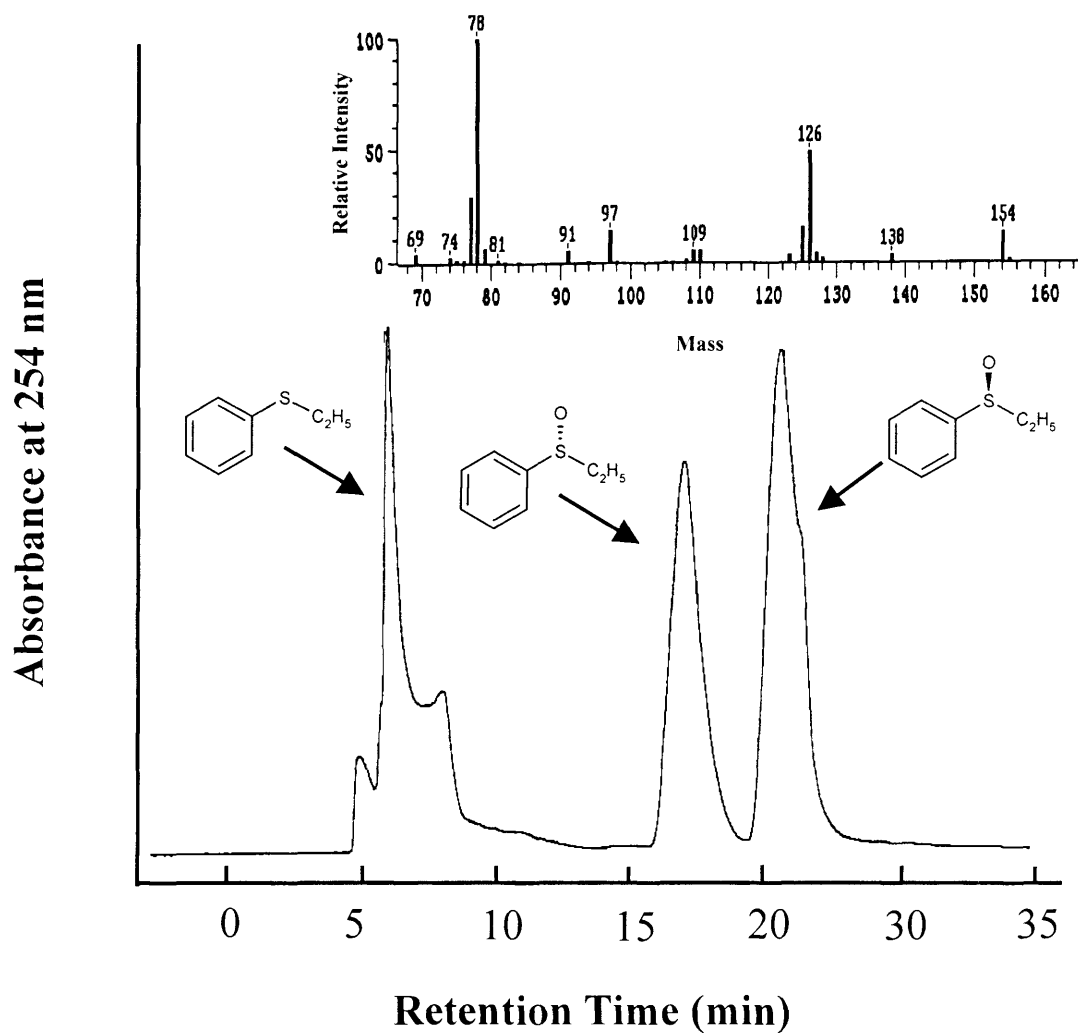
FIGURE 4.4

Chiral HPLC analysis of the enantioselectivity of the oxidation of ethyl phenyl sulphide by cytochrome P450 BM3. The HPLC conditions are given in the experimental chapter. **Inset**: Mass spectrometry analysis of ethyl phenyl sulphoxide obtained from oxidation of ethyl phenyl sulphide by cytochrome P450 BM3. The MS conditions are given in the experimental chapter.

119

TABLE 4.4

Experimental absolute stereochemistries of alkyl phenyl sulphides.

Sulphides	*R*-enantiomer (%)	*S*-enantiomer (%)
1	39	61
6	41	59
7	61	39
8	No oxidation	No oxidation

4.2.2.2 Kinetic Studies of the oxidation of Phenyl Alkyl Sulphides

Steady state parameters were measured under standard conditions following the procedure of Matson et al.[31] with small modifications. Sulphides **1, 6** and **7** were all shown to be substrates for cytochrome P450 BM3. Sulphide **8** was not oxidized, therefore it was not considered to be a substrate for P450 BM3. The kinetic measurements used a substrate concentration range of 10-500 μM. The oxidation of sulphides to sulphoxides was determined spectrophotometrically by monitoring N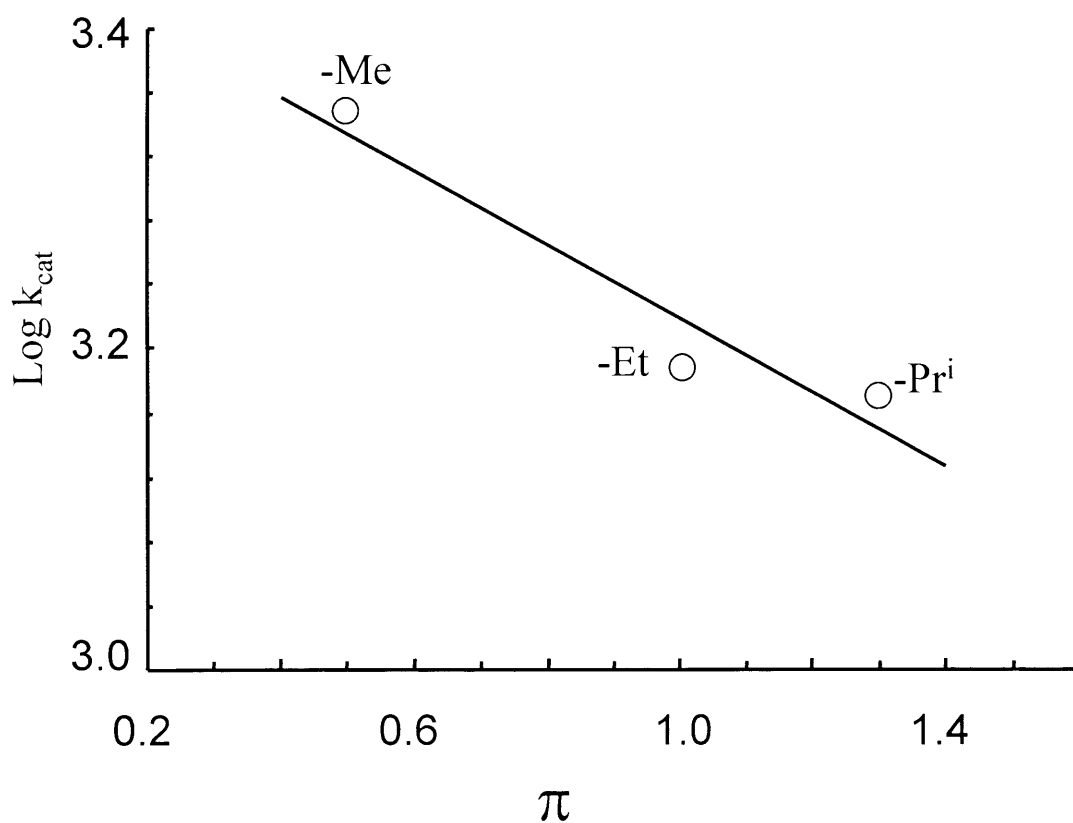ADPH consumption at 340 nm. The rates were calculated from the linear part of the graph. The kinetic parameters and errors were obtained using the Michaelis-Menten equation and are shown in Table 4.5. K_m values are not significantly different within the group. However, there is slight trend in k_{cat} parameters. Increasing alkyl group decreased the turnover number although this reduction may not be significant. Nonetheless, using the data from Table 4.5, a plot of the log k_{cat} against the hydrophobicity constant, π, shows that there is a linear relationship (Figure 4.5) between alkyl group from methyl to *iso*-propyl and π values[35]. Interestingly, an increase in the hydrophobic interaction decreases the turnover number as far as *iso*-propyl phenyl sulphide; but not *tert*-butyl phenyl sulphide. Therefore, it can be claimed that methyl-, ethyl- and *iso*-propyl- phenyl sulphides are clearly accommodated in the active site pocket of P450 BM3 and their position in the pocket is close enough to transfer oxygen from the enzyme to substrate resulting in sulphoxidation. In contrast, this is not the case for *tert*-butyl phenyl sulphide (sulphide **8**). Steric hindrance is probably the cause of the lack of oxidation of this substrate by either preventing its access to the active site pocket of cytochrome P450 BM3 or preferential binding remote from the haem group of the enzyme preventing oxygen transfer (non productive binding mode). It is well known that cytochrome P450 BM3 can accommodate the fatty acids and related compounds (up to 16 carbon chain length) in the active site and subsequently catalyse the hydroxylation of them.[36] From our findings, what can be added is that cytochrome P450 BM3 is capable of simple sulphide oxidation provided that there are no steric clashes between the substrate and residues of the active site. That is, sulphide **7** is tolerated in the active site of enzyme whereas sulphide **8** is not. As long as keeping the alky group linear or minimising the number of branches, which is probable a maximum of two, cytochrome P450 BM3 is well capable of sulphide oxidation with reasonable enantioselectivity.

TABLE 4.5

Kinetics parameters for a series of cytochrome P450 BM3 substrates

Sulphide	K_m (μM)	k_{cat} (min^{-1})	k_{cat}/K_m (μM^{-1} min^{-1})
1	28.4±6.9	2218±136	78
6	11.9±2.3	1540±46	129
7	21.3±2.6	1477±73	69
8	--	--	--

FIGURE 4.5

The relationship between the hydrophobicity of the alkyl group of the

sulphides and Log k_{cat} for the sulphoxidation catalysed by cytochrome P450

BM-3. Hydrophobicity constants, π were taken from Hansch (1970).

4.2.3 Energetics of the Formation of Enantiomers

P450 BM3-catalyzed sulphoxidation reaction leads to the formation of two enantiomers (R and S) by parallel pathways, Scheme 4.12.
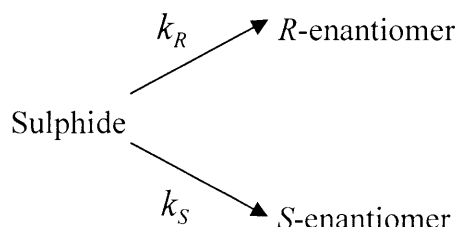
SCHEME 4.12

If two such competing routes to products R-enantiomer, and S-enantiomer have rates k_R and k_S, the enantioselectivity constant K (ratio of R-enantiomer to S-enantiomer), of the reaction should be proportional with the rates, Equation [4.2].

$$K \propto k_R/k_S \qquad ...[4.2]$$

From the equation below, the free energy differences between R- and S-enantiomers, $\Delta\Delta G°$ can be calculated using Equation [4.3].

$$\Delta\Delta G° = - RT \ln K \qquad ...[4.3]$$

Where R is gas constant (1.986 cal K^{-1} mol^{-1}) and T is temperature in Kelvin (293 K) It is clear that if $\Delta\Delta G° = 0$, then ln K = 0 and K= 1, (racemic mixture). Using the Table 4.2 and 4.4, free energy differences have been calculated and are summarized in Table 4.6. The sign of $\Delta\Delta G°$ is the indication of dominant enantiomer; (+) indicates the domination of S-enantiomers, whereas (-) indicates the domination of R-enantiomers. The maximum free energy differences was calculated to be 0.55 kcal mol^{-1} for sulphide **5**.

TABLE 4.6

Free energy differences between *R*- and *S*- enantiomers of sulphides.

Sulphides	$\Delta\Delta G^\circ$ (kcal mol^{-1})
1	0.26
2	0.07
2	-0.14
4	-0.12
5	0.55
6	0.21
7	-0.26

4.2.4 Computational Studies

Computational study has been carried out by Sutcliffe's group (University of Leicester). The 7 different alkyl aryl sulphide compounds (Scheme 4.10) were docked into the active site of Cytochrome P450 BM3, from which enantiomeric product ratios for the 7 alkyl aryl sulphides are calculated. A comparison of the experimental and modelled enantiomeric product ratios for the 7 alkyl aryl sulphides is given in Table 4.7. The modelled results suggest that all 7 sulphide compounds can be accommodated readily in the active site. There is a good agreement between the modelled and experimental enantiomeric product ratios for sulphide 1 and 2, and reasonable agreement for sulphide 4 (relative to sulphide 3,5,6,7). Notably, sulphide 1, 2, and 4 all have relatively small groups for both R (alkyl) and X (substitute). Analysis of the modelled complexes suggests that the differences between the modelled and experimental ratios for the remaining compounds could arise for two different steric reasons: sulphide 6 and 7 because an increase in the size of R could result in steric clashes with the backbone of Ala264 (I-helix), and sulphide 3 and 5 because an increase in the size of X could result in steric clashes with the side chains of Leu75 and Val78 (B'-helix). Since the protein is effectively treated as a rigid structure by GOLD, the program is unable to resolve such problems and alternative means need to be used.

Consider first sulphide 6 and 7, and their interaction with Ala264. Increasing the size of the active site slightly by moving Ala264 away from the substrate significantly improves the agreement between modelled and experimental product ratio for sulphide 7, and also improves the agreement for sulphide 6. Whilst agreement for sulphide 6 and 7 is improved, that for sulphide 1 becomes worse. This is consistent with the I-helix being displaced by substrates with larger groups in the R position. There is an experimental precedent for substrate binding displacing the region around Ala264—the binding of palmitoleic acid to P450 BM3 distorts the I-helix in the region around Ala264[37] because the normal helical hydrogen bonding pattern is disrupted, resulting in a bend in the I-helix.

TABLE 4.7

Experimental and modelled enatiomeric product ratios for the 7 different alkyl aryl

sulphide compounds.

Sulphide	Experimental (*S:R*)	Modelled Wt[a] (*S:R*)	Modelled A264[b] (*S:R*)	Modelled L75A[c] (*S:R*)	Modelled V78A[d] (*S:R*)
1	61:39	58:42	92:8	-	-
6	59:41	46:54	50:50	-	-
7	39:61	67:43	43:67	-	-
2	53:47	54:46	-	-	-
3	44:56	75:25	-	54:46	54:46
4	45:55	54:46	-	67:43	50:50
5	72:28	46:54	-	67:43	58:42

[a]Modelled into the crytal structure with no modifications.

[b]Modelled into the crystal structure with Ala264 translated.

[c]Modelled into the crystal structure with Leu75 mutated to Ala.

[d]Modelled into the crystal structure with Val78 mutated to Ala.

Now consider sulphides **3**, **4** and **5**, and their interaction with Leu75 and Val78. Increasing the size of the active site by replacing Val75 with Gly significantly improves the agreement between modelled and experimental product ratios for sulphide **3** and **5**. However, the agreement worsened for the product ratio of sulphide **4**. Similarly, increasing the size of the active site by replacing Leu78 with Gly significantly improves the agreement between modelled and experimental product ratios. In this case, the agreement for sulphide **4** improved with respect to the crystal structure with no modifications. This is consistent with the B'-helix being displaced by substrates with larger groups in the X position. Indeed, the B'-helix is displaced on substrate binding,[37] and is known to be one of the most variable parts of the structure.[38]

Clearly emerging from the above studies is the suggestion that the stereo selectivity of cytochrome P450 BM3-catalysed sulphoxidation is controlled by two major considerations. Firstly, the substrate must be sterically acceptable to the enzyme and secondly, there should be at least one polar interaction between the substrate and a group in the enzyme active site. All sulphides with the exception of *t*-butyl phenyl sulphide, do not exceed the limit of the binding site of cytochrome P450 BM3. Because of this, corresponding sulphoxides were isolated from these biotransformation.

4.3 REFERENCES

1   Ortiz de Montellano, P. R., *Cytochrome P450*, Plenum Press, New York 1995.

2   Nelson, D. R., in *Cytochrome P450: Structure, Mechanism and Biochemistry*, Ortiz de Montellano, P. R. (Ed.): Plenum Press, New York 1995, p. 575.

3   Guengerich, F. P., *FASEB*, 1992, **6**, 667.

4   Bernhardt, R., *Physiol. Biochem. Pharmacol*, 1995, **127**, 137.

5   Poulos, T. L. and Raag, R., *FASEB*, 1992, **6**, 674.

6   Newcomb, M., Shen, R., Choi, S.-Y., Toy, P. H., Hollenberg, P. F., Vaz, A. D. N. and Coon, M. J., *J. Am. Chem. Soc.*, 2000, **122**, 2677.

7   Lewis, D. F. V., *Cytochromes P450*, Taylor and Francis, London 1996.

8   Holland, H. L., *Organic Synthesis with Oxidative Enzymes*, VCH, New York 1992.

9   Dodson, R. M., Newman, N. and Tsuchia, H. M., *J. Org. Chem.*, 1962, **27**, 2707.

10   Auret, B. J., R, B. D. and Henbest, H. B., *J. Chem. Soc., Chem. Comm.*, 1966, 66.

11   Auret, B. J., R, B. D., Henbest, H. B. and Ross, S., *Journal Of the Chemical Society (C)*, 1968, 2371.

12   Holland, H. L., C, R. G., Viski, P. and Brown, F. M., *Can. J. Chem.*, 1991, **69**, 1989.

13   Holland, H. L., *Catalysis Today*, 1994, **22**, 427.

14   Argoudelis, A. D., Coats, J. M., Mason, D. J. and Sebek, O. K., *J. Antibiotics*, 1969, **22**, 339.

15   Ohta, H., Okamato, Y. and Tsuchihashi, G., *Chemical Lett.*, 1984, 205.

16   Ohta, H., Okamato, Y. and Tsuchihashi, G., *Agric. Biol.Chem.*, 1985, **49**, 671.

17   Ohta, H., Okamato, Y. and Tsuchihashi, G., *Agric. Biol. Chem.*, 1985, **49**, 2229.

18   Im, W. B., Roth, J. A., McCormick, D. B. and Wright, L. D., *J. Biol. Chem.*, 1970, **245**, 6269.

19   Roth, J. A., McCormick, D. B. and Wright, L. D., *J. Biol. Chem.*, 1970, **245**, 6264.

20   Walsh, C. T. and Jack Chen, Y. C., *Angew. Chem. Int. Ed. Engl.*, 1988, **27**, 333.

21   Carrea, G., Redigolo, B., Riva, S., Colonna, S., Gaggero, N., Battistel, E. and Bianchi, D., *Tetrahedron-Asymm.*, 1992, **3**, 1063.

22   Lu, A. H. Y. and West, S. B., *Pharm. Rev.*, 1980, **31**, 277.

23   Ryan, D. E., Levin, W., Reik, L. M. and Thomas, P. E., *Xenobiotica*, 1982, **12**, 727.

24   Ruettinger, R. T. and Fulco, A. J., *J. Biol. Chem.*, 1981, **256**, 5728.

25   Raag, R., Li, H., Jones, B. C. and Poulos, T. L., *Biochemistry*, 1993, **32**, 4571.

26   Fruetel, J., Chang, Y.-T., Collins, J. R., Loew, G. L. and Ortiz de Montellano, P. R., *J. Am. Chem. Soc.*, 1994, **116**, 11643.

27   Fukushima, D., Kim, Y. H., Iyanagi, T. and Oae, S., *J. Biochem.*, 1978, **83**, 1019.

28   Waxman, D. J., Light, D. R. and Walsh, C., *Biochemistry*, 1982, **21**, 2499.

29   Holland, H. L., *Chem. Rev.*, 1988, **88**, 473.

30   Avery, K. L., Ph.D. Thesis, Chemistry Department, University of Leicester, Leicester 1999, p. 174.

31   Matson, R. S., Hare, R. S. and Fulco, A. J., *Biochim. Biophys. Acta*, 1977, **487**, 487.

32   Ahmed, F., Al-Mutairi, E. H., Avery, K. L., Cullis, P. M., Primrose, W. U., Roberts, G. C. K. and Willis, C. L., *Chem. Commun.*, 1999, 2049.

33   Hansch, C. and Leo, A., *Substituent Constants for Correlation Analysis in Chemistry and Biology*, John Wiley and Sons, London 1979.

34   Goto, Y., Matsui, T., Ozaki, S.-i., Watanabe, Y. and Fukuzumi, S., *J. Am. Chem. Soc.*, 1999, **121**, 9497.

35   Hansch, C. and Coast, E., *J. Pharm. Sci.*, 1970, **59**, 731.

36   Miura, Y. and Fulco, A., *Biochim. Biophys. Acta*, 1975, **388**, 305.

37   Li, H. and Poulos, T. L., *Nature Struct. Biol.*, 1997, **4**, 140.

38   Hasemann, C. A., Kurumbail, R. G., Boddupalli, S. S., Peterson, J. and Deisenhofen, J., *Structure*, 1995, **2**, 41.

CHAPTER FIVE

Studies on Artificial Enzyme: Poly-L-Leucine-catalysed

Sulphide Oxidation

5.1 INTRODUCTION

Enzymes are able to catalyse a diverse range of reactions, including the hydrolysis of esters and amides, the esterification of alcohols and ketone reductions. However, the synthetically challenging but nonetheless important chiral alkene to epoxide reaction is not one that is commonly carried out enzymatically. As a result, asymmetric epoxidations performed using synthetic or natural polypeptides are of considerable interest, since these can be considered as simplified models of enzymatic reactions.[1] Indeed, if chemists could utilize amino acids and assemble polypeptide structures that were of a similar complexity as those found in enzyme structures, then an almost limitless range of novel asymmetric chemistry would be accessible. In principle, this could provide improved catalytic activities as well as high substrate specificity.

The use of polymeric amino acids as chiral catalysts in asymmetric oxidation has attracted worldwide attention and has been pioneered by Julia and co-workers.[2] One of the most significant contributions from this group has been the catalytic epoxidation of chalcone to the corresponding epoxide in high optical and satisfactory chemical yield (Scheme 5.1).
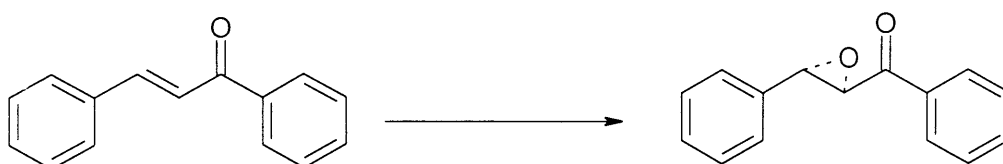
SCHEME 5.1

A general scheme for the oxidation of chalcone-type substrates

This method was a considerable improvement on a previous phase-transfer method, in which very low optical yields were generally obtained.[3]

The aim of this chapter was to expand substrate diversity of these catalysts to incorporate organic sulphides. In particular, we were interested in examining whether or not polymeric amino acid catalysts could be used for the asymmetric oxidation of alkyl aryl sulphides, as has been previously shown for the corresponding epoxidation reactions. The results from this study provided very useful information for comparison of enzymatic and *syn*-enzymatic (*i.e.* synthetic polypeptide) catalytic oxidation of sulphides.

132

5.1.1 Reactions Catalysed by Polymeric α-Amino Acids

5.1.1.1 Epoxidation Reactions

The asymmetric epoxidation of chalcones, discovered in 1980 by Julia,[2] involves the use of a simple peroxide in the presence of polyamino acids such as poly-L-leucine. Subsequently, studies on the epoxidation of chalcone were extended to chalcone-like compounds: for instance, the epoxidation of 4-methoxy-2', 4'-dimethoxymethyl-(E)-chalcone to corresponding α-hydroxydihydro chalcones was investigated by Bezuidenhoudt and co-workers.[4] This method is not only restricted to chalcones but is also applicable to other types of substrate, including enones,[5] enynone, dienone and enediones,[6] dienes,[7] and unsaturated ketoesters in which the substituent R_1 and R_2 need not to be aromatics and in which *tert*-butyl group can be accommodated adjacent to the ketone moiety. The oxidation reaction in all cases is faster than the corresponding phase-transfer methods and the yields and enantiomeric excesses have been found to be good or excellent (generally in the range 60-99 e.e.).[8]

Oxidations of the type (shown in Scheme 5.1) appear to be particularly selective and suitable for the oxidation of enones. For example, quite a large degree of variation in the structure of the enone is tolerated provided that the $-C_1=C_2-C(O)-Ph$, or a similar, motif is retained. Hence, in a series of studies[1,2,9-11] by Julia (using triphasic conditions), a number of enone derivatives were successfully oxidised in high enantiomeric excess (although other chalcone derivatives were also included as part of this study). An indication of the diversity of substrate structure tolerated by the catalyst is given in Table 5.1, in which yields and enantiomeric excesses for a representative sample of substrates are summarised. Although the range of substrates that has been examined is huge, the following simple observations and principles apply to all the oxidative reactions:

- Asymmetric epoxidation using this method has been shown to be reliable, reproducible and robust.

- As long as the 1, 3-diphenyl substituted or similar motif in the substrate structure is retained, the method is of widespread applicability for a variety of substrates.

- The oxidation of electron poor double bonds within the substrates of dramatically different structure gave inferior results.[1,9]

- The reaction time is often long (≥ 3 days).

5.1.1.2 Other Reactions

A number of other reactions have been attempted using polymeric α-amino acids as catalysts, although with rather limited success. The Darzens reaction of phenacyl chloride with benzaldehyde (Scheme 5.2) gave essentially no asymmetric induction and, although the addition of ethyl nitroacetate to chalcone (Scheme 5.3) proceeded with 6.4 % optical yield,[9] the low asymmetric induction and reaction time of 31 days renders the reaction wholly impractical. Attempts at kinetic resolution through the dehydrohalogenation of racemic chlorohydrins have also been attempted, but with little success.[9]

90 % yield

No asymmetric induction

i = Poly-L-alanine, NaOH, Toluene

SCHEME 5.2

+ EtO$_2$CCH$_2$NO$_2$

60 % yield

6.4 % optical yield

i= Poly-L-alanine, toluene

SCHEME 5.3

134
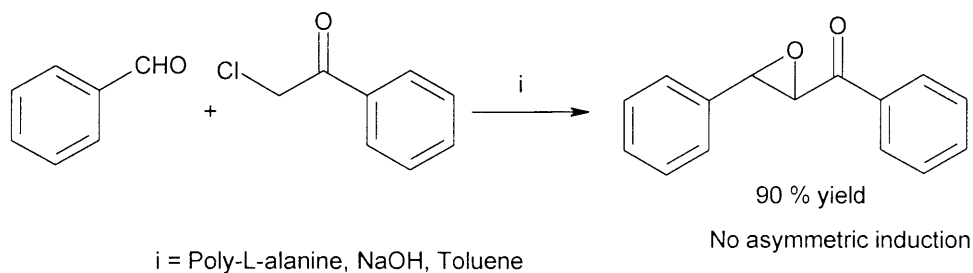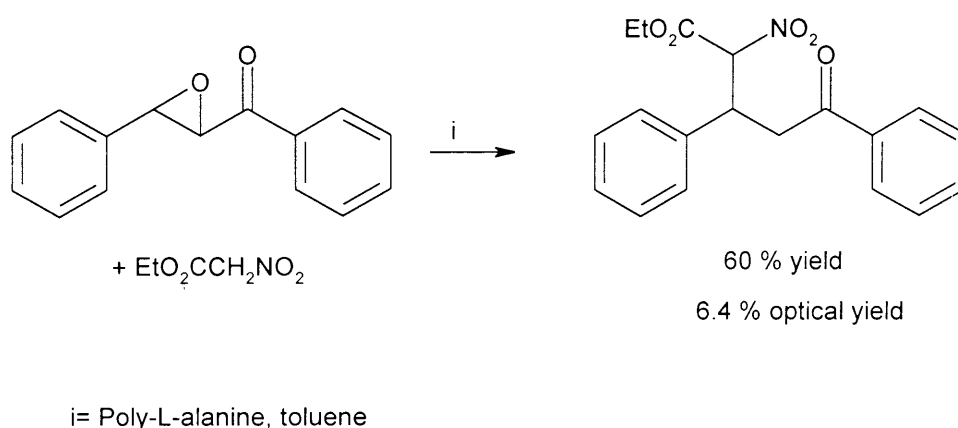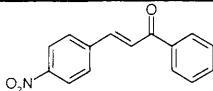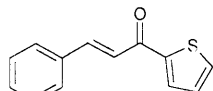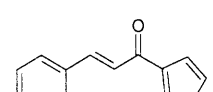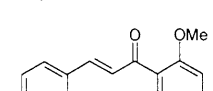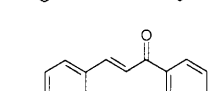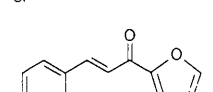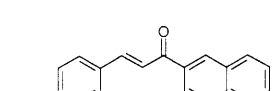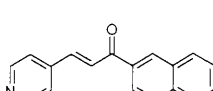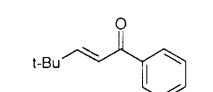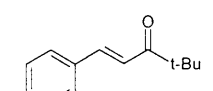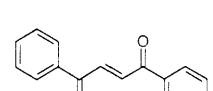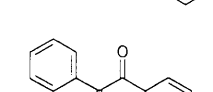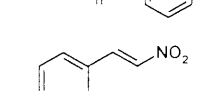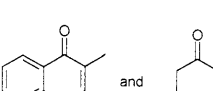
TABLE 5.1

Yields and enantiomeric excesses for the catalytic oxidation of various substrates.

Substrate	Yield (%)	Asymmetric induction (% e.e.)	Data taken from References
	83	82	9
	96	80	9
	30	70	9
	54	50	9
	47	66	9
	85	87	12
	65	96	12
	67	>96	5
	85	90	5
	92	>98	5
	76	76	6
	78	59	6
	50	7	1,9
	Not given	No asymmetric induction	1,9

Catalysis of asymmetric addition of thiols to enones using polyleucine has been attempted but very low enantioselectivity was obtained,[13] as was the case when other proteins were employed to the same end.[11]

Poly-L-leucine has found use as a chiral additive for the asymmetric carboxylation reaction of allylic alcohols (Scheme 5.4). It was found that the polymer out performed a number of chiral alcohols and phosphines in this application, generating the product lactone in 49% yield and 61 % e.e.[14]

61 % e.e.
49 % yield

i= Poly-L-leucine, PdCl$_2$, CuCl$_2$, O$_2$, HCl, THF, rt
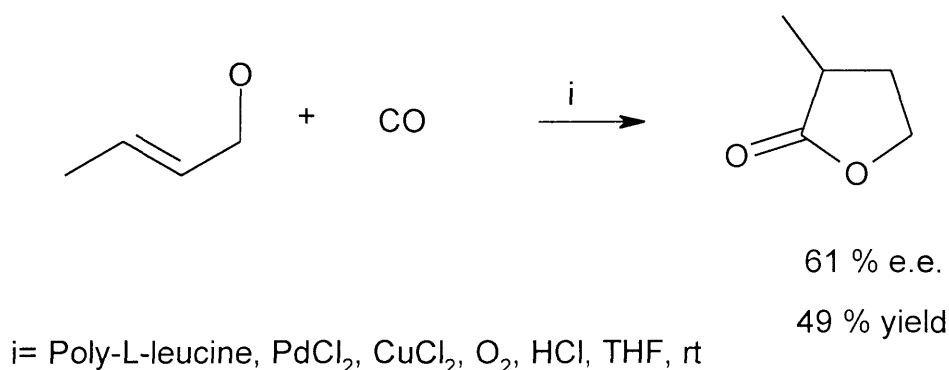
SCHEME 5.4

5.1.1.3 Reactions in Non-aqueous Media

The most significant advances to be made in recent years in this area are the reports by Roberts and co-workers on the use of non-aqueous conditions for chalcone epoxidation.[15] The original triphasic conditions had long reaction times, and insoluble substrates were found to react only very slowly, if they reacted at all. As a result, only substrates that were stable in the presence of an aqueous nucleophilic base could be used. Roberts' biphasic conditions involved a non-aqueous solvent, a water-free hydrogen peroxide source, and a non-nucleophilic amine as the base. Successful solvents included tetrahydrofuran, 1,2-dimethoxyethane, *tert*-butyl methyl ether, dimethyl sulphoxide, *N*, *N*-dimethylformamide and ethyl acetate. The best base was determined to be 1,8-diazo-bicyclo[5.4.0]undec-7-ene (DBU) and the non-aqueous peroxide source was provided by a hydrogen peroxide complex such as that formed with urea or 1,4-diazabicyclo[2.2.2]octane-peroxide complex (DABCO). The urea-hydrogen peroxide complex, UHP, is readily available. The poly-L-

leucine catalyst was generated using cross-linked aminomethyl polystyrene (CLAMPS) as initiator. The new biphasic conditions led to significantly reduced reaction times: chalcone epoxidation, for example, is complete within 30 minutes compared with 24 hours for the triphasic system. Moreover, a range of substrates that were previously found to be unreactive could be successfully converted to the corresponding epoxide, including methyl ketone 1-phenylbut-2-ene-3-one, which reacted in 4 hours giving 70% yield and 80% e.e. Thus, the use of a urea-hydrogen peroxide complex in organic solvents such as THF in the presence of DBU and poly-L-leucine resulted in epoxidation of a range of substrates within 30 minutes with high levels of asymmetric induction (Scheme 5.5).

The improvements in reactivity, yield and enantiomeric excesses afforded by the biphasic conditions effectively solves the problem of oxidant decomposition, since long reaction times are avoided. As a result, the polymer-bound polyleucine delivers a truly practical oxidation system which remains competitive with alternative methods recently reported for the transformation.[16-19]
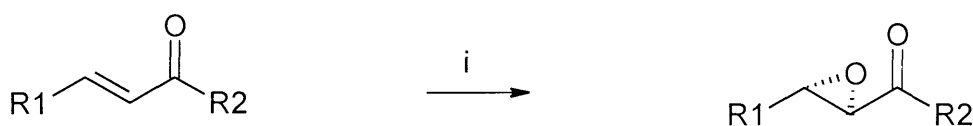
i = Immobilised poly-L-leucine, urea-H_2O_2, THF, DBU, 0.5 hr

Entry	R1	R2	Yield (%)	E.E. (%)
1	Ph	Ph	100	>95
2	CH=CHPh	2-naphthyl	85	>95
3	Ph	Me	70	83

SCHEME 5.5

Epoxidation of enones under non-aqueous conditions.[15]

5.1.2 Mechanism of Epoxidation

The exact mechanisms by which the epoxidation reaction is catalysed and the asymmetric induction is generated remain somewhat unclear. Initial speculation proposed that[23] hydrogen bonding between the chalcone and polymer chain were responsible for asymmetric induction, since performing the reaction in methanol (which is a more polar solvent capable of hydrogen bonding to the substrate) resulted in formation of racemic products. What is more, even though the secondary structures of most polypeptides are dramatically different and might, therefore, affect the binding and oxidation of various substrates, the use of poly-L-proline, which lacks N-H bonds (and cannot hydrogen bond), also gave poor results in terms of overall conversion and e.e., suggesting that hydrogen bonding is influential.[10] It is possible that the hydrophobic catalysts may enhance the reaction by providing a suitable stabilising environment for the hydrophobic substrate (Figure 5.1).
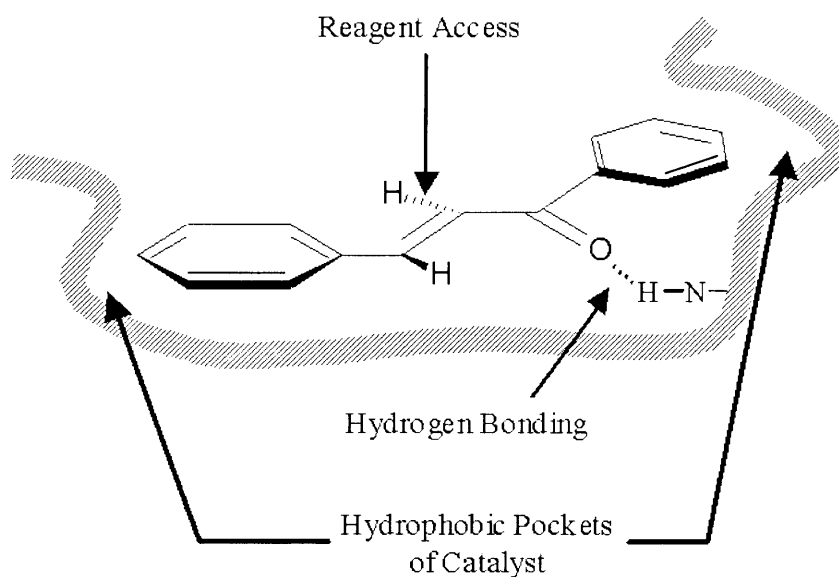
FIGURE 5.1

A cartoon showing a possible binding interaction of the catalyst with the substrate.

138

Further speculation on the mechanism proposed that catalysts with a high degree of α-helical structure, which would be likely for catalysts with 10 or more amino acids, including polyleucine and polyalanine, give the best results.[1]

A physiochemical study of the polyleucine surface during the reaction showed enhanced stabilisation of water-solvent emulsions. Together with other observations, this supports a mechanism that takes place in a monolayer.[20] X-Ray powder diffraction studies suggest a certain degree of crystallinity in the polymer.[21] However, more recent results have suggested that the polymer may actually be predominantly a β-sheet structure.[22]

A consensus of all the data indicates that the reaction between the enone and the oxidising reagent (H_2O_2) probably takes place as shown in Scheme 5.6. The first step is a type of oxa Michael addition using H_2O_2 in an alkaline medium. In this step, which overall constitutes a Michael-type addition reaction, the hydroperoxy anion, formed as a result of deprotonation of hydrogen peroxide by hydroxide, attacks the β-position of the enone leading to the formation of the intermediate. The subsequent cyclisation gives the epoxy ketone.[18]
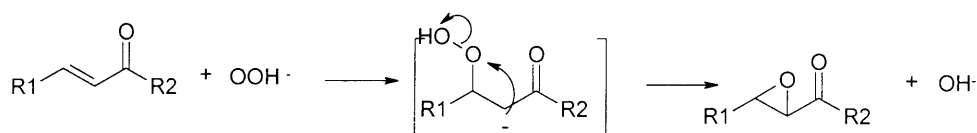
SCHEME 5.6

Proposed mechanism for the epoxidation reaction.

5.1.3 Aims of This Work

In the above discussion, the diversity of substrate oxidation by various plolymeric amino acids has been highlighted in terms of both reactivity, enantioselectivity and mechanism. The aim of this Chapter is to expand the substrate diversity of these catalysts to incorporate organic sulphides, since there are no reports of poly-L-leucine catalysed enantioselective sulphoxidation in the literature. Specifically, we are interested in examining whether or not poly-L-leucine can be used for the asymmetric oxidation of alkyl aryl sulphides.

5.2 RESULTS

5.2.1 Synthesis of Poly-L-Leucine

Automated peptide synthesis is an attractive method for the synthesis of reagents of known length and purity, but it is limited by the scale on which material can be prepared. In general, the favoured method that has been adopted in the literature[23] is the simple polymerisation of the amino acid N-carboxyanhydride derivatives, which are generally crystalline and available in one step from amino acids. Treatment of N-(benzyloxycarbonyl) amino acids (**a**) with oxalyl chloride yields N-carboxy-α-amino acids anhydrides (**b**) (Scheme 5.7).

SCHEME 5.7

Preparation of polymers of α-amino acids

For preparation of poly-L-leucine, N-carboxy-α-L-leucine anhydride (**d**) was prepared as described in the literature.[24] Hence, N-benzoxycarbonyl-L-leucine (**c**) was reacted with oxalyl chloride in benzene to yield N-carboxy-α-L-leucine anhydride (**d**) (Scheme 5.8).
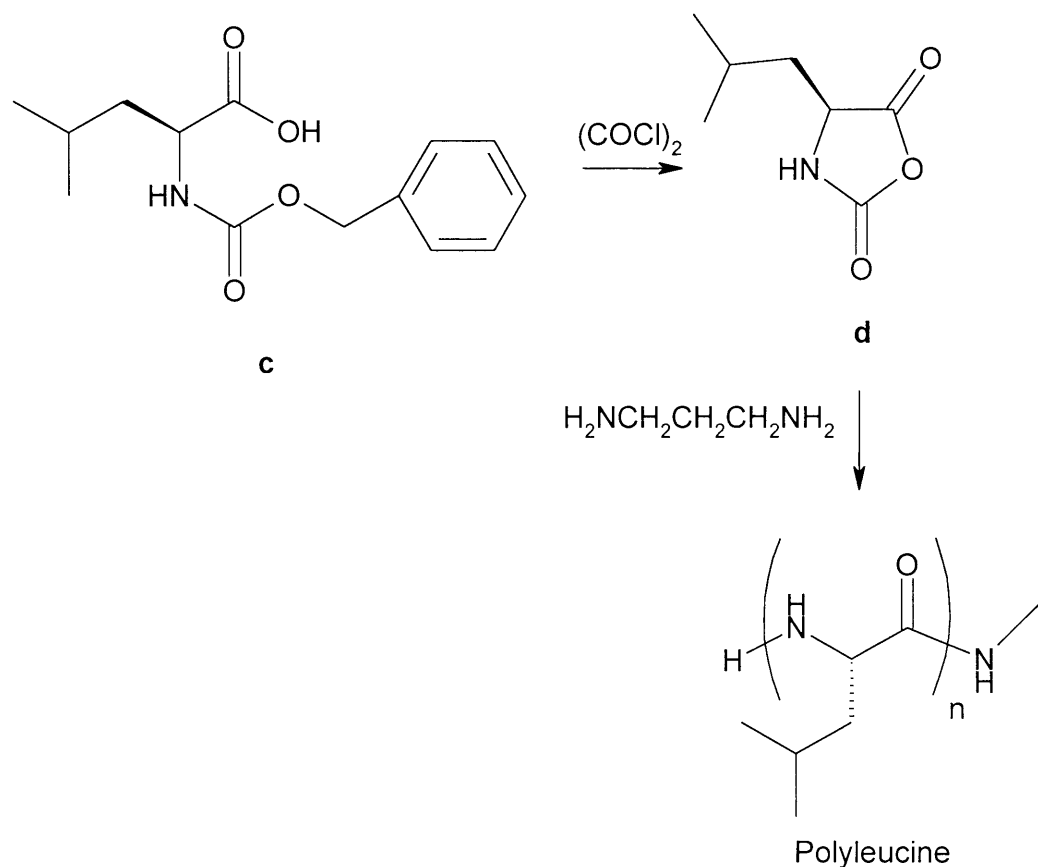
SCHEME 5.8

Preparation of poly-L-leucine

From N-carboxy-α-L-leucine anhydride, polymerized L-leucine was obtained using 1,3 diaminopropane as initiator, Scheme 5.8.[5] This method initiates polymerisation through a nucleophilic attack followed by loss of carbon dioxide and subsequent further polymerisation.

In general, the average length of the polyamino acid chain formed is assumed to be directly related to the mole percentage of initiator amine employed, in this case the ratio was 60:1 (**d**:1,3 diaminopropane). This method for poly-L-leucine synthesis has limitations, but it is reliable if the initiator has a higher reactivity than the resulting amine of the chain formed. Furthermore, the reproducible formation of higher molecular weight polymers is somewhat

limited as a result of steric hindrance at the amine terminus which is prevented by the development of secondary structure in the polymer chain.

5.2.2 Alkyl Aryl Sulphide Oxidation

Ethyl phenyl sulphide was selected as a representative alky aryl sulphide (Scheme 5.9.).

i= H_2O_2, PLL, Hexane, Water
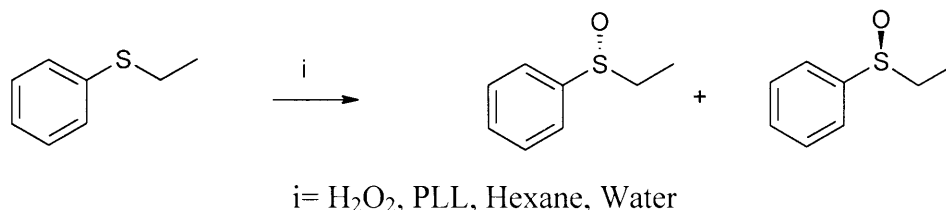
SCHEME 5.9

Oxidation in the three-phase system, comprising aqueous peroxide, organic solvent and poly-L-leucine, afforded the corresponding sulphoxide in low yield and no enantiomeric excess (Figure 5.2. and 5.3.). Hence, although a three-phase system with poly–L-leucine as catalyst provided excellent results for enantioselective oxidation of chalcone-type substrates, this system fail to produce similar results for simple sulphide oxidation. Discussions with Professor S. M. Roberts (University of Liverpool), who has carried out most of the work on poly-L-leucine oxidation, indicated that similar work in his laboratory had also failed to produce enantioselective oxidation, and this work was not pursued further.
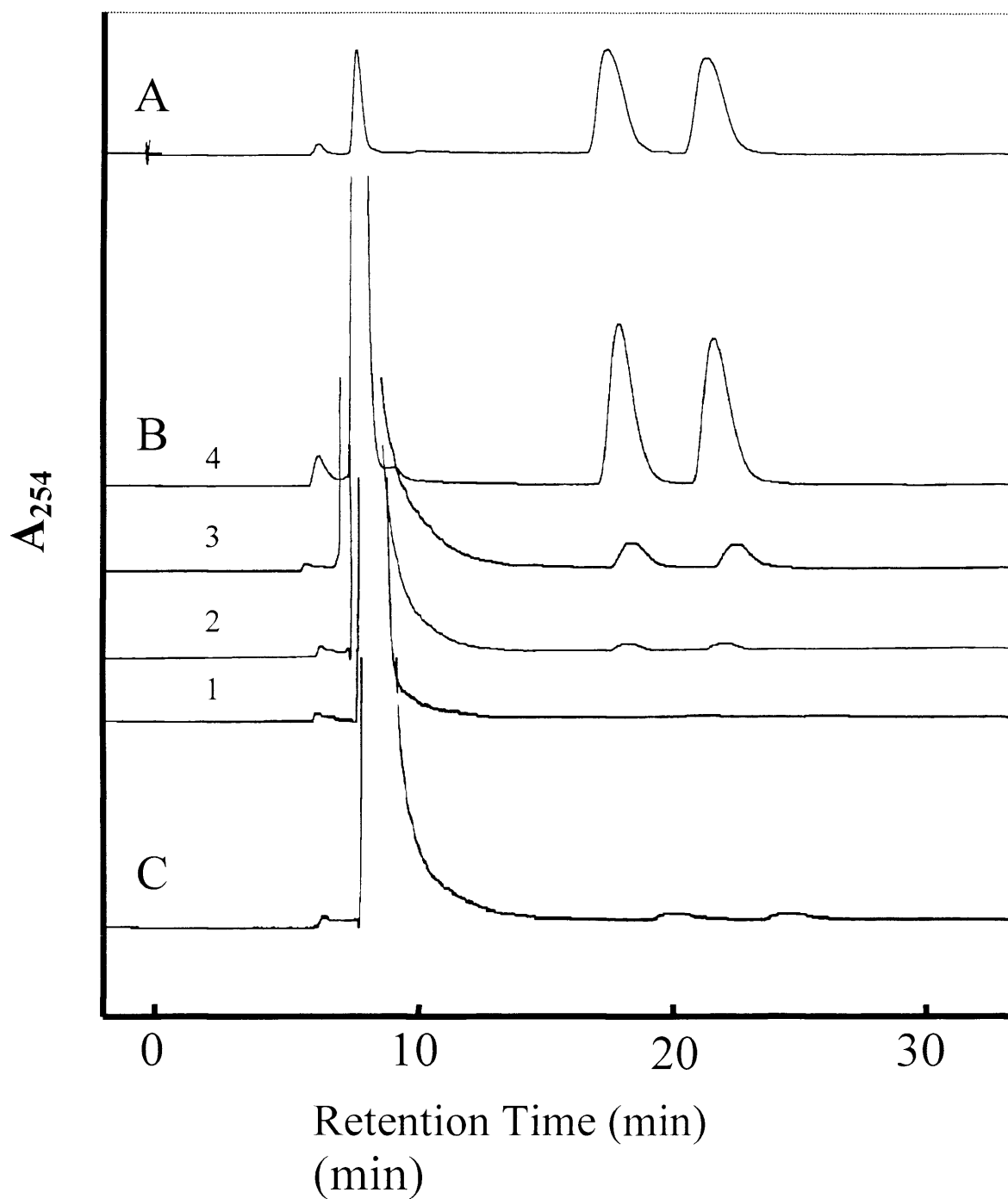
FIGURE 5.2

High Performance Liquid Chromatography traces of ethyl phenyl oxidation by poly-L-leucine. (**A**) Racemic EtPhSO standard and substrate. (**B**) Products of the reaction after mixture of EtPhS, H_2O_2 and PLL; samples were taken after (1) 30 minutes, (2) two hours, (3) 8 hours and (4) 24 hours. (**C**) Control reaction after 24 hours (mixture of EtPhS and H_2O_2 without catalyst).
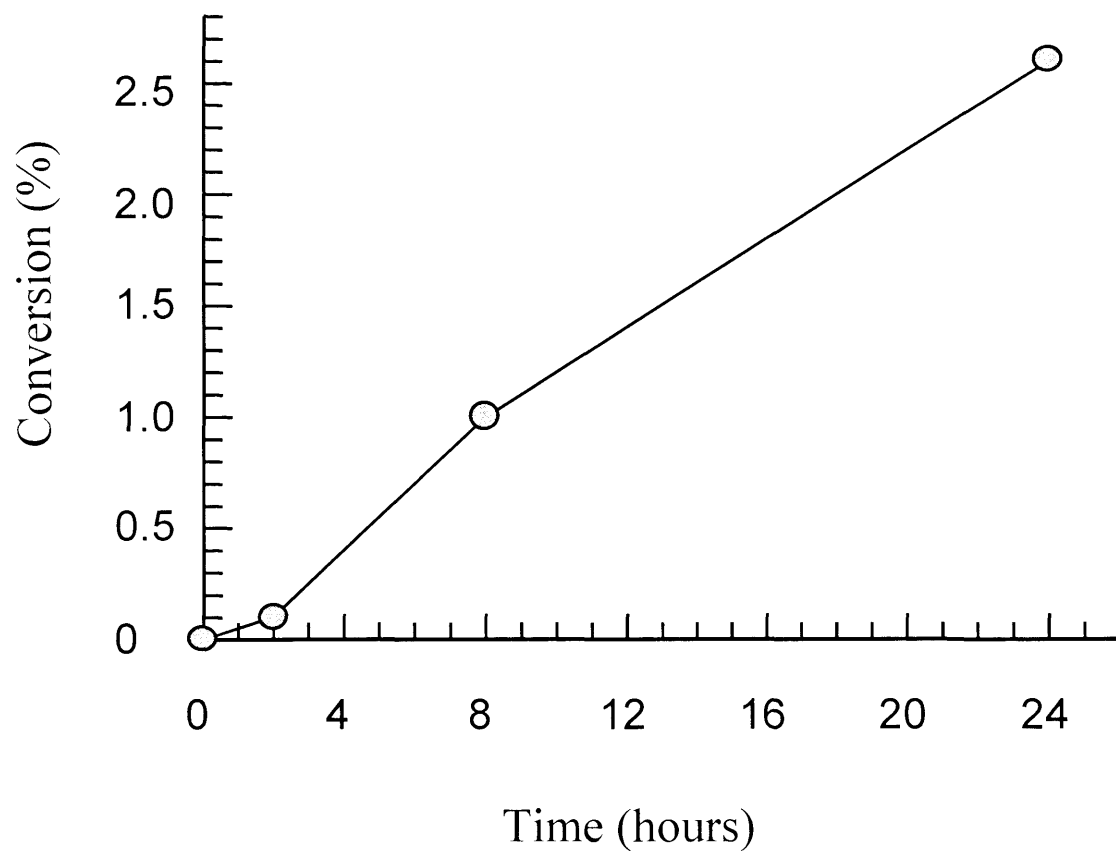
FIGURE 5.3

A graph showing the percentage conversion (as a fraction of total substrate concentration) of ethyl phenyl sulphide to the corresponding sulphoxide over time.

5.3 DISCUSSION

In this Chapter, the reactivity of poly-L-leucine towards ethyl phenyl sulphide has been examined. The procedure adopted for the preparation of poly-L-leucine has several advantages. First, it has been found that the use of 1,3-diaminopropane gives a catalyst in which n (the number of amino acid subunits, Scheme 5.8) is very close to 20 throughout the range of polymeric species produced in the reaction; this leads to homogeneous distribution of the catalyst and improved catalytic efficiencies compared to non-homogeneous mixtures in which n varies over a wider range. Second, the reaction time for generation of the catalyst is much shorter (less than three days) than for other diamines.[5] Third, the catalyst can be prepared and used on a large (>200 g) scale and has been found to be re-usable, without detrimental effects on either yield or enantiomeric excess.

The results in this work have shown that oxidation of ethyl phenyl sulphide can be catalysed by poly-L-leucine, but without any enantiodiscrimination. The possible reason for the failure of this reaction to produce enantioselectivity might arise from the absence of a carbonyl functionality on the sulphide, thus precluding hydrogen bond formation between the substrate and the catalysts (Figure 5.1). In contrast, favourable hydrogen bonding interactions in the chalcone-type substrates can account for the high degree of asymmetric induction observed in this case.[1,10] Indeed, hydrogen bonding interactions, of the type described in Section 5.1.2, between carboxylic acids and the N-H group of the catalyst have been shown to be influential in the reaction of poly-L-alanine with a variety of substrates containing carboxylic acid functionalities.[25]

We have also considered another possibility. For chalcone-type substrates, the substrate carbon atoms $C_1 - C_3$ (Figure 5.1) have sp^2 hybridisation, which makes the molecule flat and restricts rotation around the carbon-carbon bonds. The two-phenyl groups on the substrate have hydrophobic interactions with the catalyst and the carbonyl C_3 group hydrogen bonds with the catalyst. This fixes the substrate in a particular orientation, allowing the oxidation reagents to approach on the upper face but not on the bottom face. This leads to enantioselective epoxide formation. For the sulphoxidation reaction, we assume that the phenyl ring of the sulphide has a similar hydrophobic interaction with the catalyst as that observed for the epoxidation reaction and the phenyl ring therefore has no conformational mobility. However, in direct contrast to the epoxidation reaction, the

substrate now has considerably greater freedom of rotation around both the sulphur-carbon bonds (Figure 5.2). If the conformation of the phenyl ring is fixed, then rotation around the C_{phenyl}-S bond (either direction; A or B) must involve reorientation of the lone pairs on the sulphide, leading to racemic mixtures of products, since the oxidation of pro-S and pro-R lone pairs are equal. On the other hand, rotation about the S-C_{alkyl} bond would not affect the orientation of the lone pairs on the sulphide if the conformation of the phenyl ring was similarly fixed.
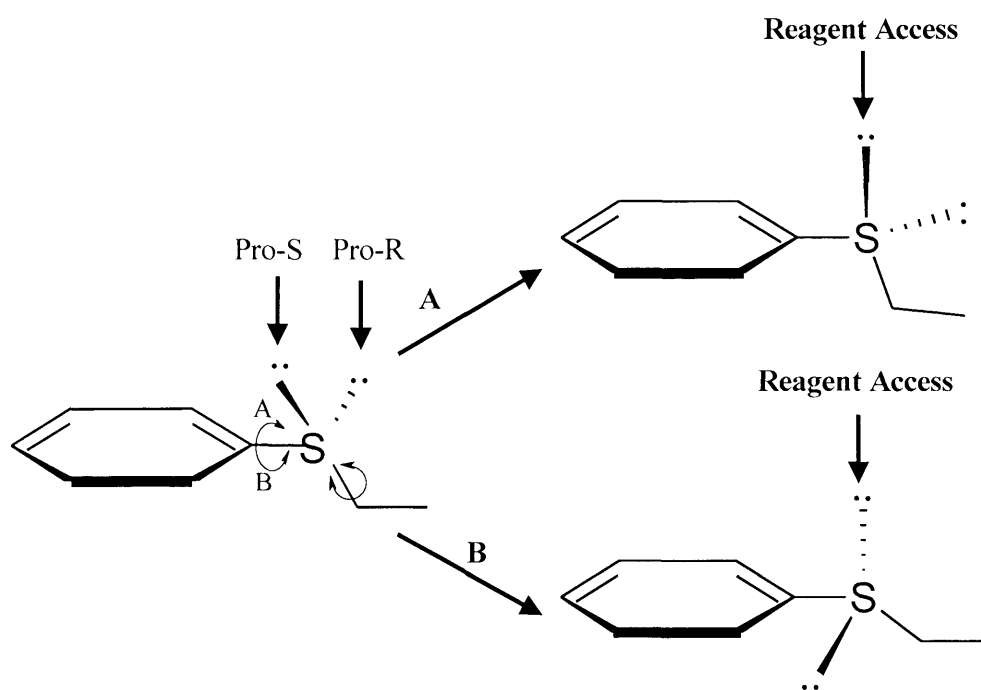
FIGURE 5.4

A cartoon showing orientation of ethyl phenyl sulphide with possible oxidation sites.

To obtain enantioselective sulphoxidation, it is likely that the sulphide atom should be fixed in the molecule and not free to rotate. The types of compound in Figure 5.5 might be likely candidates.
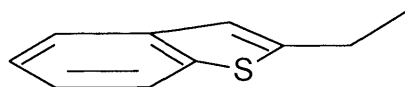
FIGURE 5.5

5.4 CONCLUSION

The use of polymeric α-amino acids as catalysts for biotransformations remains a research area with a great deal of potential. The development of these reagents has now reached a point where many of the initial difficulties involved with their preparation and use have now been overcome using supported reagents and non-aqueous reaction conditions. The methodology has proved itself a valuable synthetic tool for large scale as well as small laboratory scale applications.

Present interest now lies in the extension of polyamino acid methodology to other asymmetric applications, and to the preparation and evaluation of more complex catalysts. The potential for modification by the incorporation of other amino acids and organometal groups is obvious and will no doubt occupy researchers in this area for many years.

Poly-L-leucine proved to be a satisfactory catalyst for the oxidation of alkyl aryl sulphides although this has been shown to occur with no significant asymmetric induction. Further studies may produce satisfactory results by varying substrate structures, but that is beyond the scope of this thesis.

5.5 REFERENCES

1   Colonna, S., Molinari, H., Banfi, S., Julia, S., Masana, J. and Alvarez, A., *Tetrahedron*, 1983, **39**, 1635.

2   Julia, S., Masana, J. and Vega, J. C., *Angew. Chem. Int. Ed. Engl.*, 1980, **19**, 929.

3   Marsman, B. and Wynberg, H., *J. Org. Chem.*, 1979, **44**, 2312.

4   Bezuidenhoudt, B. C. B., Swanepoel, A., Augustyn, J. A. N. and Ferreira, D., *Tetrahedron Lett.*, 1987, **28**, 4857.

5   Lasterra-Sanchez, M. E., Felfer, U., Mayon, P., Roberts, S. M., Thornton, S. R. and Todd, C. J., *J. Chem. Soc. Perkin Trans. 1*, 1995, 343.

6   Kroutil, W., Lasterra-Sanchez, M. E., Maddrell, S. J., Mayon, P., Morgan, P., Roberts, S. M., Thornton, S. R., Todd, C. J. and Tuter, M., *J. Chem. Soc. Perkin Trans. 1*, 1996, 2837.

7   Allen, J. V., Cappi, M. W., Kary, P. D., M, R. S., Williamson, N. M. and Wu, L. E., *J. Chem. Soc. Perkin Trans. 1*, 1997, 3297.

8   Kroutil, W., Mayon, P., Lasterra-Sanchez, M. E., Maddrell, S. J., Roberts, S. M., Thornton, S. R., Todd, C. J. and Tuter, M., *Chem. Commun.*, 1996, 845.

9   Julia, S., Guixer, J., Masana, J., Rocas, J., Colonna, S., Annunziata, R. and Molinari, H., *J. Chem. Soc. Perkin Trans. 1*, 1982, 1317.

10   Banfi, S., Colonna, S., Molinari, H., Julia, S. and Guixer, J., *Tetrahedron*, 1984, **40**, 5207.

11   Papagni, A., Colonna, S., Julia, S. and Rocas, J., *Synt. Commun.*, 1985, **15**, 891.

12   Lasterra-Sanchez, M. E. and Roberts, S. M., *J. Chem. Soc. Perkin Trans. 1*, 1995, 1467.

13   Aglietto, M., Chiellini, E., Dantone, S., Ruggeri, G. and Solaro, R., *Pure Appl. Chem.*, 1988, **60**, 415.

14   Alper, H. and Hamel, N., *J. Chem. Soc., Chem. Comm.*, 1990, 135.

15   Bentley, P. A., Bergeron, S., Cappi, M. W., Hibbs, D. E., Hursthouse, M. B., Nugent, T. C., Pulido, R., Roberts, S. M. and Wu, L. E., *J. Chem. Soc., Chem. Comm.*, 1997, 739.

16   Enders, D., Zhu, J. Q. and Raabe, G., *Angew. Chem. Int. Ed. Engl.*, 1996, **35**, 1725.

17   Elston, C. L., Jackson, R. F. W., MacDonald, S. J. F. and Murray, P. J., *Angew. Chem. Int. Ed. Engl.*, 1997, **36**, 410.

18   Enders, D., Zhu, J. and Kramps, L., *Liebigs Ann.*, 1997, 1101.

19   Bougauchi, M., Watanabe, S., Arai, T., Sasai, H. and Shibasaki, M., *J. Am. Chem. Soc.*, 1997, **119**, 2329.

20   Valencia-Parera, G., Solans-Marsa, C., Reigh-Isart, F. and Garcia-Anton, J. M., *J. Coll. Int. Sci.*, 1986, **114**, 140.

21   Sela, M. and Berger, A., *J. Am. Chem. Soc.*, 1953, **75**, 6350.

22   Bentley, P. A., Kroutil, W., Littlechild, J. A. and Roberts, S. M., *Chirality*, 1997, **9**, 198.

23   Ebrahim, S. and Wills, M., *Tetrahedron-Asymm.*, 1997, **8**, 3163.

24   Konopinska, D. and Siemion, I. Z., *Angew. Chem. Int. Ed. Engl.*, 1967, **6**, 248.

25   Stephens, R. M. and Bradbury, E. M., *Polymer*, 1976, **17**, 563.

CHAPTER SIX

Experimental

6.1 GENERAL EXPERIMENTAL PROCEDURES

6.1.1 Solvents and Materials

All solvents and reagents were of the highest possible purity, were obtained from commercial sources and used without further purification unless otherwise stated. Petroleum ether (PE) refers to the fraction boiling between 40°C and 60°C and was distilled prior to use.

All buffers and other aqueous solutions were prepared using water purified through the Milli-Q system (Millipore Corp.). Hydrogen peroxide solutions were prepared by dilution of a 30% (v/v) solution.

6.1.2 Instrumentation

6.1.2.1 Analytical Thin Layer Chromatography (TLC)

Analytical thin layer chromatography (TLC) was performed on Merck aluminum backed, thin layer chromatography plates pre-coated with a 0.25 mm layer of 60 F_{254} silica gel containing a fluorescent indicator. Visualization was achieved either by UV light (254nm), or by staining with iodine, alkaline potassium permanganate solution. Evaporation under reduced pressure was achieved on a Büchi rotary evaporator, using a water aspirator.

6.1.2.2 Nuclear Magnetic Resonance Spectrometry (NMR)

^{1}H Nuclear magnetic resonance spectra were recorded at 250 MHz on a Bruker AM250NMR, at 300 MHz on a Bruker DPX300NMR or at 400 MHz on a Bruker DRX400NMR. Chemical shifts are reported in parts per million (ppm) relative to residual $CHCl_3$ (δ 7.27ppm) or tetramethylsilane as the internal reference (δ 0.00 ppm). The following abbreviations are used to describe the multiplicity of a given signal: s = singlet, d = doublet, t = triplet, q = quartet, m = multiplet, br = broad. Coupling constants, J, are given in Hertz.

6.1.2.3 High Performance Liquid Chromatography (HPLC)

HPLC analyses were performed using an isocratic HPLC system (Shimadzu) fitted with a UV-visible detector at 290, 300 or 254 nm. The columns used were: (1) a reverse phase C-18 column with the mobile phase as methanol/water (40:60 v/v) containing 0.25% trifluoroacetic acid, and (2) Chiralcel OD-H column with the mobile phase as 5-30 % (depending on the application) isopropanol in hexane.

6.1.2.4 Gas Chromatography-Mass Spectrometry (GC-MS)

GC-MS analyses were performed at 70 eV on a KRATOS Concept mass spectrometer fitted with a gas chromatograph (Shimadzu, GC-14A) and a fused capillary column (HP35). A temperature gradient was used unless stated otherwise in the GC separations: the initial temperature (50 °C, 5 minutes) was increased to 250 °C at a rate of 10 °C / minute.

6.1.2.5 Uv-Visible Spectroscopy

Spectra were obtained using variable slit Perkin Elmer Lambda 14 and 40 spectrometers, which were operated under computer control. Temperature control (± 0.1 °C) was achieved using a circulating water bath (Julabo U3) and a water cooler (MK refrigeration Ltd.).

6.2 EXPERIMENTAL PROCEDURES RELATING TO CHAPTER 2

6.2.1 Expression and Purification of Pea Cytosolic Ascorbate Peroxidase

6.2.1.1 Protein Expression

Pea cytosolic APX cDNA was obtained from Dr. Barbara Zilinkas (Rutgers University, New Jersey, USA). Enzyme purification followed a protocol adapted from published procedures.[1] LB-ampicillin plates (see Appendix) were streaked with *E.coli* TOPP3 cells transformed with the pMAL-c2 vector, which is ampicillin resistant, taken from a frozen (-20 °C) glycerol stock. The streaked plates were incubated at 37 °C overnight. A single

colony was picked from this plate using a sterilized wooden toothpick and was transferred into a 250 ml conical flask containing 100 ml rich medium and ampicillin (100 mg / ml) (Appendix). The cell culture was allowed to grow for 10-12 hours in a shaker incubator at 37 °C and with shaking at ~250 rpm. A 10-ml sample of this culture was used to inoculate each of six flasks of rich medium (750 ml) containing ampicillin (100 mg / ml) (Appendix) and incubated at 37 °C and with shaking at ~250 rpm. At 30 minutes intervals, 1-ml aliquots were removed from the culture and the cell growth was assessed spectrophotometrically using the absorbance at 600 nm. When the absorbance at given wavelength had reached 0.5 (corresponding to a cell density of $\sim 2 \times 10^8$ cells/ml), the cells were induced using isopropyl-ß-D-thiogalactoside (IPTG), added to a final concentration of 0.3 mM. Six hours after induction, the cells were collected by centrifugation (10,000 rpm for 20 minutes at 4°C) and the supernatant discarded. Pelleted cells were resuspended in 100 ml lysis buffer (see Appendix), using 5 ml for every gram of cells (wet weight), before being frozen at –20 °C. SDS-PAGE analysis was used to confirm MBP-Fusion product over expression (Figure 6.1.(a)).

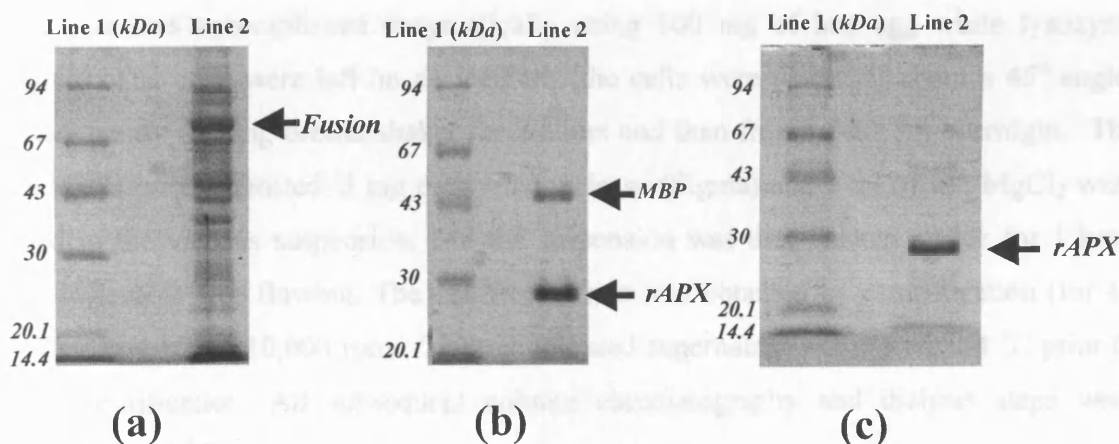**(a)**   **(b)**   **(c)**

FIGURE 6.1

10-15% SDS-PAGE Gel of protein samples from APX isolation and purification. **(a)** cell protein after 6 hours of IPTG induction; **(b)** a sample from trypsin digest; **(c)**, a pooled fraction from FFQ column. The masses of the markers are indicated on the left hand side of each figure (from top: 94.0, 67.0, 43.0, 30, 20.1 and 14.4 kDa);.

6.2.1.2. Purification of APX

Frozen cells were thawed overnight at 4 °C and phenylmethylsulphonyl fluoride (PMSF) and dithiothreitol (DTT) were added to the suspension to a final concentration of 1 mM. Cell lysis was accomplished enzymatically using 100 mg of hen egg white lysozyme (Sigma). The cells were left on an ice bath (the cells were placed at about a 45° angle) upon a gently moving orbital shaker for 2 hours and then frozen (-20 °C) overnight. The lysed cells were defrosted, 5 mg deoxyribonuclease (Sigma) and 1 ml of 1M $MgCl_2$ were added to the viscous suspension, and the suspension was then shaken on ice for 1 hour until it became free flowing. The cell-free extract was obtained by centrifugation (for 40 minutes at 4 °C) at 10,000 rpm. The red-coloured supernatant was stored at 4 °C prior to further purification. All subsequent column chromatography and dialysis steps were performed at 4 °C.

The first stage of purification was to isolate the MBP-fusion product from the numerous solubilized proteins present in the cell-free extract. An amylose (New England Biolabs) affinity column (2.5 × 20 cm) was pre-equilibrated using > 5 column volumes of AC buffer (see Appendix). The cell-free extracts were pooled and applied to the equilibrated amylose column at a flow rate of 1ml/min. The column was washed thoroughly with >5 column volumes of AC buffer until the flow-through protein absorbance at 280 nm (A_{280}) approached the base-line level. Elution of the bound fusion protein was achieved using AC buffer containing 10 mM maltose at a flow rate of 1ml/min; all red-colored fractions were pooled. The MBP-fusion protein solution was concentrated to 20 ml using a stirred ultrafiltration cell (Amicon, model 8050) fitted with an Amicon YM10 membrane and the maltose removed through exhaustive exchanges with AC buffer. Cleavage of the MBP-fusion protein was achieved using trypsin (Sigma) in a ratio of 1:100 trypsin:MBP-fusion product (w/w) (Figure 6.1 (b)). Cleavage was complete after 60 minutes incubation at ambient temperature and further digestion was inhibited by the addition of a corresponding amount of trypsin inhibitor (twice the number of moles of trypsin) (Sigma). The trypsin-digested solution was diluted with cold AC buffer, to a total protein concentration of < 2.5 mg/ml, before being applied to a freshly equilibrated amylose column at a flow rate 1 ml/min. The MBP bound to the resin whilst the red colored rAPX fractions were collected as eluant from the column. The pooled APX fractions (~ 100 ml), which were eluted from the second amylose column, were transferred into a pre-treated dialysis membrane. The

rAPX solution was dialyzed for 5 hours on three separate occasions: twice progressively against 1 l of high quality-dH_2O (drawn from an Elgastad Option 2 water purifier, which is fed with deionised water) and finally against 1 l of FFQ column buffer. A 2.5 × 20 cm column of FFQ-Sepharose anion exchange resin was prepared and equilibrated with >5 column volumes of FFQ column buffer. The dialyzed APX was applied to the anion exchange column at a flow rate of 1 ml/min and a dark band was observed as the enzyme bound to the top of the packed resin. Once the APX solution had been loaded, the column was washed thoroughly with >5 column volumes of FFQ column buffer and elution of the enzyme was achieved using a linear KCl gradient 0-15 mM (about 250 ml used). Coloured fractions were analyzed spectroscopically by measuring the absorbance at 403 and 280 nm: those fractions with a calculated R_z purity number of (A_{403}/A_{280}) ≥ 1.95 were pooled (Figure 6.1 (c)). A stirred ultrafiltration cell fitted with an Amicon YM10 membrane was used to exchange the enzyme into high- quality dH_2O and concentrate the enzyme to a minimum volume (~3 ml, 8 mg/ml). The enzyme solution was divided into 500 µl aliquots and transferred into cryovials for storage under liquid nitrogen.

6.2.2 Ascorbate Peroxidase Activities

Enzyme activities assays were carried out using a Perkin Elmer Lambda 14 UV-visible spectrophotometer linked to an Exacta 366D computer and a circulating water bath (Julabo U3). One unit of enzyme activity is defined as the amount of enzyme that oxidizes 1 µmol of substrate per minute.

6.2.2.1 l-Ascorbic Acid Oxidation

APX was assayed in a reaction mixture (1 ml) containing 50 mM sodium phosphate buffer (μ = 0.10 M, pH 7.0), 0.25 mM l-ascorbic acid, and 1.01 mM hydrogen peroxide and 25 nM enzyme solution at 25 °C. The reactions were initiated by addition of hydrogen peroxide. The activity values for APX are based on linear rates observed after an initial lag phase at 290 nm. The activity was calculated using the published absorption coefficient for l-ascorbic acid at 290 nm (ε_{290} = 2.8 $mM^{-1}cm^{-1}$).[2,3] Corrections were made for the low rates of ascorbate disappearance due to nonenzymatic oxidation.

6.2.2.2 Oxidation of 2,2'-Azino,Di-(3-Ethyl-Benzothiazoline-6-Sulfonic Acid) (ABTS)

Assays were carried out in a reaction mixture (1 ml) containing 50 mM sodium phosphate buffer (μ = 0.10 M, pH 7.0), 0.23 mM ABTS and 1.01mM hydrogen peroxide and the enzyme solution (23 nM) at 25 °C. The activity was calculated, based on linear rates observed after an initial lag phase, using an absorption coefficient of ε_{405}=18.6 mM^{-1}cm^{-1} for ABTS [4].

6.2.3 Oxidation of p-Cresol

p-Cresol (3.50 g, 32 mmol) was dissolved in 300 ml of phosphate buffer (pH 7.0, μ = 0.10 M). Hydrogen peroxide or cumene hydroperoxide (97 mmol) in 50 ml of water was added slowly to the continuously-stirred solution of *p*-cresol with 10 intermediate additions of 0.5 ml of 4.40 μM APX over a period of 3 hours. The cream-white oily precipitate was extracted three times with 100 ml of ethyl acetate. Four spots for the hydrogen peroxide-supported reaction and six spots for the cumene hydroperoxide-supported reaction were observed by thin layer chromatography, developed with ethyl acetate and petroleum ether (1:5). The effect of enzyme concentration on the ratio of products was determined at constant *p*-cresol concentration (0.25 mM) and varying [APX] (0.20 - 1.36 μM). Hydrogen peroxide was added over 1 hour in 10 equal portions giving a final [H_2O_2] = 1.25 mM and reaction mixtures were incubated for a further one hour at room temperature before termination of the reaction by addition of 6 M HCl (0.5 ml). Prior to HPLC analysis, APX was removed from the mixture by ultrafiltration.

6.2.4. Oxidation of 2-Naphtol

The enzymatic oxidation of 2-napthol (25 mg), Scheme 6.1, was performed with APX (4 x 50 μl of 8.79 g/ml stock) in sodium phosphate buffer (20 ml, pH 7.0, μ = 0.10 M) with 5 % DMSO as organic co-solvent and equivalent amount of H_2O_2 (45 ml of 3.87 mM stock) at room temperature. Hydrogen peroxide was slowly added using a peristaltic pump. After 15 hours, the products were extracted with diethyl ether (3x30 ml), dried over anhydrous sodium sulphite and evaporated *in vacuo*. Purification was performed using preparative

TLC on a spinning plate (Chromatotron) with petroleum ether and ethyl acetate as eluents (1:1 v/v). GC-MS analysis was carried out to characterise the product.

2-Napthol(**1**)   2,2'-Binapthol(**2**)
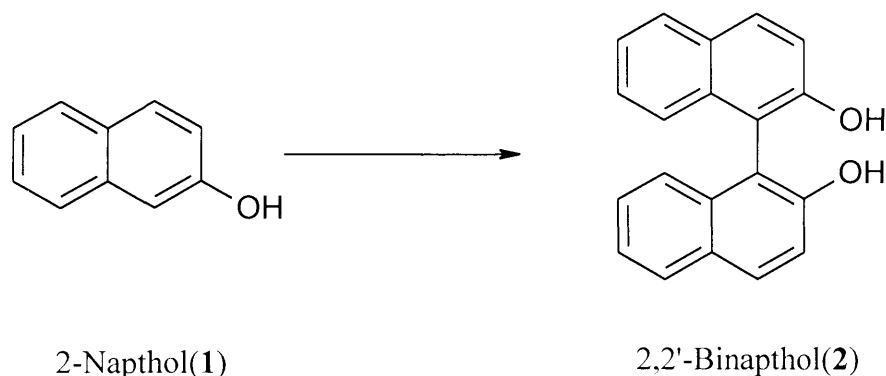
SCHEME 6.1

Characterisation of product, by direct comparison with authentic sample, revealed the formation of 2,2'-binaphtol (**2**), Scheme 6.1. GC temperature programming was used for separation and the settings were as follows: 100 °C for 4 min, 10° min^{-1}, 250 °C for 10 min.

GC: (Retention time, min): 27.5.

MS (EI): m/z 286 ([M$^+$], 100%), 268 (18%), 239 (20%), 207 (20%), 119 (10%), 77, (5%).

For an authentic sample of 2,2'-binaphtol, the following properties were recorded:

GC: (Retention time, min): 27.5.

MS (EI): m/z 286 ([M$^+$], 100%), 268 (12%), 257 (25%), 239 (23%), 207 (5%), 120 (20%).

6.2.5 Synthesis of Pummerer's Ketone (3)

(**3**)
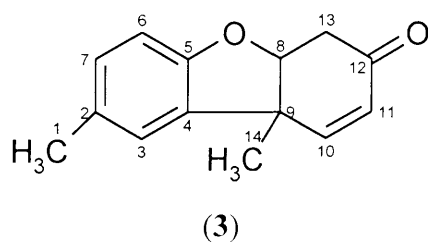
Pummerer's ketone (**3**) was synthesised non-enzymatically using the original protocol.[5] *p*-Cresol (16.09 g, 0.594 mol) and sodium carbonate (21.16 g, 0.199 mol) was dissolved in

300 ml of water. Potassium ferricyanide (59 g, 0.179 mol) was added intermittently over a period of 30 minutes to the continuously stirred solution. After 24 hours of stirring at 30 °C, the solution was acidified with HCl and the reaction mixture was extracted with dichloromethane. The mixture was separated by vacuum distillation at 4 to 5 mmHg and the product (obtained in 10 % yield) distilled at 170-180 °C and recrystallized from boiling methanol. The melting point (120–125 °C) corresponded well with the literature (121 °C).[5]

NMR: δ_H (250 MHz; $CDCl_3$) 7.04 (dd, 2H, J = 8.1 and 2.3); 6.99 (d, 2H, J = 2.3); 6.85 (d, 2H, J = 8.1); 5.6 (s, 2H, broad); 2.32 (s, 6H).

MS (EI): 214 (M^+, 100%), 199 (10.3%), 195 (9.5%), 186 (4.3%), 171 (15.5%), 145 (5.2%), 128 (5.2%), 77 (2.6%).

6.2.6 Kinetic Studies

6.2.6.1 Time-dependent Multiple Wavelength Spectra

Time-dependent multiple wavelength spectra were obtained using an Applied Photophysics Photophysics SX.18MV stopped flow spectrophotometer fitted with a Neslab RTE200 circulating water bath, photodiode array detector and X-Scan software. Spectral deconvolution was performed by global analysis and numerical integration methods using PRO-K software (Applied Photophysics).

6.2.6.2 Transient State Kinetics

Transient kinetics were carried out using an Applied Photophysics SX.18MV stopped flow spectrophotometer fitted with a Neslab RTE200 circulating water bath. Reported values for k_{obs} were an average of at least 3 measurements. All experiments were carried out in sodium phosphate buffer (pH 7.0, μ = 0.10 M) at 5.0 ± 0.1 °C. Data obtained were analysed using non-linear least squares regression analysis on an Archimedes 410-1 microcomputer utilizing Applied Photophysics Spectrakinetics software.

(a) Determination of k_1

The single-mixing method was used to monitor absorbance changes at 403 nm. Protein solutions (0.250 μM) were reacted with varying concentrations of H_2O_2 (2.5 –15 μM) under pseudo first order conditions. The transients obtained were fitted to a single exponential Equation [6.1], to obtain rate constants for the formation of compound I.

$$A_t = A_o \exp^{(-k_{obs}t)} + c \qquad \qquad ...[6.1]$$

Where A_t is the absorbance at time t, A_o the absorbance at time 0, k_{obs} is the observed rate constant, and c is the equilibrium absorbance signal. Plots of k_{obs} *versus* hydrogen peroxide concentration yielded a linear plot of slope k_1. Three determinations for transients were made to ascertain values for k_{obs}.

(b) Determination of k_2

Pseudo-first-order rate constants for reaction of Compound I with *p*-cresol $(k_{2,obs})$ were monitored at 408 nm (isosbestic point between APX and Compound II) in sequential mode by mixing APX (1 μM) with H_2O_2 (1 μM) followed by subsequent reaction (after 50 ms delay) with varying concentrations of *p*-cresol (0–80 μM). The data obtained were fitted to Equation 6.1 with values of k_2 determined in the same way as for k_1. Plots of k_{obs} vs. *p*-cresol concentration yielded a linear plot of slope k_2.

(c) Determination of k_3 and K_d

Pseudo-first-order rate constants for the reduction of Compound II $(k_{3,obs})$ were determined at 421 nm (isosbestic point between native enzyme and Compound I). Enzyme (1 μM) was reacted with one equivalent of H_2O_2. After 10 minutes, this reaction was followed by subsequent reaction with varying concentrations of *p*-cresol. A fit of the data to equation 6.1, using Applied Photophysics software package, was used to determine values for k_{obs}. From the plot of *p*-cresol ([PC]) vs. k_{obs}, k_3 and K_d were obtained according to Equation [6.2].

160

$$k_{obs} = \frac{k_3}{1 + K_d / [PC]} \qquad \qquad ...[6.2]$$

Where [PC] is *p*-cresol concentration, K_d is the dissociation constant of the bound complex in Equation [2.8] in Chapter 2.

6.2.6.3 Steady State Kinetics

Oxidation of *p*-cresol was monitored by an increase in absorbance at 300 nm (ε_{300} = 2450 $M^{-1}cm^{-1}$),[6] which is an isosbestic point between products II and III and where *p*-cresol itself does not absorb.

6.3 EXPERIMENTAL PROCEDURES RELATING TO CHAPTER 3

6.3.1 Site Directed Mutagenesis

Site-directed mutagenesis was carried out using the QuikChange™ mutagenesis kit (Stratagene Ltd., Cambridge).

6.3.1.1 Oligonucleotides Synthesis and Purification

Two complementary oligonucleotides (below) containing the desired mutation were synthesized by The Protein and Nucleic Acid Chemistry Laboratory (PNACL) at University of Leicester. Purification of the oligonucleotides was carried out by ethanol precipitation, in which 180 µl of oligonucleotides were mixed with 20 µl of 3 M sodium acetate buffer, pH 5.2. To this, 400 µl of 100 % ethanol was added and mixed fully. The mixture was spun at 13 K for 30 minutes. Washing was carried out with 500 µl of 70 % ethanol. After drying, the pellets were re-suspended in 100 µl ddH$_2$O.

```
                    5' ------------------------------------3'
Primer 1 (forward)  CGT TTG GCA GCT GAA TCT GCT GGT AC
Primer 2 (reverse)  GCA AAC CGT CGA CTT AGA CGA CCA TG
                    3' ------------------------------------5'
```

6.3.1.2 Polymerase Chain Reaction

Control reactions were prepared by mixing 5 μl of 10 × reaction buffer (Appendix), 2μl (10 ng) of Whitescript ™ 4.5-kb control plasmid (5 ng / μl), 1.25 μl (125 ng) of oligonucleotide control primer 1 [34-mer (100 ng / μl)], 1.25 μl (125 ng) of oligonucleotide control primer 2 [34-mer (100 ng / μl)] and 1μl of dNTP mix. Double-distilled water was added to a final volume of 50 μl, and 1 μl of *Pfu* DNA polymerase (2.5 units / μl) was added. Two transformation reactions (sample reactions, S1 and S2) were prepared by mixing 5 μl of 10 × reaction buffer, 2.5 μl (for S1) and 0.5 μl (for S2) (5-50 ng) of dsDNA template, 2 μl (125 ng) of oligonucleotide primer 1, 2 μl (125 ng) of oligonucleotide primer 2 and 1 μl of dNTP mix. To the mixture, double-distilled water was then added to a final volume of 50 μl, and finally, 1 μl of *Pfu* DNA polymerase (2.5 unit / μl) was added.

Both the control and sample reactions were overlaid with 30 μl of mineral oil. Each reaction was cycled using following cycling parameters: for the control reaction, a 12-minute extension time was used and the reaction was run for 12 cycles; for the sample reactions, extension time was 17 min and the reaction was run for 16 cycles (Table 6.1). At the end of the reaction, the mixtures were placed on ice for 2 minutes to cool to ≤ 37 °C.

TABLE 6.1

Cycling parameters for mutagenesis

Segment	Cycles	Temperature	Time	
	1	95 °C	30 seconds	
Denaturation	16	95 °C	30 seconds	⎫
Annealing		55 °C	1 minute	⎬ 16 cycles
Extension		68 °C	17 minutes	⎭

162

The digestion of parental DNA (recombinant wild type DNA) was achieved by addition of 1 μl of the restriction enzyme D*pn* I (10 units / μl) to each PCR reaction and the reaction mixture mixed by pipetting the solution up and down several times.

The reaction mixtures were spun down in a microcentrifuge for 1 minute and immediately incubated at 37 °C for 1 hour to digest the parental supercoiled dsDNA.

6.3.1.3 Transformation of Epicurian Coli Xl1-Blue Supercompetent Cells

Epicurian Coli XL1-Blue supercompetent cells (Stratagene Ltd., Cambridge) were thawed on ice and 10μl of the *Dpn I*-treated DNA was transferred from each control and sample reaction to separate aliquots of the supercompetent cells (50 μl) to a prechilled Falcon® 2059 polypropylene tube (Stratagene Ltd., Cambridge). The transformation reactions were swirled gently to mix and then left on ice for 30 minutes. After heating for 45 seconds at 42 ° C, the reactions were returned to ice for 2 minutes. LB broth media (0.5 ml) (see Apendix), preheated to 42 ° C, was added and the transformation reactions were incubated at 37°C for 1 hour with shaking at 225-250 rpm. The control transformation reaction (100 μl) was plated onto LB-ampicillin agar plates that had been spread with 20μl of 10% (w/v) X-gal and 20μl of 100 mM IPTG. It should be noted that IPTG and X-gal should not be mixed, since these chemicals will precipitate. X-gal should be prepared in dimethylformamide (DMF) and the IPTG should be prepared in filter-sterilized deionised water. Each sample transformation reaction was precipitated by brief microcentrifugation and was resuspended in 100 μl LB and plated onto LB-ampicillin plates. The transformation plates were incubated at 37 °C overnight.

6.3.1.4 DNA Sequencing

The transformed plasmid DNA was sequenced in order to verify the introduction of the W41A mutation without additional mutations across the whole APX gene. Automated sequencing was performed in The Protein and Nucleic Acid Chemistry Laboratory (PNACL) at University of Leicester, using an ABI 377 DNA sequencer using BigDye terminator chemistry. The oligonucleotides used are pMAL-c2 and M13 (New England Biolabs).

6.3.2 Expression and Purification of W41A APX

Expression and purification of W41A variant were carried out in the same manner as for recombinant APX. The only exception was the time allowed for cleavage of the MBP-fusion protein into MBP and W41A variant by trypsin. For W41A, cleavage was complete after 20 rather than 60 minutes incubation at ambient temperature and further digestion was inhibited by the addition of a corresponding amount of trypsin inhibitor (twice the number of moles of trypsin) (Sigma). The rest of the purification steps were carried out in the same way as APX described in section 6.2.1.

6.3.3 Determination of Extinction Coefficient for W41A APX

The procedure, according to published protocols,[7] was used to calculate the molar extinction coefficient of W41A. A protein stock solution (500 µl), the absorbance of which had been determined earlier, was added to 1.5 ml of the pyridine solution (2 ml of pyridine, 600µl of 1 M NaOH and distilled water to a final volume of 6 ml). Samples with an absorbance of 0.3-0.9 in the visible region are required to provide reliable data. The resulting solution of oxidized haemochromogen was divided into two 1 ml aliquots. After five minutes (to allow for complete conversion to haemochromogen) a UV-visible spectrum was recorded for the oxidised haemochromogen of one of the aliquots. The second aliquot was left for several hours to ensure complete extraction of haem had occurred.

Assay of the haem concentration of the solution was carried out spectroscopically by measuring the absorbance at 557 nm of the reduced pyridine-haemochromogen that was formed immediately after addition of a solid of sodium dithionite (<1 mg). The concentration of the protein stock is determined from the concentration of the haemochromogen formed in the reaction. The absorption coefficient of the reduced pyridine-haemochromogen measured at 557 nm is 32.0 $mM^{-1}cm^{-1}$,[7] and permits calculation of the concentration using Beer's Law. The experiment was repeated on the remaining aliquot to check reproducibility.

164

6.3.4 Measurement of W41A: APX Activities

6.3.4.1 l-Ascorbic Acid Oxidation

W41A variant was assayed in a reaction mixture (1 ml) containing 50 mM sodium phosphate buffer (μ=0.10M, pH 7.0), 0.25 mM l-ascorbic acid, and 1.01 mM hydrogen peroxide and the enzyme solution (27 nM) at 25 °C. The reactions were initiated by addition of hydrogen peroxide. The activity values for APX are based on linear rates observed after an initial lag phase at 290 nm. The activity was calculated using an absorption coefficient of l-ascorbic acid (ε_{290} = 2.8 mM^{-1}cm^{-1}).[2,3] Corrections were made for the low rates of ascorbate disappearance due to nonenzymatic oxidation.

6.3.4.2 Oxidation of 2,2'-Azino,di-(3-ethylbenzothiazoline-6-Sulphonic Acid) (ABTS)

Assays were carried out in a reaction mixture (1 ml) containing 50 mM sodium phosphate buffer (μ = 0.10M, pH 7.0), 0.23 mM ABTS and 1.01mM hydrogen peroxide and the W41A solution (140 nM) at 25 °C. The activity was calculated, based on linear rates observed after an initial lag phase, using an extinction coefficient of ε_{405}=18.6 mM^{-1}cm^{-1} for ABTS.[4]

6.3.5 Sulphoxidation of Alkyl Aryl Sulphides

The sulphides used were methyl phenyl sulphide, ethyl phenyl sulphide, isopropyl phenyl sulphide (all from Aldrich Chemical Co.), n-propyl phenyl sulphide, p-chlorophenyl methyl sulphide, p-nitrophenyl methyl sulphide and methyl naphthalene sulphide (all from Lancaster Synthesis Ltd.). Stock solutions (100 mM) were prepared in methanol (HPLC Grade, Aldrich Chemical Co.); methanol is necessary to solubilize the sulphides in the aqueous reaction mixture. (-)-(S)-t-Butylphenylphosphinothioic acid was kindly provided by Dr Martin Harger (University of Leicester). Hydrogen peroxide solutions were freshly prepared by dilution of a 30% (v/v) solution (Sigma): exact concentrations were determined by titration with 0.05 M Ce(IV) standards[8] and confirmed by Uv-visible spectroscopy (ε_{240}= 39.4 M^{-1}cm^{-1})[9]

In a typical reaction, all sulphides except *p*-nitrophenyl methyl sulphide (in methanol, 10 μL total) were diluted into sodium phosphate (μ= 0.10 M and pH 7.0) buffer (2 ml) to give a final concentration of 10 mM. To this solution, APX or W41A (10 μM) were added, followed by H_2O_2 in 10 μl-aliquots over 90 minutes to give a final concentration of 10 mM. The total reaction time was 120 minutes. The mixture then extracted with dichloromethane (3 x 2ml) and the extract concentrated and analysed by GC-MS. For the oxidation of *p*-nitrophenyl methyl sulphide, the reaction procedure was scaled up 10-fold and, after evaporation of the dried organic layer under vacuum, gave a crude product that was further purified using a preparative TLC on a spinning plate (Chromatotron) with petroleum ether and ethyl acetate as eluents (1:5 v/v). For APX-catalysed reactions, approximately 40-50 % of starting sulphide was recovered; for W41A-catalysed reactions, approximately 5-20 % of starting sulphide was recovered.

6.3.6 Kinetic Studies

Kinetic experiments were carried out in sodium phosphate buffer (μ = 0.10 M and pH 7.0) at 25.0 °C. The reaction mixture contained APX (10 μM) or W41A (5 μM), 100 μM H_2O_2 and sulphides (0-250 μM). Reactions were initiated by addition of H_2O_2 and the rate of sulphide oxidation was followed by monitoring the decrease in absorbance of the sulphides recorded over 5 minutes. The rate of oxidation in the absence of either APX or W41A was negligible. Initial rates at a single concentration of sulphide were calculated using the $\Delta\varepsilon$ values between sulphides and corresponding sulphoxides. $\Delta\varepsilon$ ($mM^{-1}cm^{-1}$) values and the monitored wavelength (nm) were as follows: methyl phenyl sulphide, 7.87 (254); ethyl phenyl sulphide, 7.27 (251); isopropyl phenyl sulphide, 5.28 (252); *n*-propyl phenyl sulphide, 6.32 (252); *p*-chlorophenyl methyl sulphide, 8.65 (256); *p*-nitrophenyl methyl sulphide, 10.70 (338); methyl naphthalene sulphide, 35.28 (250.5). All determinations of initial rates were carried out at least three times and steady state kinetic parameters, k_{cat} and K_m, were determined by a fit of the averaged data at each concentration to the Michaelis-Menten equation using a non-linear regression analysis program (Grafit32 version 4, from Erithacus Software Limited, Middlesex, UK).

6.3.7 Computational Studies

Computational work was carried in the laboratory of Dr. M. J. Sutcliffe (University of Leicester). The interactive molecular graphics program Sybyl (Tripos Inc, St. Louis, MO, USA) was used to construct the sulphides. These were energy minimised using the Tripos forcefield.[10] The protein coordinates for wild-type APX (accession number 1APX; Patterson & Poulos, 1995) were obtained from the Protein Data Bank (Bernstein et al., 1977) and hydrogen atoms added within Sybyl. The W41A variant was modelled by replacing Trp41 in the crystal structure (1APX) with an alanine. For both wild-type APX and W41A, an oxygen atom was modelled in the sixth coordination site of the haem iron.

The program GOLD[11] was used to dock the 7 different sulphides into the active site of recombinant wild-type APX and W41A. A 15 Å radius was specified to encompass the active site around the Trp41 residue in wild-type APX and the Ala41 residue in W41A. An (Fe)O–S(substrate) upper distance restraint of 4 Å was applied, with a force constant k = 10 kcal mol^{-1}. Twenty dockings, into both wild-type APX and W41A, were produced for each of the seven compounds. To check if 20 dockings were sufficient, one of the sulphides (phenyl, n-propylsulphide) was used to produce 50 dockings in W41A APX, and compared with the product ratio obtained from 20 dockings. The resulting dockings were analysed using InsightII and lone pairs were added to the sulphur atoms. The distance of the pro-R lone pair and the pro-S lone pair from the O on the haem iron were measured for each of the compounds: if this distance differed by more than 0.3 Å, the product was taken to correspond to the closest lone pair to the oxygen. The arginine residue at position 38 was identified as likely to sterically hinder the substrate orientation, and the sidechain conformation of Arg38 was therefore modified (using InsightII) so that it was further from the haem iron, and in an energetically favourable conformation.

6.3.8 Synthesis of Sulphoxides Standards

Sulphoxide standards were prepared from sulphides using literature procedures.[12] A stock solution of periodide was prepared by dissolving 10.7g of $NaIO_4$ in 100 ml de-ionized water. To 13.1 ml (6.6 x mmol) of $NaIO_4$ at 4 °C was added 6.6 mmol of sulphides and the mixture was stirred in an ice-bath overnight. The precipitated sodium iodide was removed by filtration and the filtrate was extracted with chloroform. The extract was dried over

anhydrous MgSO$_4$ and the residue was subjected to flash column chromatography (petroleum ether: ethyl acetate = 5:1) to give the desired sulphoxides. NMR and MS data are given below.

Methyl phenyl sulphoxide

NMR: δ_H (250 MHz; CDCl$_3$) 7.65 (d, 2H), 7.48-7.30 (m, 3H), 2.65 (s, 3H).

MS (EI): m/z 140 (M$^+$, 80 %), 125 (100 %), 109 (15 %), 97 (85 %), 77 (75%).

Ethyl phenyl sulphoxide

NMR: δ_H (250 MHz; CDCl$_3$) 7.66-7.60 (d, 2H), 7.50-7.38 (m, 3H), 2.83 (q, 2H), 1.22 (t, 3H).

MS (EI): m/z 154 (M$^+$, 20 %), 126 (50 %), 109 (10 %), 97 (15 %), 78 (100 %).

n-Propyl phenyl sulphoxide

NMR: δ_H (250 MHz; CDCl$_3$) 7.65 (d, 2H), 7.50-7.32 (m, 3H), 2.78 (t, 2H), 1.68 (m, 2H), 0.97 (t, 3H).

MS (EI): m/z 168 (M$^+$, 30 %), 151 (10 %), 126 (100 %), 97 (15 %), 78 (85 %).

Isopropyl phenyl sulphoxide

NMR: δ_H (250 MHz; CDCl$_3$) 7.60 (d, 2H), 7.48-7.32 (m, 3H), 3.10 (m, 1H), 1.20 (d, 6H).

MS (EI): m/z 168 (M$^+$, 30 %), 152 (4 %), 126 (100 %), 97 (5 %), 78 (70 %).

t-Butyl phenyl sulphoxide

NMR: δ_H (250 MHz; CDCl$_3$) 7.31-7.36 (m, 2H), 7.19-7.10 (m, 3H), 1.1 (s, 9H).

MS (EI): m/z 182 (M$^+$), 165 ([M-H]$^+$, 100%), 124 (28%), 94 (32%), 78 (60%).

p-Chlorophenyl methyl sulphoxide

NMR: δ_H (250 MHz; CDCl$_3$) 7.32 (d, 2H), 7.24 (d, 2H), 2.53 (s, 3H).

MS (EI): m/z 174 (M$^+$, 10 %), 158 (100 %), 143 (60 %), 125 (15 %), 108 (40 %), 75 (20 %).

p-Nitrophenyl methyl sulphoxide

NMR: δ_H (400 MHz; CDCl$_3$) 8.40 (d, 2H), 7.85 (d, 2H), 2.8 (s, 3H).

MS (EI): m/z 185 (M$^+$, 100 %), 170 (40 %), 134 (15 %), 96 (3 %), 76 (3 %).

p-methylphenyl methyl sulphoxide

NMR: δ_H (250 MHz; CDCl$_3$) 7.64-7.60 (d, 2H), 7.43-7.38 (d, 2H), 2.78 (s, 3H), 2.49 (s, 3H).

MS (EI): m/z 154 (M$^+$), 100%), 124 (28%), 94 (32%), 78 (60%).

p-Methoxyphenyl methyl sulphoxide

NMR: δ_H (300 MHz; CDCl$_3$) 7.30-7.40 (d, 2H), 6.60 (d, 2H), 3.10 (s, 3H), 2.10 (s, 3H).

MS (EI): m/z 170 (M$^+$, 30 %), 155 (100 %), 139 (20 %), 123 (25 %), 92 (30 %), 77(30 %).

Methyl naphthalene sulphoxide

NMR: δ_H (250 MHz; $CDCl_3$) 7.70-7.80 (m, 3H), 7.40 (t, 1H), 7.30 (t, 1H), 7.15 (m, 2H), 2.63 (s, 3H).

MS (EI): m/z 190 (M^+, 50 %), 175 (100 %), 159 (20 %), 147 (35 %), 127 (40 %), 77 (10 %).

6.4 EXPERIMENTAL PROCEDURES RELATING TO CHAPTER 4

6.4.1 Preparation Cytochrome P450 BM3

Cytochrome P-450 BM3 was kindly provided by Dr F. Ahmed (University of Leicester). The P450 BM3 concentrations were measured by the method of Omura and Sato[14] using an absorption coefficient of ε = 91 mM^{-1}cm^{-1} at 448 nm for the reduced P450-carbon monoxide (P450-CO) complex. Protein purity was confirmed by SDS/PAGE, and by assessments of the ratio A_{418}/A_{280}, where a high level of purity is represented by a ratio of 0.7 or above.

6.4.2 Oxidation of Alkyl Aryl Sulphides

The sulphides used were methyl phenyl sulphide, ethyl phenyl sulphide, isopropyl phenyl sulphide, *t*-butylphenyl sulphide, *p*-chlorophenyl methyl sulphide, *p*-nitrophenyl methyl sulphide and *p*-methylphenyl methyl sulphide and *p*-methoxyphenyl methyl sulphide (purchased from Aldrich Chemical Co.).

6.4.2.1 Procedure 1

This procedure was used to determine if the title reaction occurs. The sulphides were added (2 mM, 10 ml) to 20 ml buffer (sodium potassium phosphate buffer, pH 8.0, 50 mM, containing 5% DMSO as a co-solvent) and NADPH (2 mM, 10 ml). The reaction was initiated by addition of P450 BM3 (150 µl, 4.4µM). The reaction mixture was stirred at room temperature for 3 hours. Extraction was then carried out using dichloromethane (3 x 40 ml). Organic extract was left in fume cupboard overnight in order to evaporate the solvent until dryness. The sample was dissolved in a minimum amount of HPLC solvent and analysed by HPLC or NMR.

6.4.2.2 Procedure 2

This procedure was used to obtain large amount of sulphoxides for analysis. Alky aryl sulphides were added (2mM, in 100 ml sodium potassium phosphate buffer, pH 8.0, 50

mM, containing 5% DMSO as a co-solvent) to the NADPH regeneration system (2 mM, see Appendix). The reaction was initiated by addition of P450 BM3 (300 μl, 4.4μM). The reaction mixture was stirred at room temperature for 3 hours. Extraction was then carried out using CH_2Cl_2 (3 x 100 ml). Solvent was evaporated under vacuum until dryness. The sample was analysed by direct comparison of HPLC and MS data with the sulphoxide standards (see Section 6.3.8).

6.4.3 Synthesis of tert-Butyl Phenyl Sulphide(4)
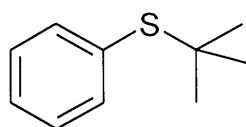
(4)

A solution of 70 % (v/v) H_2SO_4 was saturated with isobutene for 20 minutes. Thiophenol (3 ml) was added dropwise at 0°C. Stirring was maintained for another 45 minutes and the temperature allowed to warm from 0°C to room temperature. The reaction was then stopped and extraction carried out with diethyl ether. The organic extract was dried over anhydrous sodium sulphate, filtered and concentrated under reduced pressure. The resulting crude product was purified using a preparative TLC on a spinning plate (Chromatotron) with petroleum ether and ethyl acetate as eluents (1:5 v/v). The title compound was obtained as white crystalline solid.[13]

NMR: δ_H (250 MHz; $CDCl_3$) 7.31-7.36 (m, 2H), 7.19-7.10 (m, 3H), 1.1 (s, 9H).

MS (EI): m/z 165 ([M-H]$^+$, 100%), 124 (28%), 94 (32%), 78 (60%).

6.4.4 Kinetic Studies

Kinetic experiments were carried out in sodium potassium phosphate buffer, pH 8.0, (containing 5 % DMSO, 10 % for *p*-nitrophenyl methyl sulphide) at 25 °C, in 1 mL cuvettes, 1 cm path length.[15] The reaction mixtures contained P450 BM3 (22 nM), NADPH (0.2 mM) and sulphides (5-500 μM). The oxidation of sulphides to sulphoxides was determined spectrophotometrically by monitoring NADPH consumption at 340 nm with the background wavelength at 250 nm over 10 seconds by using a Beckman DU7500 instrument with a diode array detector. The rates were calculated from the linear part of

the graph. The K_m and V_{max} values were obtained by fitting the date to Michaelis-Menten equation using *Origin 5* software.

6.4.5 Computational Studies

Computational work was carried by the laboratory of Dr. M. J. Sutcliffe (University of Leicester). The alkyl aryl sulphide compounds were constructed using the interactive molecular modelling program Sybyl (Tripos Inc, St. Louis, MO, USA). These were then energy minimised using the Tripos forcefield.[10] The coordinates of the ferric form of the haemoprotein domain of P_{450} BM3 complexed with parmitoleic acid (accession number 1FAG[16]) were obtained from the PDB[17] and hydrogens added within Sybyl. To mimic the ferryl oxygen species, an oxygen atom was positioned 1.7 Å above the haem iron, on the opposite side of the haem to the cysteinyl ligand.

The 7 different alkyl aryl sulphide compounds were docked into the active site using the program GOLD.[11] A 15 Å radius was specified to encompass the active site around the ferroxyl oxygen. To ensure that the substrate sulphur was close enough to the ferroxyl oxygen for oxidation to take place, a (Fe)O–S(substrate) upper distance restraint of 3.8 Å was applied, with a force constant k = 10 kcal mol^{-1}. For each compound, 25 protein-substrate complexes were generated. The best 12 dockings (on the basis of best overall energy) were then analysed, and lone pairs were added to the sulphurs, using Sybyl. The distance of the pro-R lone pair and the pro-S lone pair from the O on the haem iron were measured for each of the compounds; if this distance differed by more than 0.25 Å, the product was taken to correspond to the closest lone pair to the oxygen.

Three residue positions were identified as likely sterically hindering the substrate orientation—Ala 264 (I-helix) interacts with **R** groups, and Leu 75 and Val 78 (B'-helix) interact with **X** groups. To gauge any likely influence on enantioselectivity of these three residues, the following modifications were modelled (one at a time) into the protein structure, and the docking process repeated. Leu 75 was replaced with alanine, Val 78 was replaced with alanine, and Ala 264 was translated by 0.4 Å along the vector running from Leu 439 Cγ2 to Ala 264 Cα. In all three cases, the modification potentially gave the substrate more conformational freedom within the active site.

172

6.5 EXPERIMENTAL PROCEDURES RELATING TO CHAPTER 5

6.5.1 Synthesis of N-Carboxy-α-L-Leucine Anhydride (5)

(5)
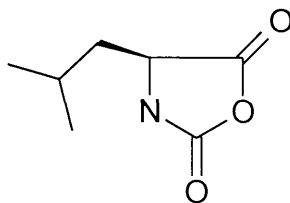
N-Carboxy-α-L-Leucine anhydrides (5) was prepared as described by Konopinska and Siemion.[18] N-benzoxycarbonyl-L-leucine (1 mmol) was allowed to react with 3 mmol of oxyl chloride in 2 ml of boiling benzene for 2 to 3 min. The reaction mixture was cooled in ice. The title compound was crystallized after addition of diethyl ether.

Melting point: 73-75 °C (literature values range from 65 to75 °C[18]).
Yield: 55 %.

NMR: δ_H (250 MHz; CDCl$_3$) 6.43 (br, 1H), 4.27 (dd, 1H, J_1 8.82 Hz, J_2 4.08 Hz), 1.53-1.82 (m, 3H),) 0.93 (t, 6H, J 5.98 Hz).

MS (FAB): m/z 180 ([MNa]$^+$, 11%), 158 ([MH]$^+$, 55%), 130 (100%), 120 (10%), 107 (22%), 86 (28%), 77 (22%).

6.5.2 Synthesis of Poly-L-Leucine

Neat 1,3 Diaminopropane (0.038 mmol) was added to a solution of an N-carboxy-α-L-leucine anhydrides (2.3 mmol) in CH$_2$Cl$_2$ (anhydrous; 10 ml). After stirring for three days under nitrogen at room temperature, the solvent was removed under reduced pressure. The residue was washed with diethyl ether and dried in *vacuo* to yield polymerized L-leucine (0.200 g). The melting point was found to be over 300 °C.[19]

6.5.3. Oxidation of Alkyl Aryl Sulphides

6.5.3.1 Procedure 1

To water (2 ml), phenyl ethyl sulphide (0.1 mmol) and poly-L-leucine (127 mg) were added and stirred for 6 hours to swell the polymer. Subsequently, hydrogen peroxide (1 mmol) in water (2 ml) was added. After 4 hours of reaction, the product(s) were extracted and analysed by HPLC.

6.5.3.2 Procedure 2

To a solution of hexane (2 ml), phenyl ethyl sulphide (0.2 mmol) and poly-L-leucine (100 mg) were added and stirred for 6 hours to swell the polymer. Subsequently, hydrogen peroxide (2 mmol) in water (2 ml) was added over 2 hours. After 24 hours of reaction, the mixture was filtered to re-claim the catalyst. The filtrate was separated and the organic phase was dried over anhydrous sodium sulphate and the solvent was evaporated under vacuum until dryness. The remaining sample was dissolved in minimum amount of hexane:isopropanol mixture (v/v, 80:20,) and analysed by HPLC using a chiral column (Chiralcel OD-H).

6.6 REFERENCES

1   Patterson, W. R. and Poulos, T. L., *J. Biol. Chem.*, 1994, **269**, 17020.

2   Mittler, R. and Zilinskas, B. A., *Plant Physiol.*, 1991, **97**, 962.

3   Nakano, Y. and Asada, K., *Plant Physiol.*, 1981, **22**, 867.

4   Putter, J. and Becker, R., in *Methods of Enzymatic Analysis*, Verlag Chemie, Weinheim 1983, p. 286.

5   Pummerer, R., Melamed, D. and Puttfarcken, H., *Chem. Berr.*, 1922, **55**, 3116.

6   Casella, L., Poli, S., Gullotti, M., Selvaggini, C., Beringhelli, T. and Marchesini, A., *Biochemistry*, 1994, **33**, 6377.

7   Antonini, E. and Brunori, M., *Hemoglobin and Myoglobin in Their Reactions with Ligands*, , North Holland 1971.

8   Jeffery, G. H., Bassett, J., Mendham, J. and Denney, R. C., *Vogel's Textbook of Quantitative Chemical Analysis*, John willey & Sons, New York 1989.

9   Nelson, D. P. and Kiesow, L. A., *Anal. Biochem.*, 1972, **49**, 474.

10   Clark, M., Cramer, R. D. and Van Opdenbosch, N., *J. Comp. Chem.*, 1989, **10**, 982.

11   Jones, G., Willet, P., Glen, R. C., Leach, A. R. and Taylor, R., *J. Mol. Biol.*, 1997, **267**, 727.

12   Johnson, C. R. and Keiser, J. E., *Org. Synt.*, 1973, **5**, 791.

13   Ipatieff, V. N., Pines, H. and Friedman, B. S., *J. Am. Chem. Soc.*, 1938, **60**, 2731.

14   Omura, T. and Sato, R., *J. Biol. Chem.*, 1964, **239**, 2370.

15   Matson, R. S., Hare, R. S. and Fulco, A. J., *Biochim. Biophys. Acta*, 1977, **487**, 487.

16   Li, H. and Poulos, T. L., *Nature Struct. Biol.*, 1997, **4**, 140.

17   Bernstein, F., Koetzle, T. F., Williams, G. J. B., Meyer, E. F., Brice, M. D., R, R. J., Kennard, O., Shimanouchi, T. and Tasumi, M., *J. Mol. Biol.*, 1977, **112**, 535.

18   Konopinska, D. and Siemion, I. Z., *Angew. Chem. Int. Ed. Engl.*, 1967, **6**, 248.

19   Lasterra-Sanchez, M. E., Felfer, U., Mayon, P., Roberts, S. M., Thornton, S. R. and Todd, C. J., *J. Chem. Soc. Perkin Trans. 1*, 1995, 343.

APPENDIX

APPENDIX

1000x AMPICILLIN

100 mg ampicillin per ml of dH$_2$O, filter sterilised.

LB-AMPICILLIN PLATES

10 g NaCl, 10 g tryptone, 5 g yeast extract, 20 g agar to 1 liter with dH$_2$O; autoclave, allow to cool to $\leq$ 55 °C, and add 0.5 ml of 1000 x ampicillin and pour ~50 ml into each petri dish, allow to set.

GLYCEROL STOCKS

300 μl glycerol (50%) and 700 μl of an overnight culture; stored frozen at -20 °C.

RICH MEDIUM

5 g NaCl, 10 g tryptone, 5 g yeast extract, 2 g glucose to 1 liter with dH$_2$O; autoclave, allow to cool to $\leq$ 55 °C, and add 0.7 ml of 1000x ampicillin.

LYSIS BUFFER

50 mM tris(hydroxymethyl) aminomethane-HCl, pH 8.0, 10 mM diaminoethanetetraacetic acid.

AC BUFFER

20 mM tris(hydroxymethyl)aminomethane-HCl, pH 7.5, 200 mM NaCl.

FFQ COLUMN BUFFER

10 mM KPi pH 7.0.

10 X REACTION BUFFER

100 mM KCl, 100 mM (NH$_4$)$_2$SO$_4$, 200 mM Tris-HCl (pH 8.8), 20 mM MgSO$_4$, 1 % Triton® X-100 and 1 mg/ml nuclease-free bovine serum albumin(BSA) (Stratagene Ltd., Chambridge).

LB BROTH

For per liter, 10 g of NaCl, 10 g of tryptone and 5 g of yeast extract to 1 liter with deionised H_2O; autoclave plus 2.5 ml of 1M $MgCl_2$ and 12.5 ml of 1 M $MgSO_4$ and 10 ml of a 2 M filter-sterilised glucose solution.

NADPH REGENERATING SYSTEM

For 100 ml, 2 mM: 0.041 g $MgCl_2$, 61 mg of Glucose-6-phosphate, Glucose-6-phosphate dehydrogenase (1 unit) and 153 mg of NADP.

PUBLICATIONS

1. **Celik, A.**, Cullis, PM., and Raven, EL., Catalytic Oxidation of p-Cresol by Ascorbate Peroxidase, *Arch.,Biochem. Biophy.* (2000), **373**, pp 175-181

2. **Celik, A.**, Cullis, PM., Sautcliffe, MJ., Sangar, R., and Raven, EL., Engineering the Active Site of Ascorbate Peroxidase, *Eur. J. Biochem..* (2001), **268**, pp 78-85

3. **Celik, A.**, Raven, EL and Cullis, PM., Cytochrome P450 BM3 Catalysed Enantioselective Sulphoxidation, in preperation.

FUTURE WORK

Future Work

Enzymatic oxidation has been called the technology of the future in various industries, such as pharmaceutical, paper and bleaching, waste water treatment and so on. Among the ideal oxidants, peroxidases and cytochrome P450s are good candidates, which are inexpensive and readily available. Therefore to understand these enzymes, in particular, ascorbate peroxidase and cytochrome P450 in terms of structure function relationship are becoming more important and demanded. Thus, we have investigated such structure-function relationship in certain degree. But this is, of course, not the end of the work. The investigation could be extended in various ways. Here, the future work could be, as outlined below, in general and in specific.

In general;

The compounds range for APX and its mutant (W41A) could be extended to other substrates, in particular, phenolic compounds and aliphatic sulphides in order to obtain more detailed picture of structure-function relationship within each series of similar compounds.

Since APX and its mutant reduce hydrogen peroxide to water, the use of racemic hydroperoxides could yield chiral alcohols if APXs catalyse an enantioselective reduction of racemic peroxides.

Site-directed mutagenesis is a powerful tool to utilize for understanding the roles of various amino acids residues by replacing them with others. Therefore it would be used to get more detailed information about APX and cytochrome P450 BM3. Effects of mutations of various residues could be investigated further.

In specific;

In chapter two, the concentration range of p-cresol in Figure 2.9 can be extended in order to elucidate the origin of the apparent sigmoidal kinetics. This data may serve a clue for two independent binding sites.

In chapter two, the concentration range for APX-catalysed ABTS oxidation could be extended in order to obtain more detailed picture of steady state kinetics. A comparison with kinetics of oxidation of p-cresol and ascorbic acid could also be investigated further.

In chapter three, the thermodynamic effects (compound I/II stability) that could result from formation of stabilizing hydrogen bond in between residues in distal packet of APX, is clearly destroyed in the W41A mutant, since no clear formation of compound II observed. This could be extended, and more detailed information will be obtained by making additional mutation of distal residues of APX.